Chapter 3

Where Is Geothermal in New Mexico? Exploring Our Underground Heat Abundance

Shari Kelley, New Mexico Bureau of Geology and Mineral Resources, New Mexico Institute of Mining and Technology
Mark Person, Department of Earth and Environmental Science, New Mexico Institute of Mining and Technology
Luke Martin, New Mexico Bureau of Geology and Mineral Resources, New Mexico Institute of Mining and Technology
Martin Reyes Correa, New Mexico Bureau of Geology and Mineral Resources, New Mexico Institute of Mining and Technology

An important note: As mentioned in the Executive Summary and elsewhere in this report, New Mexico was a target for extensive geothermal exploration of hydrothermal—or conventional—resources during the 1970s and 1980s. This first section of this chapter describes geologic and conceptual models used to identify and develop a few of the key hydrothermal resources in the state. At the end of this chapter, you'll find a summary of the extensive subsurface possibilities, with a focus on next-generation geothermal development in New Mexico.

New Mexico is ranked sixth in the nation in geothermal potential (**Figure 3.1**).[1,2] That is, in part, due to an important north-trending geologic feature that bisects the state—the Rio Grande rift, a place where the Earth's crust is stretched and thinned, bringing elevated temperatures closer to the surface (**Figure 3.2**). Seismic profiles across the rift show that the crust is 40 to 50 kilometers thick to the east and west of the rift, but the crust thins to 30 to 40 kilometers beneath the rift.[3,4] More recent seismic studies document a 150-kilometer-wide, low-velocity zone in the mantle beneath the rift, indicative of hot mantle.[5,6]

In addition to the Rio Grande rift, another significant geologic feature, the northeast-trending Jemez Lineament, influences geothermal potential (**Figure 3.2**). The Jemez Lineament intersects the Rio Grande rift in the vicinity of the Valles Caldera. Passive seismic

and more recently magnetotelluric data[7,8] indicates the presence of a moribund (slowly cooling) magma body under the Valles Caldera. The Jemez Lineament is an alignment of 10 volcanic fields that are generally less than 10 million years old; the aligned fields stretch from eastern Arizona to southeastern Colorado (**Figure 3.2**).[9,10] The volcanic fields have no spatial or temporal or chemical progression along the Jemez Lineament. Late Cenozoic volcanism along the Jemez and in the Rio Grande rift in New Mexico is predominantly basaltic. Holocene basalt flows include the Bandera flow (11,000 years old) and the McCartys flow (3,900 years old) in the Zuni-Bandera volcanic field and the 5,200-year-old Carrizozo flow in the Tularosa Basin in central New Mexico. Although several hot springs are associated with the volcanic fields along the lineament, the only volcanic field with a significant high-temperature geothermal system is the Jemez Mountains volcanic field, which culminated with the eruption of the 0.07 million to 1.23 million-year-old Valles Caldera.

GEOTHERMAL POTENTIAL IN THE UNITED STATES

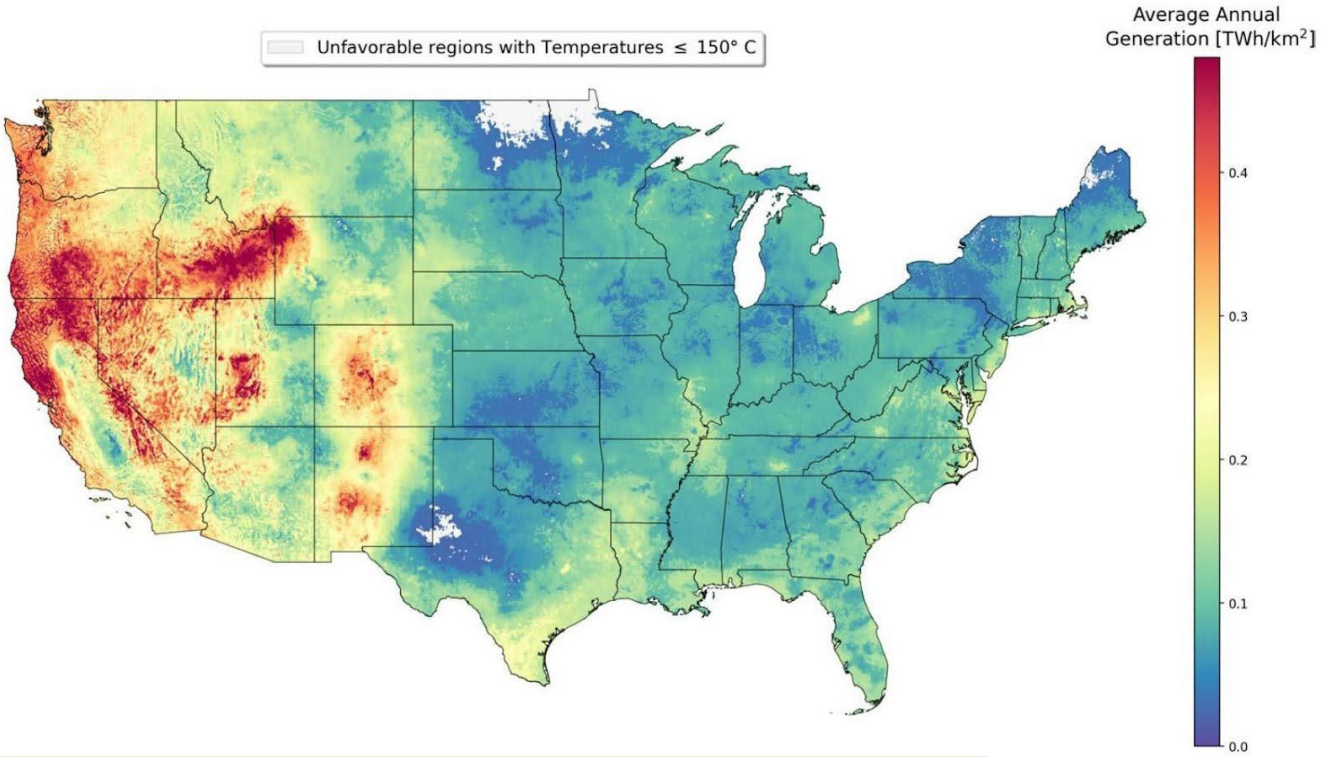

Disclaimer: While the maps and analyses in this chapter and insert highlight areas of geothermal potential, additional site-specific analyses, including economic, engineering, and fluid production rate analyses, are required to identify potential uses and drill-ready prospects.

Figure 3.1. *Map illustrating why New Mexico is ranked sixth in the nation for geothermal potential. This map shows the average annual engineered geothermal system (EGS) power generation per unit area (TWh/km²) for geothermal projects spanning depths of 1 km–7 km. High EGS capacity follows a north-south trend that bisects New Mexico. White areas indicate techno-economically infeasible locations, with temperatures of less than 150°C (302°F) at a depth of 7 kilometers.* Source: Aljubran, M. J., & Horne, R. N. (2024). Thermal Earth model for the conterminous United States using an interpolative physics-informed graph neural network. *Geothermal Energy, 12*(1), 25. https://doi.org/10.1186/s40517-024-00304-7

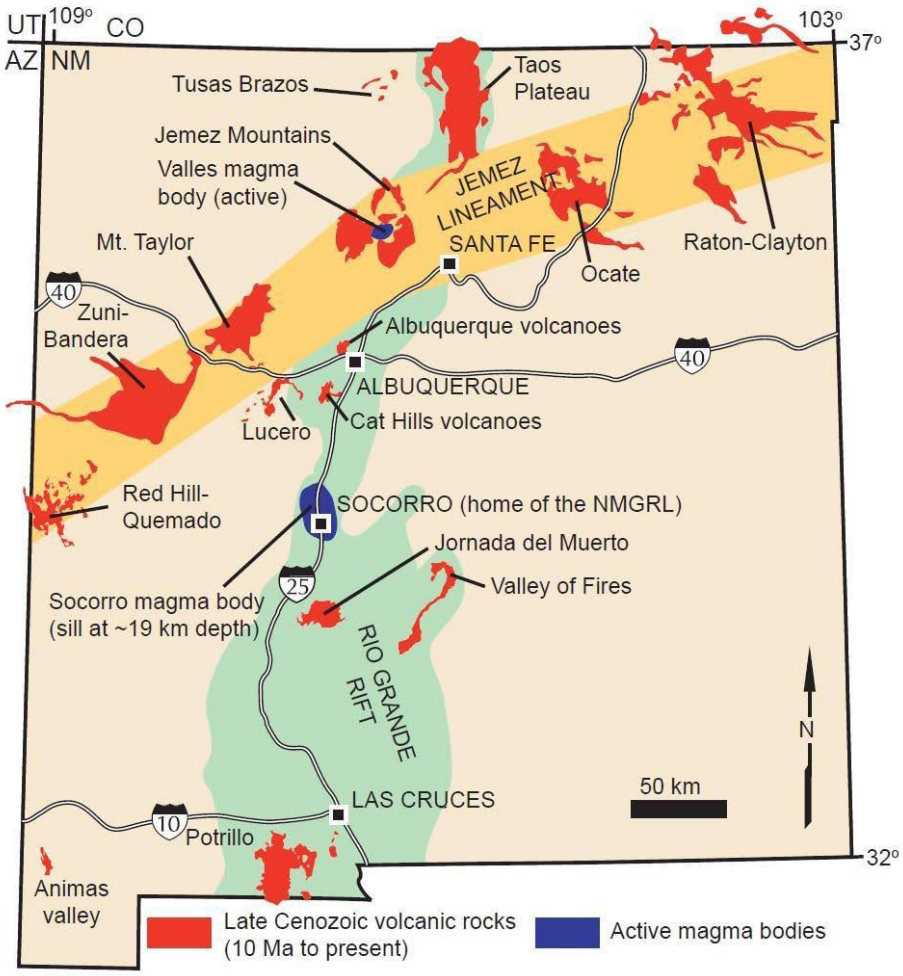

Figure 3.2. *Map of the Rio Grande rift (green) and the young volcanic rocks (red areas) in New Mexico.* Source: Zimmerer, M. J. (2024). A temporal dissection of late Quaternary volcanism and related hazards within the Rio Grande rift and along the Jemez lineament of New Mexico, USA. *Geosphere, 20*(2), 505–546. https://doi.org/10.1130/GES02576.1

The concept of extracting heat from the Earth using a hot dry rock system was originally developed in Los Alamos (the Los Alamos Scientific Laboratory at the time) by Burnham and Stewart,[11] who used nuclear explosives to create a fractured cavity surrounding well-penetrating crystalline basement rocks. Because of technical and environmental concerns about using nuclear material, hydraulic fracturing—a different design using a technology already in use by the oil and gas industry—was investigated starting in 1970 and was implemented at a site on the west side of the Valles Caldera starting in spring 1972.[12] The Los Alamos developments and the 1973 oil crisis triggered extensive exploration for geothermal resources in New Mexico in the 1970s and 1980s. Many companies—including Unocal, Hunt Oil Company, Phillips, Sunedco, and Geothermix—drilled hundreds of shallow exploration holes across the state; the well records from these companies are archived in the Geologic Information Center at the New Mexico Bureau of Geology and Mineral Resources. During this same time frame, New Mexico State University in Las Cruces,[13,14,15,16] the University of New Mexico in Albuquerque,[17] and the New Mexico Institute of Mining and Technology in Socorro[18,19,20,21] developed geothermal research programs that instilled interest in geothermal research for a generation of students.

Figure 3.3 shows the locations of hot springs and wells in New Mexico. The use of geothermal heat in the Land of Enchantment during the 1970s and 1980s focused on direct-use projects in the Rio Grande rift, particularly in southern New Mexico (**Figure 3.3**). As mentioned, New Mexico has one geothermal power plant located near Lordsburg in southwestern New Mexico (**Figure 3.4**). The original 4 megawatt electric power plant Lighting Dock

HOT SPRINGS AND WELLS WITH TEMPERATURES ABOVE 30°C (86°F)

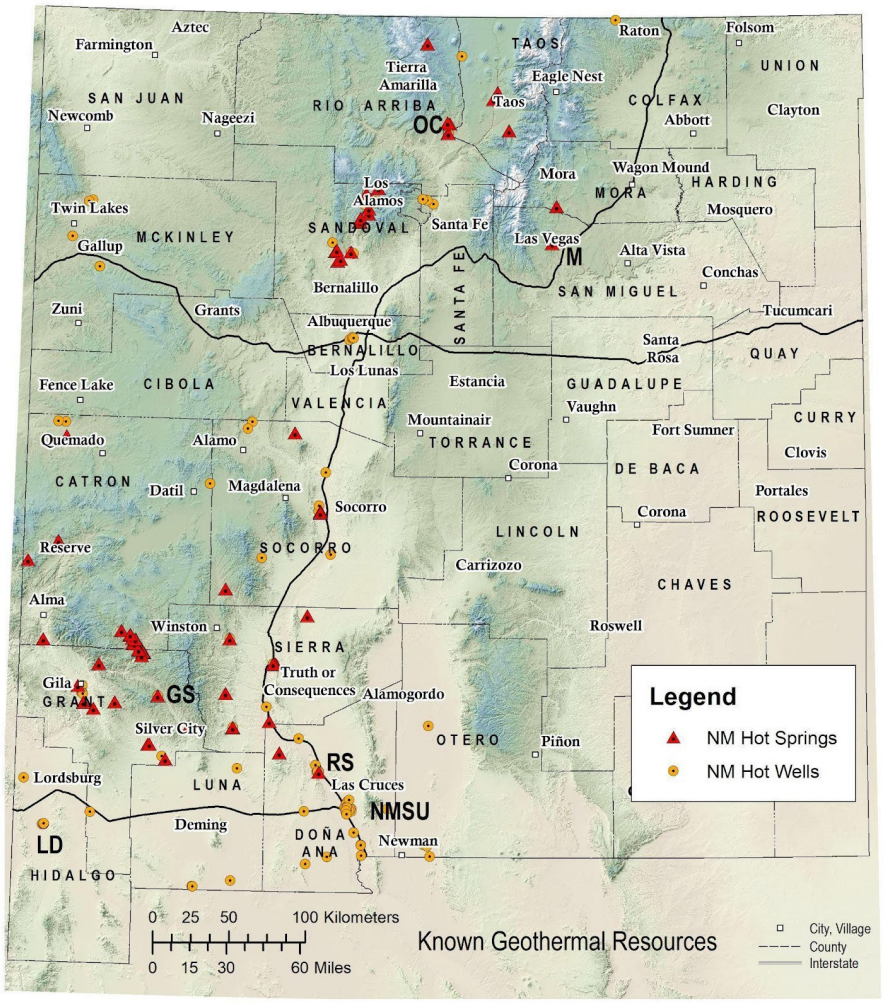

Figure 3.3. *Locations of hot springs and wells with temperatures above 30°C (86°F) in New Mexico. M = Montezuma Hot Springs. OC = Ojo Caliente. RS = Radium Springs. GS = Gila Hot Springs. LD = Lightning Dock. NMSU = New Mexico State University.* Source: *Shari Kelley.*

was built by Cyrq in 2013. The original plant was replaced with a new, more efficient 10 megawatt electric power plant that went online in 2018. Zanskar purchased the property from Cyrq in 2024 and drilled a successful new step-out well in 2025. The geologic setting for Lightning Dock is described in more detail later in the report.

Now, with the expansion of modern horizontal drilling technologies into geothermal fields that use concepts derived from the shale revolution in the oil and gas industry, **the entire spectrum of Earth's heat—from low temperatures needed for heating and cooling buildings via ground source heat pumps to intermediate temperatures for direct-use applications to higher temperatures for producing electricity from hydrothermal systems (also called conventional systems), engineered systems, and advanced systems—is available in New Mexico.**

As discussed later in this chapter, hydrothermal geothermal systems in New Mexico are commonly associated with fractured basement rocks, faults, and juxtaposition of aquitards and aquifers across faults. Conceptual models for these systems are fairly well established (see "Geothermal Resources in New Mexico" section). Proterozoic rocks in parts of the state have been intensely fractured by mountain-building events during late Pennsylvanian compression (Ancestral Rocky Mountains), late Jurassic to early Cretaceous extension (Bisbee Basin), late Cretaceous to Paleogene compression (Laramide), and middle to late Cenozoic extension (Rio Grande rift and Basin and Range). The Proterozoic metavolcanic, metasedimentary, and plutonic rocks that form the basement of New Mexico have variable capacities to fracture. For example, brittle rocks such as plutonic rocks and quartzite

fracture more readily than metamorphic schist. Part of the reason that recent engineered geothermal system (EGS) development in Utah at the Frontier Observatory for Research in Geothermal Energy (FORGE) and Fervo sites has been so successful is because new horizontal wells are penetrating uniform rocks with sealed natural fractures that are not faulted, which improves drilling speed and reduces induced seismic risk.[22,23]

Nw exploration in New Mexico should focus on finding Proterozoic rocks like those in Utah that are ideal for next-generation geothermal technology development.

Figure 3.5 shows estimated depths to temperatures across the state. Across New Mexico, as explored in Chapter 4, "Geothermal Heating and Cooling," there are depths to temperatures that are good for uses such as heating of greenhouses and other direct-use applications (**Figure 3.5A**).

Yellow to red areas in **Figure 3.5B** indicate that favorable temperatures for electricity production can be reached at depths greater than or equal to 3,500 meters (close to 11,500 feet) in the southwestern corner of New Mexico. This depth is commonly reached via wells drilled by the

HISTORY OF LIGHTNING DOCK GEOTHERMAL RESOURCE AREA

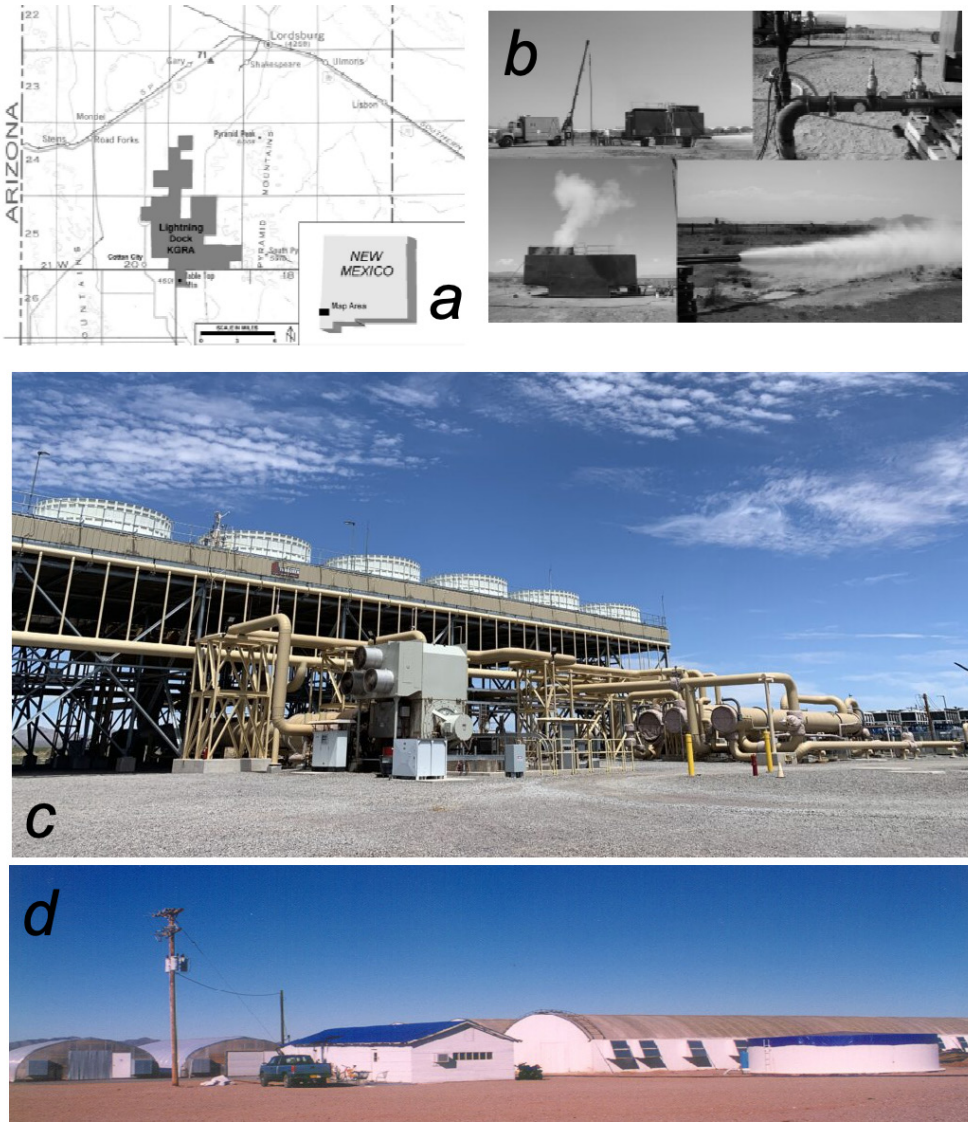

Figure 3.4. *(a) Location of the Lightning Dock geothermal area in southwestern New Mexico. (b) Images of early geothermal production test (1948) in which boiling conditions were encountered at depths of less than 30 meters. (c) The current binary geothermal power plant that became operational in 2018 and is now operated by Zanskar, Inc. (d) The Americulture tilapia geothermal heated aquaculture facility opened in 1995. Photos courtesy of Jim Witcher and from Elston et al. (1983).*

ESTIMATED DEPTHS AT TEMPERATURES

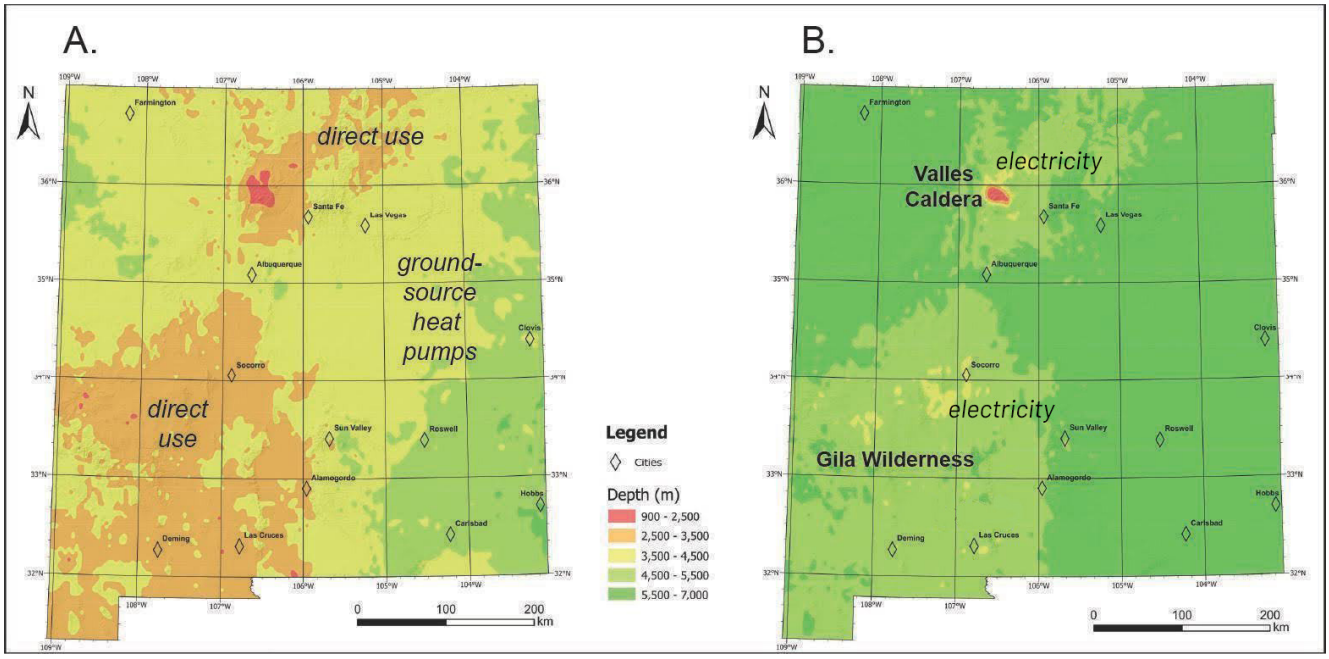

Figure 3.5. *(A) Estimated depth to at least 100°C (212°F), a temperature favorable for direct-use applications like heating a greenhouse. The red and orange areas are favorable for direct use. Ground source heat pumps are currently being installed statewide, particularly in new public schools and other public buildings. (B) Estimated depth to at least 150°C (302°F), a favorable temperature for producing electric power using a binary power plant. The red to yellow areas are favorable for electricity development, and the darker green areas are less favorable.* Source: Aljubran, M. J., & Horne, R. N. (2024). Thermal Earth model for the conterminous United States using an interpolative physics-informed graph neural network. *Geothermal Energy, 12*(1), 25. https://doi.org/10.1186/s40517-024-00304-7

oil and gas community. Southwestern, south-central, and north-central New Mexico and the Raton Basin in the northeastern part of the state have high electricity potential. The red areas on **Figure 3.5B** suggest favorable temperatures can be reached at depths of about 2,500 meters (about 8,000 feet). However, factors other than temperatures must be considered when evaluating geothermal potential (permeability of basement, proximity to tectonic provinces, etc.). Additionally, two of the state's highest-potential geothermal sites are currently off-limits to development due to their federally protected status (Gila Wilderness and the Valles Caldera National Preserve).

GEOLOGIC OVERVIEW

The complex geologic evolution of New Mexico has influenced the location of shallow geothermal reservoirs that have been used in the past. Understanding that history will guide future exploration and development of geothermal resources in the state. In this chapter, we consider the state as divided into six physiographic provinces with distinctive yet common geologic histories and geothermal resource potential (**Figure 3.6**): the Colorado Plateau, which includes the San Juan Basin in northwestern New Mexico; the Southern Rocky Mountains in north-central New Mexico; the extensional Rio Grande rift basins and adjacent mountains that occupy most of the central part of New Mexico; the Southern High Plains region that includes the Raton Basin in the northeast and the Permian and Delaware Basins in the southeastern parts of the state; the Southern Basin and Range, an extensional province in southwestern New Mexico; and the Eocene to Oligocene Mogollon-Datil volcanic field. The San Juan, Raton, and Delaware Basins are important oil- and gas-producing regions in New Mexico. The San Juan and Raton Basins and the Southern Rocky Mountains

SIX PHYSIOGRAPHIC PROVINCES IN NEW MEXICO

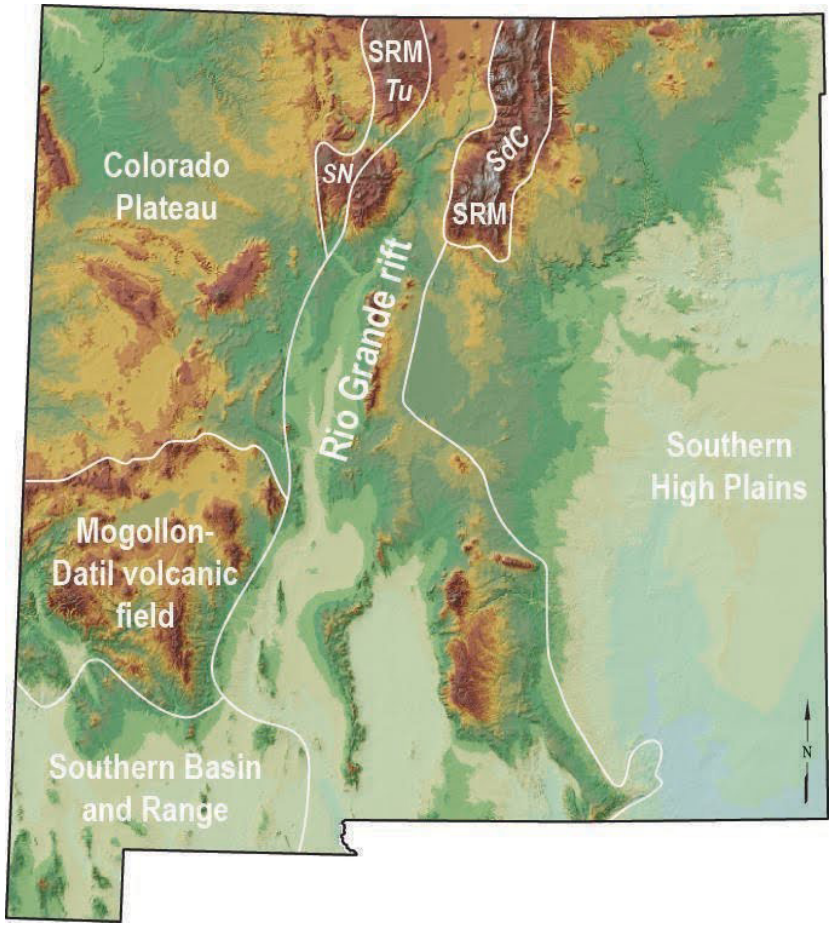

Figure 3.6. *Six physiographic provinces in New Mexico. SRM = Southern Rocky Mountains; SdC = Sangre de Cristo Mountains; Tu = Tusas Mountains; SN = Sierra Nacimiento. Source: Shari Kelley.*

formed starting about 75 million years ago during compressional Laramide deformation. The Delaware Basin formed during Permian time.

The Colorado Plateau is a relatively undeformed region that is occasionally interrupted by sharp monoclines and gentle folds. The Southern Rocky Mountains include the Sangre de Cristo and Tusas Mountains and the Sierra Nacimiento (**see Figure 3.6**); these three high-elevation ranges are cored by Proterozoic basement and serve as important sources of groundwater recharge in northern New Mexico. The High Plains occupy the region between tectonically active areas to the west and the tectonically quiescent mid-continent to the east. Narrow ranges bounded by normal faults that are separated by basins filled with sedimentary deposits derived from the adjacent highlands characterize both the Rio Grande rift and the Southern Basin and Range provinces. The basins between the ranges tend to be deeper in the Rio Grande rift than in the Southern Basin and Range, and the number of Quaternary faults and youthful volcanic fields (<1 million years old) is higher within the rift. The Mogollon-Datil volcanic field is an erosional remnant of an extensive volcanic highland formed by multiple andesitic volcanic and rhyolitic caldera eruptions 40 to 25 million years ago that was subsequently faulted during basin and range extension.[24] Extension in the rift began 30 to 25 million years ago, with activity generally waning at 10 million years ago. Local extension has continued into the Pleistocene and Holocene.[25] GPS measurements indicate that the rift is still extending at a very slow rate of between 1 millimeter and 2 millimeters per year.[26] Extension in the Southern Basin and Range peaked in the Miocene, with minor extension continuing into the Quaternary. Most previous geothermal exploration efforts in New Mexico have focused on the extensional terrains of the Rio Grande rift and Southern Basin and Range provinces.

GENERALIZED MAP OF RIFT AND PETROLEUM BASINS

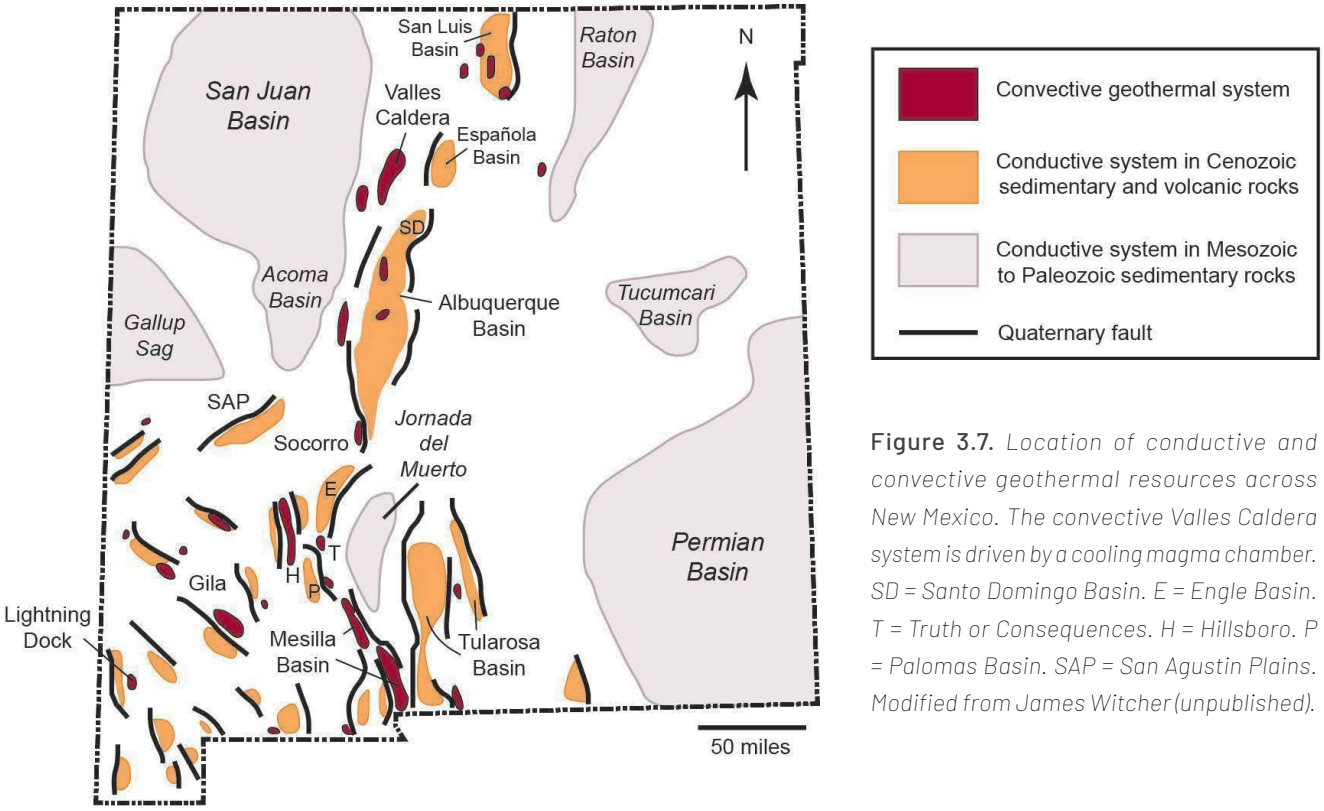

Figure 3.7. *Location of conductive and convective geothermal resources across New Mexico. The convective Valles Caldera system is driven by a cooling magma chamber. SD = Santo Domingo Basin. E = Engle Basin. T = Truth or Consequences. H = Hillsboro. P = Palomas Basin. SAP = San Agustin Plains. Modified from James Witcher (unpublished).*

GEOTHERMAL RESOURCES IN NEW MEXICO

New Mexico hosts three types of geothermal resources: magmatic, conductive, and convective (**Figure 3.7**). Chapter 1 explains the differences in each of these resources. Geothermal heat is concentrated near the Earth's surface in places where volcanic activity has recently occurred or is actively happening. Active faulting enhances geothermal potential by convectively bringing hot water toward the surface.

The only magmatically heated geothermal system in New Mexico is underneath the Valles Caldera in the Jemez Mountains volcanic field in north-central New Mexico. This volcanic field has been active since about 14 million years ago, culminating with two massive caldera-forming eruptions at 1.6 million (Toledo Caldera) and 1.2 million years ago (Valles Caldera). Immediately after the formation of the Valles Caldera, remaining magma pushed up the floor of the caldera, creating a dense fracture network on the resurgent dome, which hosts the modern geothermal system. Post-caldera ring-fracture rhyolite domes were emplaced between 1.23 million and 0.5 million years ago. The two most recent ring-fracture eruptions occurred at 74,000 and 69,000 years ago along the southwestern margin of the ring-fracture system.[27]

Numerous deep-drilling projects that accompanied geothermal exploration in the Jemez Mountains in the 1970s to mid-1990s illuminate subsurface stratigraphic relationships and thermal conditions beneath the western and central caldera (**Figure 3.8**). Unocal drilled 24 deep exploration wells into the resurgent dome, encountering temperatures of between 250°C and 300°C (482°F-572°F). The deepest industry well was 3.2 kilometers deep and was in the Proterozoic basement at total depth.[28] Three deep research boreholes (up to 1762 meters deep; maximum temperatures of 200°C [392°F]) drilled on the west side of the caldera that were supported by the

GEOLOGIC MAP AND EAST-WEST CROSS-SECTION OF THE VALLES CALDERA

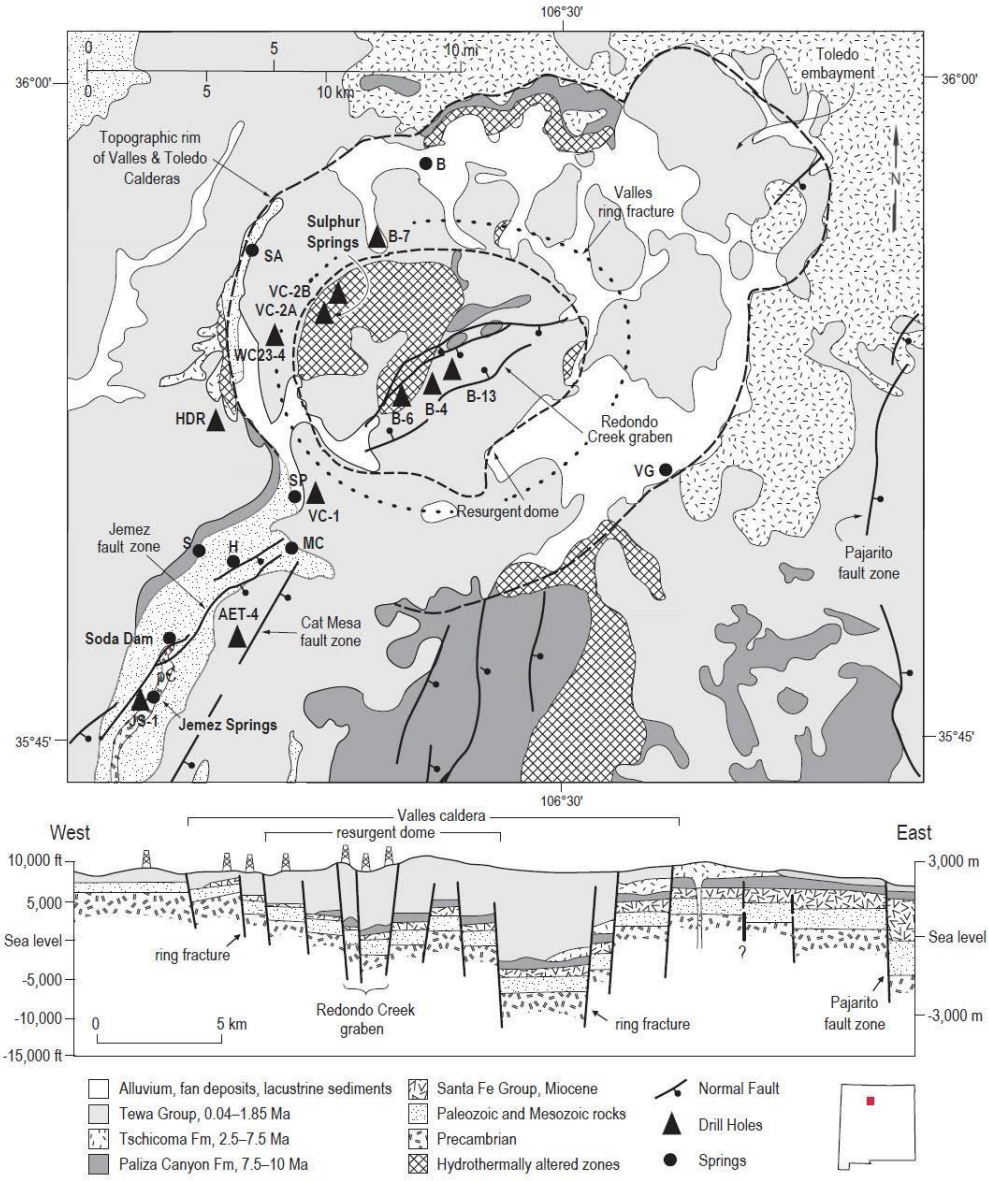

Figure 3.8. *Geologic map and east-west cross-section of the Valles Caldera.* Source: Goff, F., & Goff, C.J. (2017). *Energy and mineral resources of New Mexico: Overview of the Valles caldera (Baca) geothermal system.* New Mexico Bureau of Geology and Mineral Resources. https://doi.org/10.58799/M-50F

U.S. Continental Scientific Drilling Program provided important insights into intracaldera stratigraphy and the temperatures, alteration, and mineralization associated with the hydrothermal system.[29,30,31,32]

Several hot and warm springs (89°F–165°F, or 74°C–32°C)[33] in Cañon de San Diego southwest of the margin of the caldera are associated with an outflow plume from the caldera (**Figure 3.9**). In addition, the stratigraphy and structure of the southwestern topographic rim of the caldera were characterized to depths of 4.5 kilometers during the hot dry rock experiment.[34,35] Learnings from that experiment have guided the vast improvements in developing EGS in recent years at FORGE in Utah.[36,37,38] Because this system is within the Valles Caldera National Preserve, this resource has been retired from development since 2006.

Conductive resources are typically located in Laramide and Permian oil-producing sedimentary basins that have

undergone little tectonic upheaval since the formation of the basins (**Figure 3.7**). These basins include the San Juan, Permian/Delaware, and Raton basins. In these settings, the average geothermal gradient (typically 16°C–37°C/kilometer [0.9°F–2.0°F/100 feet]) shows the increasing temperatures with depth (**Figure 3.10**). **Figure 3.10** illustrates the uncorrected bottom-hole temperature measurements in petroleum wells in the three major conductive basins in New Mexico. The Raton Basin in northeast New Mexico lies in proximity to the Jemez Lineament and thus is the warmest basin at relatively shallow depths in the state. At three kilometers deep, the temperature within sandstone and limestone reservoirs in the Raton Basin can reach 212°F (100°C). The groundwater in these basins is typically saline (three times the salinity of seawater; greater than 100 parts per thousand). Provided that these sandstone and limestones are permeable, "dry" petroleum wells could potentially be repurposed to be geothermal wells. However, sedimentary formations with a temperature of about 302°F (150°C) would need to be pumped at a rate of at least 4,000 cubic meters per day (about 800 of gallons per minute) to generate about 1.3 megawatts of electricity using a binary power plant.[39] Few oil wells have the capacity or the permeability to accommodate such flow rates.

Amagmatic geothermal systems are common in New Mexico along the Rio Grande rift, where the Earth's crust is extending and thinning and the hot mantle rocks move closer to the surface as the crust thins. These systems are also widespread in the Southern Basin and Range. The multiple tectonic events that have affected New Mexico (discussed in the previous section) have fractured the crystalline basement rocks beneath the Paleozoic-Mesozoic and rift-fill sedimentary strata, promoting groundwater circulation to depths of 6–8

VALLES CALDERA MAGMATIC GEOTHERMAL SYSTEM

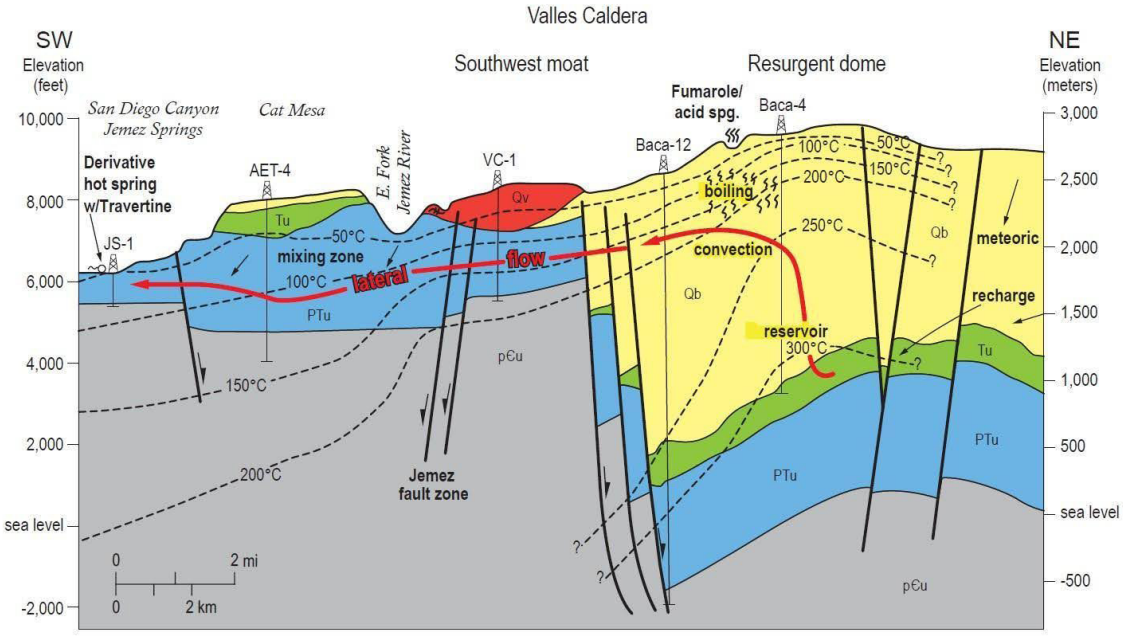

Figure 3.9. *The Valles Caldera is the only example of a magmatic geothermal system in New Mexico. pCu = Proterozoic basement. PTu = Paleozoic and Triassic sedimentary rocks. Tu = Tertiary sedimentary and volcanic rocks. Qb = Bandelier Tuff. Qv = ring fracture rhyolite and associated sedimentary rocks. Fluids in the caldera are heated by a moribund magma chamber in the southwest corner of the caldera. The water then flows southwest along northeast-striking faults (Jemez fault zone; Figure 3.8), paralleling Cañon de San Diego, and traveling primarily in fractured Pennsylvanian limestone.* Source: Goff, F., & Goff, C.J. (2017). *Energy and mineral resources of New Mexico: Overview of the Valles caldera (Baca) geothermal system.* New Mexico Bureau of Geology and Mineral Resources. https://doi.org/10.58799/M-50F

BOTTOM-HOLE TEMPERATURES IN NEW MEXICO BASINS

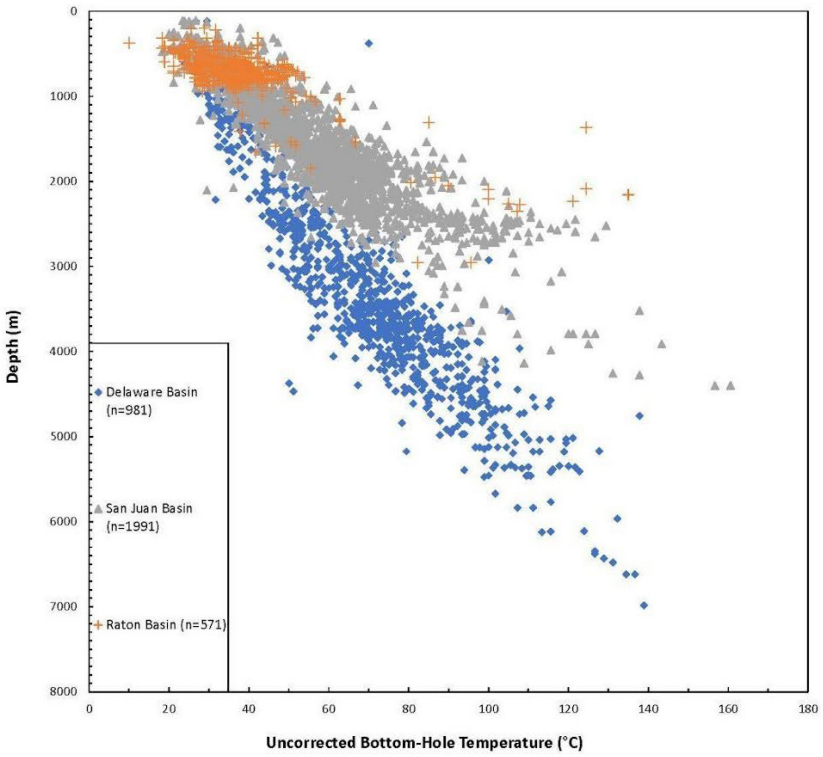

Figure 3.10. *Uncorrected bottom-hole temperature measurements for the conductive, oil-producing Raton, San Juan, and Permian Basins in New Mexico (New Mexico Bureau of Geology and Mineral Resources Geothermal Database). The gradients were calculated using the surface intercept of mean annual surface temperature from the NOAA 2006–2020 data set. Raton Basin: 2°F/100 ft (37°C/km) with 48.2°F (9°C) surface temperature intercept (9 stations); San Juan Basin: 1.6°F/100 ft (29°C/km) with 50°F (10°C) surface temperature intercept (16 stations); Delaware Basin: 0.9°F/100 ft (16°C/km) with 60°F (16°C) surface temperature intercept (10 stations).* Source: Palecki, M., Durre, I., Applequist, S., Arguez, A., & Lawrimore, J. (2021). *U.S. climate normals 2020: U.S. hourly climate normals (1991–2020).* NOAA National Centers for Environmental Information. Retrieved March 6, 2025, from https://www.ncei.noaa.gov/metadata/geoportal/rest/metadata/item/gov.noaa.ncdc:C01622/html

kilometers.[40,41] Convective amagmatic geothermal systems form as a consequence of two conditions: (i) There is significant (greater than 0.5 meters per year)[42] groundwater recharge in mountainous terrains; and (ii) the permeability of fractured crystalline basement rocks is high enough to result in flow rates on the order of meters per year. Permeability is typically represented in units of square meters by hydrogeologists and milliDarcies (mD) by the petroleum industry. Fractured bedrock or sandstone with a permeability of 1,000 mD (equivalent to 10^{-12} m^2) is considered by petroleum engineers to be an excellent oil reservoir.[43] Assuming that Snow's law[44] is valid, a permeability of this magnitude can result from a distributed fracture network with a spacing of 100 millimeters. A pumping test carried out in the crystalline basement beneath the Truth or Consequences hot springs district at a depth of about 70 meters below the land surface had a permeability of 3.6×10^{-10} m^2 (36,000 mD) (Unpublished data collected by the second author.). Calibrated hydrothermal models suggest that the average crystalline basement rocks at 6 kilometers have a permeability of about 10^{-14} m^2 to 10^{-13} m^2.[45,46]

Figure 3.11 illustrates a gravity-driven hydrothermal system that redistributes heat across a regional groundwater flow system in the vicinity of Socorro (**Figures 3.2** and **3.3**). Groundwater flow within a gravity-driven geothermal system is controlled by water table topographic gradients between the mountains and lowlands. The water table elevation drop between the Magdalena Mountains located west of Socorro and the Rio Grande in **Figure 3.11** is about 500 meters. As groundwater flows to depths of 5 kilometers or more, groundwater temperatures increase. Concentrations of dissolved silica and other cations suggest that fluid temperatures exceed 120°C (248°F) at these depths. The distribution of temperatures shown in **Figure 3.11** is based on temperature profiles from Barroll and Reiter[47] at shallow levels and from a hydrothermal model of the area west of Socorro at depth.[48] Due to vigorous downward circulation of cold meteoric water proximal to the Magdalena Mountains, which are in the groundwater recharge zone, temperature isotherms are deflected downward, reducing thermal gradients in wells at high elevations (see temperature profiles for Wells #17 and #48 in **Figure 3.11**). In the lowlands,

CONCEPTUAL MODEL OF AN AMAGMATIC GEOTHERMAL SYSTEM

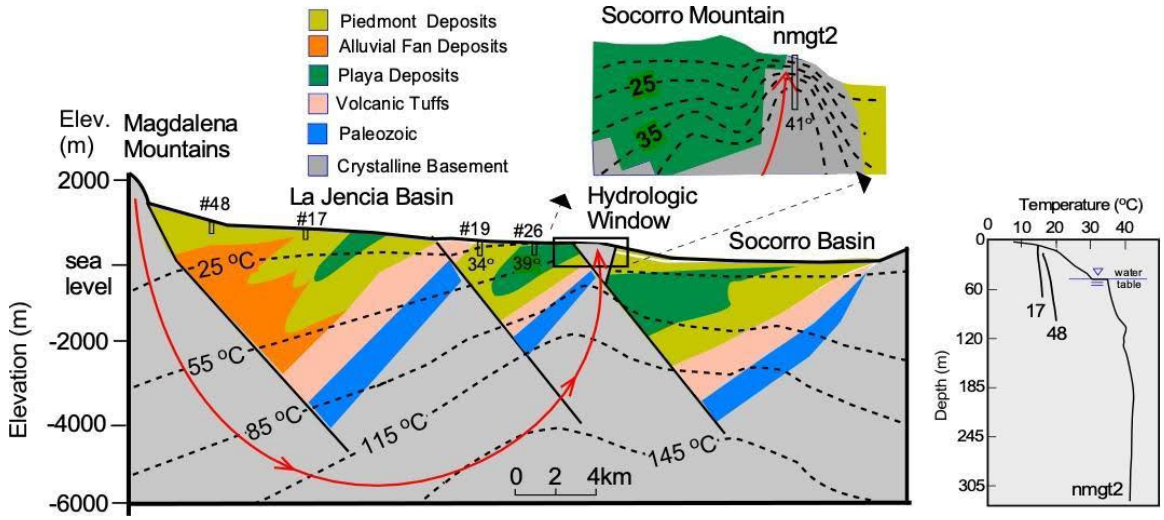

Figure 3.11. *Conceptual model of an amagmatic geothermal system. New Mexico has abundant convective geothermal resources along the Rio Grande Valley. This figure illustrates a gravity-driven convective geothermal model in a rift-flank setting with possible flow paths shown as red arrows.* Adapted from Barroll, M. W., & Reiter, M. (1990). Analysis of the Socorro hydrogeothermal system: Central New Mexico. *Journal of Geophysical Research, 95*, 21949–21964. https://doi.org/10.1029/JB095iB13p21949; Mailloux, B. J., Person, M., Kelley, S., Dunbar, N., Cather, S., Strayer, L., & Hudleston, P. (1999). Tectonic controls on the hydrogeology of the Rio Grande Rift, New Mexico. *Water Resources Research, 35*(9), 2641–2659. https://doi.org/10.1029/1999WR900110

EXAMPLES OF HYDROGEOLOGIC WINDOWS

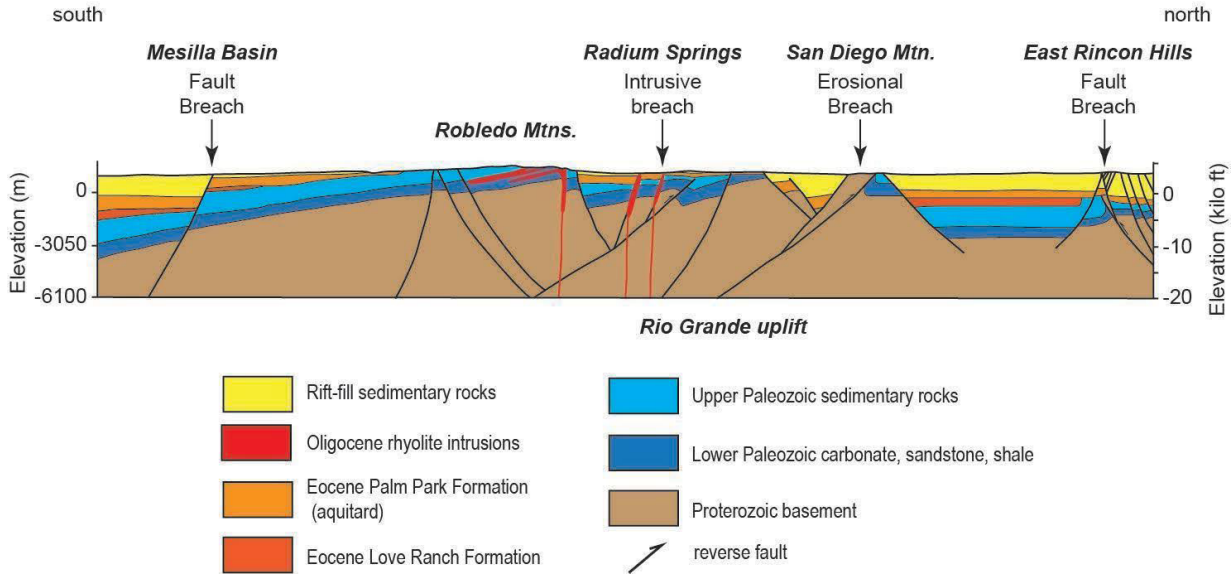

Figure 3.12. *Different types of hydrologic windows through the volcaniclastic Palm Park Formation aquitard in southern New Mexico, including fault, erosional, and intrusive windows.* Adapted from Seager, W. R., Hawley, J. W., Kottlowski, F. E., & Kelley, S. A. (1987). *Geology of east half of the Las Cruces and northeast El Paso 1 degree by 2 degree sheets* (GM-57: 1:250,000). New Mexico Bureau of Mines and Mineral Resources.

SUBCROP MAP AND MACHINE LEARNING RESULTS

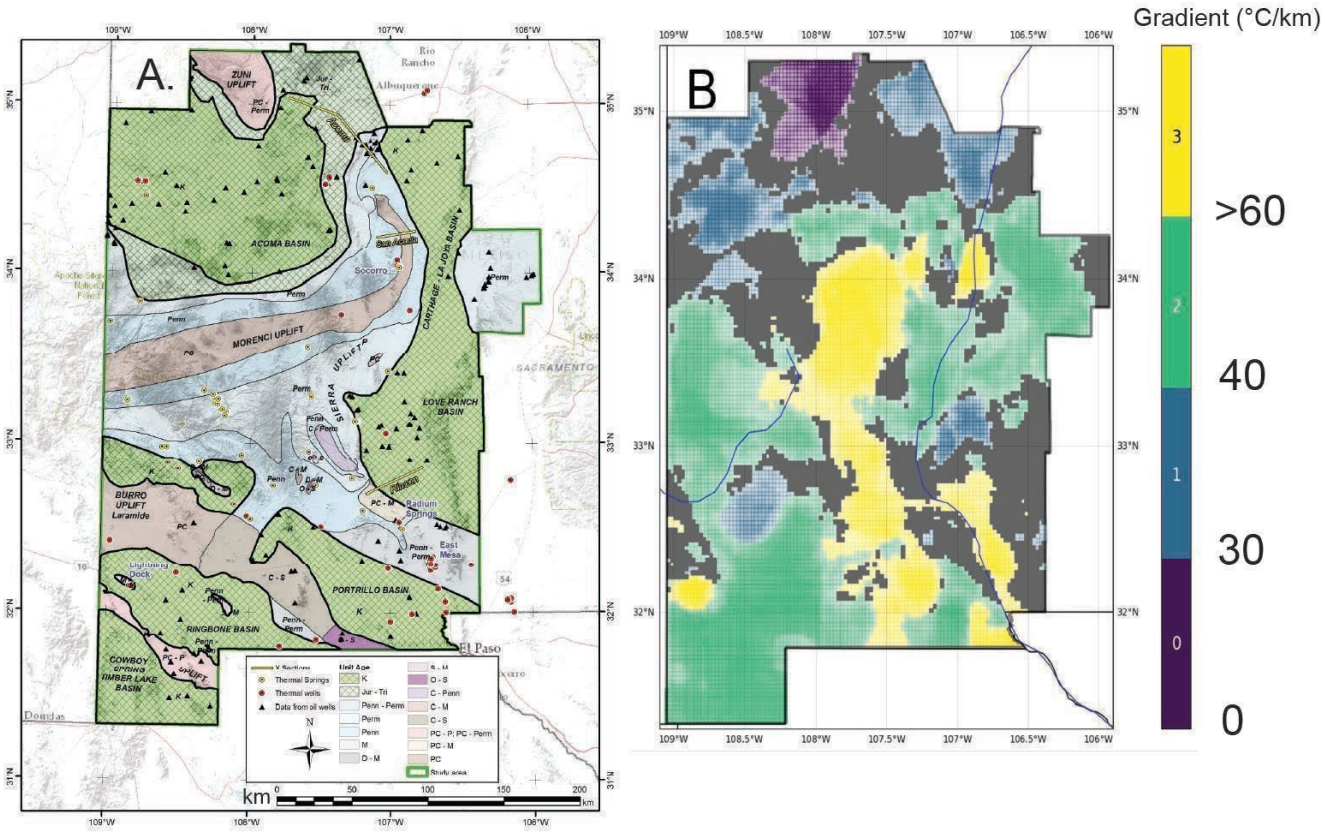

Figure 3.13. *(A) subcrop map of southwestern New Mexico depicting the landscape at the end of Laramide deformation, just prior to deposition of Eocene to Oligocene volcanic and volcaniclastic rocks from the Mogollon-Datil volcanic field. (Bielicki et al., 2015). The various colors represent the rock unit or units that lie below the unconformity. The northwest-striking fabric of southwestern New Mexico is inherited in part from Jurassic rifting associated with the formation of the Bisbee Basin (Lawton, 2000). (B) ensemble prediction map of geothermal gradients produced by supervised machine learning (Holmes and Fournier, 2022). The gray areas highlight areas of high uncertainty.* Sources: Bielicki, J., Blackwell, D., Harp, D., Karra, S., Kelley, R., Kelley, S., Middleton, R., Pepin, J., Person, M., Sutula, G., & Witcher, J. (2015). *Hydrogeologic windows: Regional signature detection for blind and traditional geothermal Play Fairways applied to Southwestern New Mexico* [Data set]. Geothermal Data Repository. Los Alamos National Laboratory. https://gdr.openei.org/submissions/611; Lawton, T. F. (2000). Inversion of late Jurassic-early Cretaceous extensional faults of the Bisbee Basin, southeastern Arizona and southwestern New Mexico. *New Mexico Geological Society Guidebook, 51,* 95–102. https://doi.org/10.56577/FFC-51.95; Holmes, R. C., & Fournier, A. (2022). Machine learning-enhanced Play Fairway analysis for uncertainty characterization and decision support in geothermal exploration. *Energies, 15*(5), 1929. https://doi.org/10.3390/en15051929

heated groundwater flows upward before discharging at the surface or to the water table. Within the Socorro Basin, this is facilitated by the absence of confining units such as playa deposits (**Figure 3.11**). Upward flow of groundwater in the discharge area transports heat toward the surface, resulting in an amagmatic convective geothermal resource. Well nmgt2 has a temperature of about 41°C (106°F) near the water table.

The Socorro system is an excellent example of how the juxtaposition of aquitards and aquifers across faults and disruption of aquitards by erosion and faulting can control discharge in hydrothermal systems. The concept of hydrogeologic windows was first described by Witcher et al.[49] The hydrologic window within the Socorro Basin, as exemplified in **Figure 3.11**, formed as a result of faulting and erosional processes occurring

over millions of years.[50] The window provides a pathway of least resistance for groundwater discharge. Although the sediments overlying the crystalline basement can host permeable aquifers, the overlying deposits also contain regionally extensive clay or shale formations that can block upward flow. A breach related to faulting and erosion is only one type of a hydrologic window (**Figure 3.12**).[51] In southern New Mexico, a regionally extensive andesite debris-flow deposit called the Palm Park Formation acts as an aquitard that covers potential blind geothermal resources developed in fractured basement rocks and Paleozoic limestone.[52,53] Hot springs and shallow geothermal systems occur in fractured volcanic dikes that act as hydrologic windows, as well as in other areas where the Palm Park aquitard is breached (**Figure 3.12**).

An exploration map created as part of a Department of Energy–funded Play Fairway project[54] depicting regions where hydrologic windows may exist below aquitards in the subsurface is shown in **Figure 3.13A** for southwestern New Mexico. This map was first presented by Witcher et al. and many of the concepts used in the 2015 Play Fairway analysis are described in the 1988 paper.[55] Rock units below the Eocene-Oligocene volcaniclastic debris flows and lahars (aquitards) mentioned earlier were identified, and the landscape developed on Laramide structures preserved beneath the unconformity in southwestern New Mexico was mapped. Cretaceous basins filled with intercalated shales (e.g., Mancos Shale) or fine-grained tight sandstones that act as aquitards are shown in the green-cross hatched pattern in **Figure 3.13A**. These areas are not likely to have post-Laramide windows, but deeper windows related to earlier Ancestral Rocky Mountain deformation may exist beneath the Cretaceous rocks. Possible hydrogeologic windows in the northwest-striking Proterozoic- to Paleozoic-cored Laramide highlands are shown in shades of brown, pink, and blue. Areas where a Devonian shale aquitard has been stripped from Ordovician to Silurian karstic carbonate aquifers are among the best targets for geothermal exploration in the state.

Data collected as part of the 2015 Play Fairway project were analyzed with machine-learning algorithms to better understand which geologic, geochemical, and geophysical parameters have high correlation in known geothermal systems, as well as to quantify parameter uncertainty.[56,57] These studies consider 18 to 25 independent parameters related to geothermal prospectivity. The unsupervised machine-learning algorithm used by Vesselinov and colleagues identified five geographic areas that have a unique set of dominant data attributes.[58] The key data attribute used to distinguish between low-temperature (less than 194°F, or 90°C) and medium-temperature (194°F–302°F, or 90°C–150°C) hydrothermal systems was the silica geothermometer, a geochemical proxy for reservoir temperature. The two medium-temperature systems are in the northern part of the Mogollon-Datil volcanic field and in the Rio Grande rift near Las Cruces. Interestingly, Swanberg came to similar conclusions primarily using silica geothermometry.[59] Holmes and Fournier used four different types of machine-learning supervised algorithms to evaluate three types of data uncertainty related to the choice of model, errors in the parameters estimated by the models, and input data preparation.[60] The results from the four models were combined to form a weighted-average ensemble model (**Figure 3.13B**). Holmes and Fournier note that the analysis of uncertainty can be used to find areas where the four models do not agree, which can be used to target additional data collection.[61]

The effects of convective heat transfer are illustrated in the heat flow map of New Mexico (**Figure 3.14**). In the northern part of New Mexico, the Valles Caldera (VC) stands out as a geothermal anomaly. In the Albuquerque Basin (A), heat flow is lowest along the eastern flanks of the rift due to convective anomalies associated with meteoric "cold" groundwater recharge. In the center and along the western flank of the rift, heat flow is elevated. This is likely due to convective warming. Within the Socorro-La Jencia basin (S), a classic pattern of low heat flow (17 milliwatts per square meter) in the La Jencia Basin adjacent to the Magdalena Mountains in the region of groundwater recharge occurs. At the base of the Socorro Mountain block, heat flow reaches 490 milliwatts per square meter in a hydrologic window, where the crystalline basement crops out at the land surface. The high heat-flow values such as those observed in the Socorro geothermal system are deceiving. High and low shallow temperature gradients beneath the land surface are due to convective upwelling and downwelling.

NEW MEXICO HEAT FLOW MAP IN MILLIWATTS PER SQUARE METER

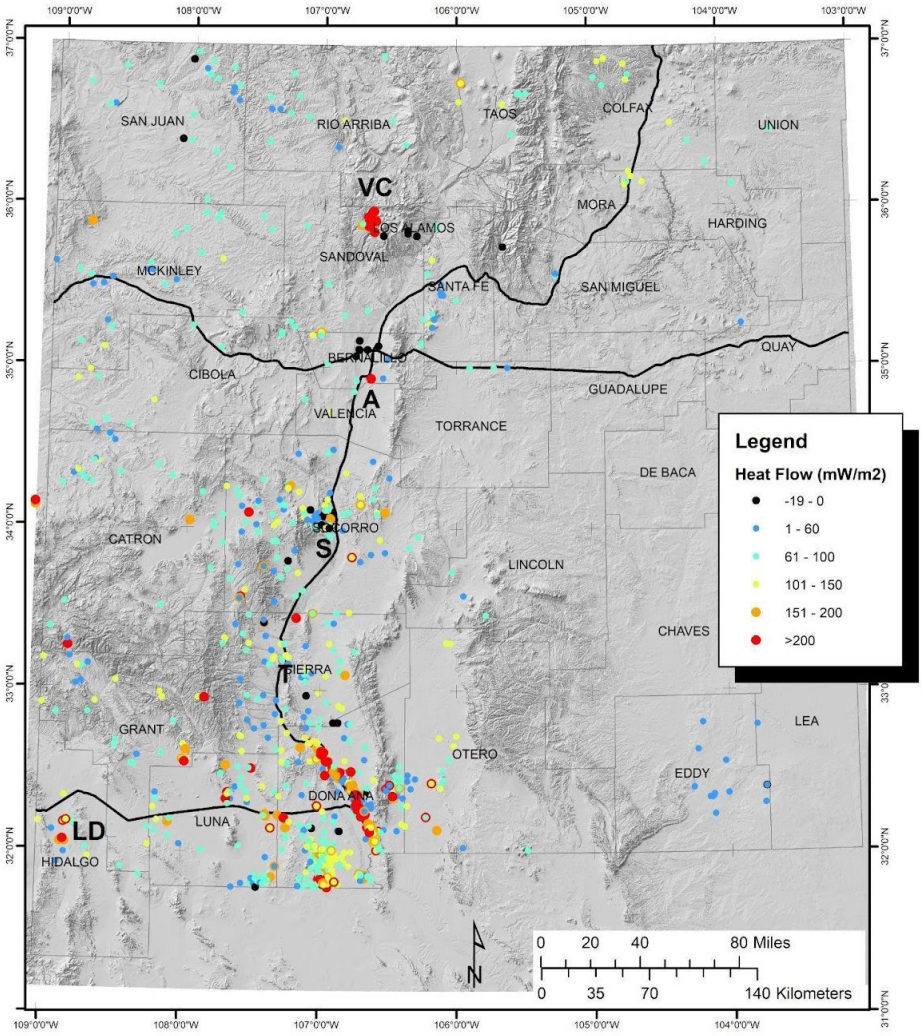

Figure 3.14. *New Mexico heat flow map in mW/m²; data compiled from published and industry data sources. VC = Valles Caldera, A = Albuquerque Basin, S = Socorro Basin, T = Truth or Consequences, LD = Lightning Dock. Source: Shari Kelley.*

Temperatures within the discharge area do not exceed 41°C (106°F). Beneath this area, isothermal conditions exist. The same is true for the Truth or Consequences geothermal system. The crystalline basement is exposed just below the land surface. Measured temperatures do not exceed 109°F (43°C). Further to the southwest in the "bootheel" region of New Mexico at Lightning Dock, temperatures approach boiling conditions. Here, discharge occurs along a fault zone. Lightning Dock discharge is likely focused in a narrow outflow zone associated with the fault, allowing for higher temperatures. Within the Truth or Consequences and Socorro geothermal systems, upflow is more diffuse because flow is less restricted to a narrow zone.

DETAILED ANALYSIS

Due to page constraints, only a few geothermal areas are discussed in detail in this chapter. Many areas in New Mexico do not have the thermal and geophysical data needed for rigorous analysis of geothermal potential. The examples described here are areas with significant, but not complete, quantities of useful data. The geothermal potential of the Socorro magma body at the intersection of the southern Albuquerque and northern Socorro Basins; the San Agustin, Engle, and Mesilla Basins; and the Rincon system is discussed. Lightning Dock in the southern Basin and Range is briefly described. We close with a discussion of the geothermal potential of the three conductive petroleum basins with large amounts of stratigraphic and bottom-hole temperature data.

Socorro Magma Body

The Socorro magma body is considered to be the largest active magma chamber in the U.S. continental crust (**Figure 3.15**).[62,63] This unique feature is located between the southern terminus of the Albuquerque Basin and northern Socorro Basin (**Figure 3.2**). Seismic data suggests that the intrusion is at a depth of about 19 kilometers.[64,65] The footprint of the body is about 3,400 square kilometers. The sill has a thickness of only 100 to 150 meters.[66,67] Williams and colleagues report evidence of mantle-derived helium associated with a saline spring near the town of San Acacia, located about 20 kilometers north of Socorro.[68] The magma body is associated with a region of dome-like uplift detected by Interferometric Synthetic Aperture Radar (InSAR) that is presently rising at a rate of between 2 millimeters and 3 millimeters per year.[69] The uplift is interpreted to be the result of thermal expansion and magma injection into the sill.[70] Studies of the deformation of terrace deposits, the deformation of the railroad grade near the Rio Grande detected in the 1970s, and InSAR studies in the Socorro area indicate two episodes of inflation between 26,000 to 3,000 years ago and more modern inflation detected during the 1970s and continuing to the present day.[71] Swarms of earthquakes are common, and studies of the swarms can be used to distinguish between fluid-related swarms and fault-related swarms.[72,73] The largest event in the 2005 swarm studied by Stankova and colleagues[74] had a magnitude of 2.4 and the largest event in the 2009 swarm studied by Ruhl and colleagues[75] had a magnitude of 2.5.

Because there is no clear regional temperature anomaly at the surface, magma injection appears to occur episodically. Reiter and colleagues hypothesized that episodic magma injection with associated pressure increases could result in the observed seismic anomalies.[76] The regional heat flow above the Socorro magma body is about 90 milliwatts per square meter, indicating that the thermal regime related to sill emplacement at 19 kilometers at 1–3 million years ago has yet to reach the surface.[77,78] The only hint of hydrothermal fluid flow related to a possible geothermal upflow zone is a discharge temperature of 83.4°F (28.8°C) that was recorded at the San Acacia municipal well about 22 kilometers north of Socorro, near the southern Albuquerque Basin boundary;[79] the well is 164 meters deep.

SOCORRO MAGMA BODY AND SOCORRO SEISMIC ANOMALY

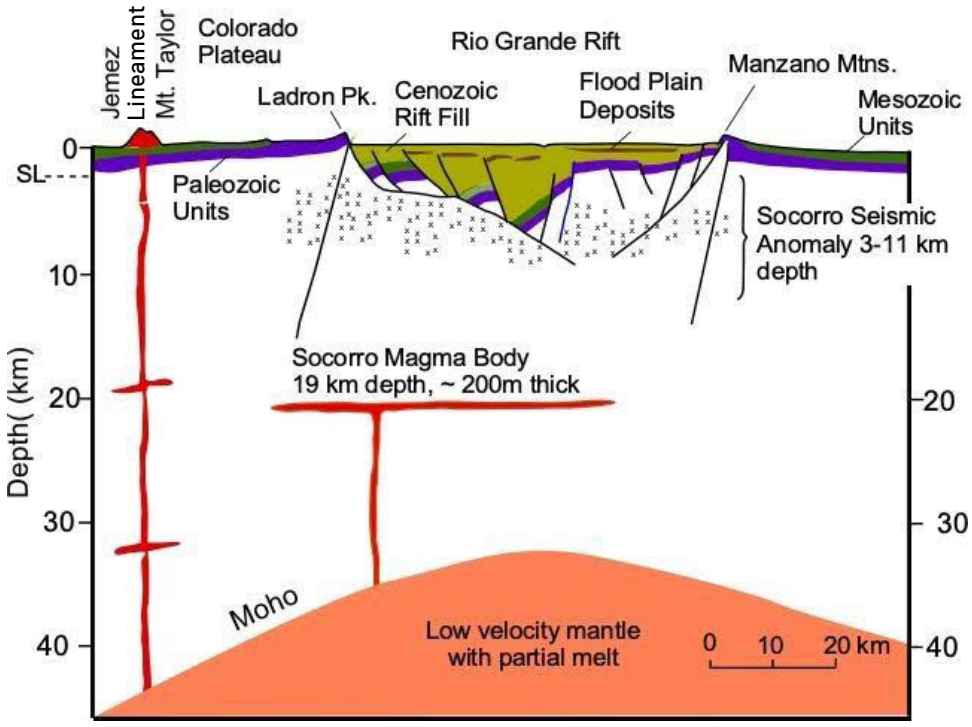

Figure 3.15. *General east-west cross-section across the Rio Grande rift showing the Socorro magma body and Socorro seismic anomaly near the southern Albuquerque Basin terminus. X=earthquakes.* Adapted from Williams, A. J., Crossey, L. J., Karlstrom, K. E., Newell, D., Person, M., & Woolsey, E. (2013). Hydrogeochemistry of the Middle Rio Grande aquifer system—Fluid mixing and salinization of the Rio Grande due to fault inputs. *Chemical Geology, 351*, 281–298. https://doi.org/10.1016/j.chemgeo.2013.05.029

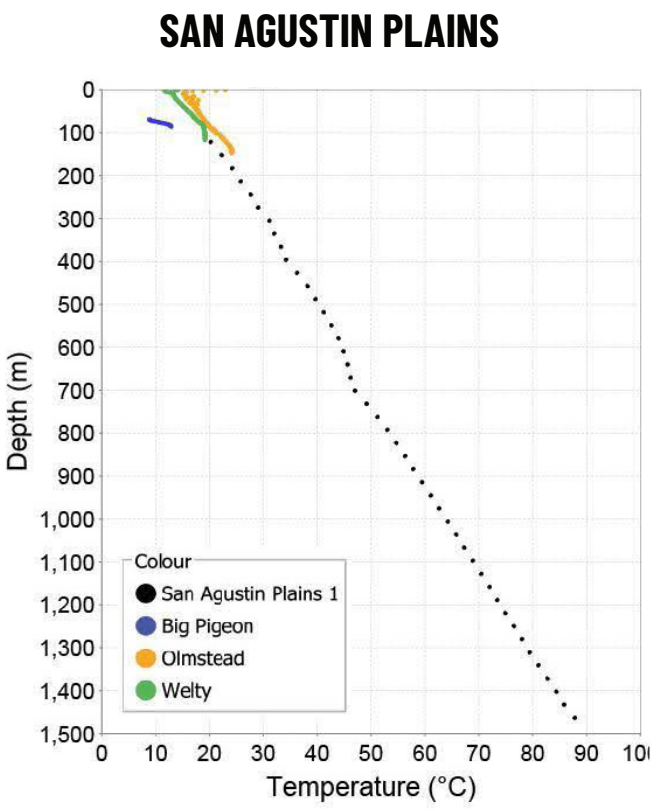

Figure 3.16. *Measured temperature-depth profiles from four wells from the San Agustin Plains. Source: Shari Kelley.*

San Agustin Plains

Reiter and colleagues[80] present the results of repeat temperature measurements in the upper part of Sun Oil Co. 1 San Agustin Plains (API 30-003-05002; SAP); the most recent log measured in December 1975 is shown by dotted line in **Figure 3.16.** This well encountered temperatures of 194°F (90°C) at 1500 meters. Geothermal gradient was calculated in three intervals in the well. The gradients range from 48.9°C/km (2.7°F/100 ft) to 59.9°C/km (3.3°F/100 ft). The average calculated heat flow is 73.2 milliwatts per square meter. This well penetrated Cenozoic tuff and volcaniclastic sediments to a depth of 2,016 meters, then penetrated Cretaceous, Triassic, Permian, and Pennsylvanian sections before bottoming in Proterozoic gneiss at 3,744 meters.

Several middle Cenozoic rhyolite intrusions were encountered during the drilling of this well; according to the driller's log, the thickest interval is 463 meters. The equilibrium temperature log of Reiter and colleagues[81] is in the Cenozoic section. The uncorrected bottom-hole temperature readings for the oil well are 280°F–309°F (138°C–154°C). Given the conductive nature of the geothermal gradient shown in **Figure 3.16**, this site might be attractive for the development of engineered geothermal systems, advanced geothermal systems, and other options.

Temperature logs in three shallow water wells (**Figure 3.16**) were measured and analyzed as part of the current investigation. Two of the wells have geothermal gradients that are similar to those encountered in the top of the deep oil well. The geothermal gradient in the Olmstead well is 67.4°C/km (3.7°F/100 ft) below the water table. The Welty log is located just north of the divide that separates the San Agustin Plains from the Alamosa Creek, a tributary of the Rio Grande. The geothermal gradient measured above the water table is about 3.3°F/100 ft (60°C/km), but the gradient is much lower below the water table due to influx of cold groundwater. The Big Pigeon well is in a recharge zone in the San Mateo Mountains, and thus the log records cold temperatures.

Engle Basin

The Engle Basin hosts the Truth or Consequences geothermal system.[82] A geologic cross-section extending from the recharge area in the San Mateo Mountains and Sierra Cuchillo eastward to the Rio Grande in the Truth or Consequences hot spring district is shown in **Figure 3.17.** The location of this cross-section is shown in **Figure 3.17A** (black line a to a') and is perpendicular to the regional water table elevation contours. The large fault in the middle of the cross-section is the Mud Springs fault, and the portion of the Engle Basin to the west of the fault is the Monticello graben. The broad Cuchillo Negro fault zone, which has Quaternary offset, lies to the west of the Mud Springs fault; Pepin reports a warm well (86°F, or 30°C) that is 262 meters deep along Alamosa Creek near the Cuchillo Negro fault zone.[83]

Mark Person and colleagues, with the support of town officials in Truth or Consequences, conducted a study to assess the sustainability of the geothermal system in light of increased development in the area.[84] Person and associates[85] and Pepin and colleagues[86] collected temperature-depth profiles in wells less than or equal to 25 meters deep in and around the Truth or

THERMAL MODEL AND MAGNETOTELLURIC DATA INTERPRETATION FOR THE TRUTH OR CONSEQUENCES GEOTHERMAL SYSTEM

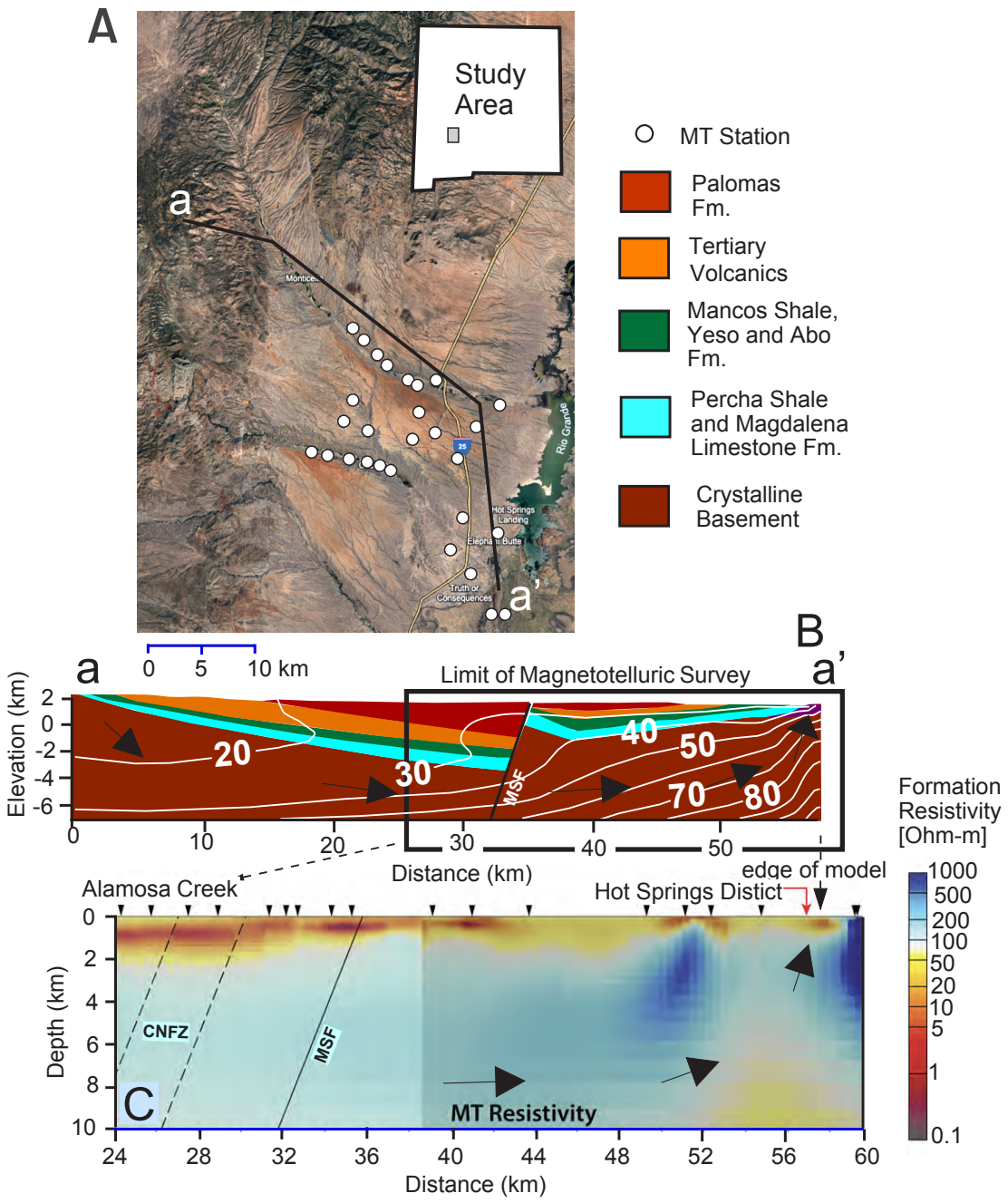

Figure 3.17. *(A) Location of magnetotelluric (MT) soundings and hydrothermal model within the Engle Basin and the northernmost Palomas Basin. (B) Simplified geologic cross-section. Solid black line shows location of MT survey and inversion (from Person et al., 2013). Temperature-depth contours calculated from the hydrothermal model are shown as white lines (°C). (C) MT inversion showing formation resistivity map. CNFZ = Cuchillo Negro fault zone. MSF = Mud Springs fault.* Sources: Pepin, J. (2018). *New approaches to geothermal resource exploration and characterization* [Doctoral dissertation]. New Mexico Institute of Mining and Technology; Person, M., Phillips, F., Kelley, S., Timmons, S., Pepin, J., Blom, L., Haar, K., & Murphy, M. (2013). *Assessment of the sustainability of geothermal development within the Truth or Consequences Hot-Springs District, New Mexico* (Open-file Report 551). New Mexico Bureau of Geology and Mineral Resources. https://doi.org/10.58799/OFR-551 *(from Pepin, 2018).*

Consequences hot springs district. Temperature-depth profiles were isothermal at depth with significant curvature near the water table, indicative of groundwater upflow. The maximum temperatures range from 30°C to 45°C (86°F–113°F). Pepin collected three-dimensional magnetotelluric data in portions of the Engle Basin and the northernmost Palomas Basin in Sierra County (**Figure 3.17C**).[87] The station spacing was between 2 kilometers and 5 kilometers (**Figure 3.17C**). A fence diagram showing the results of the three-dimensional MT inversion is presented in **Figure 3.17C**. At shallow depths, the Palomas Formation, within the Santa Fe Group, is conductive (less than 1 Ohm-meter) to depths of around 1.5 kilometers. The rift-fill sediments were deposited when the Engle Basin was hydrologically closed and include playa deposits, which likely accounts for the low formation resistivity at the top of the model. The subsurface becomes more resistive with depth, and at the base of the Paleozoic units, the resistivity has increased to about 200 Ohm-meters. Pepin interprets this region as containing relatively fresh groundwater (less than 0.5 parts per thousand total dissolved solids).[88] The transition between the crystalline basement and the lower Paleozoic units is not apparent, suggesting that the crystalline basement is highly fractured. The Paleozoic rocks include the basal Pennsylvanian limestone aquifer system. Below 2.5 kilometers, the subsurface beneath the Truth or Consequences hot spring district becomes more conductive with depth and commonly has resistivity values that are less than 100 Ohm-meters. Pepin interprets these values to indicate salinity buildup along the flow path through the crystalline basement.[89]

Person and colleagues[90] and Pepin[91] conclude that upward groundwater flow in the hot spring district has diminished since the study by Theis and associates,[92] that many of the wells drilled in the 1940s no longer exist or are in poor repair, and that buried faults compartmentalize the reservoirs beneath Truth or Consequences. The district has been closed to further development to ensure the system's sustainability.

TOPOGRAPHIC MAP OF JORNADA DEL MUERTO BASIN, HYDROGEOLOGIC CROSS-SECTION, AND SIMULATED TEMPERATURES

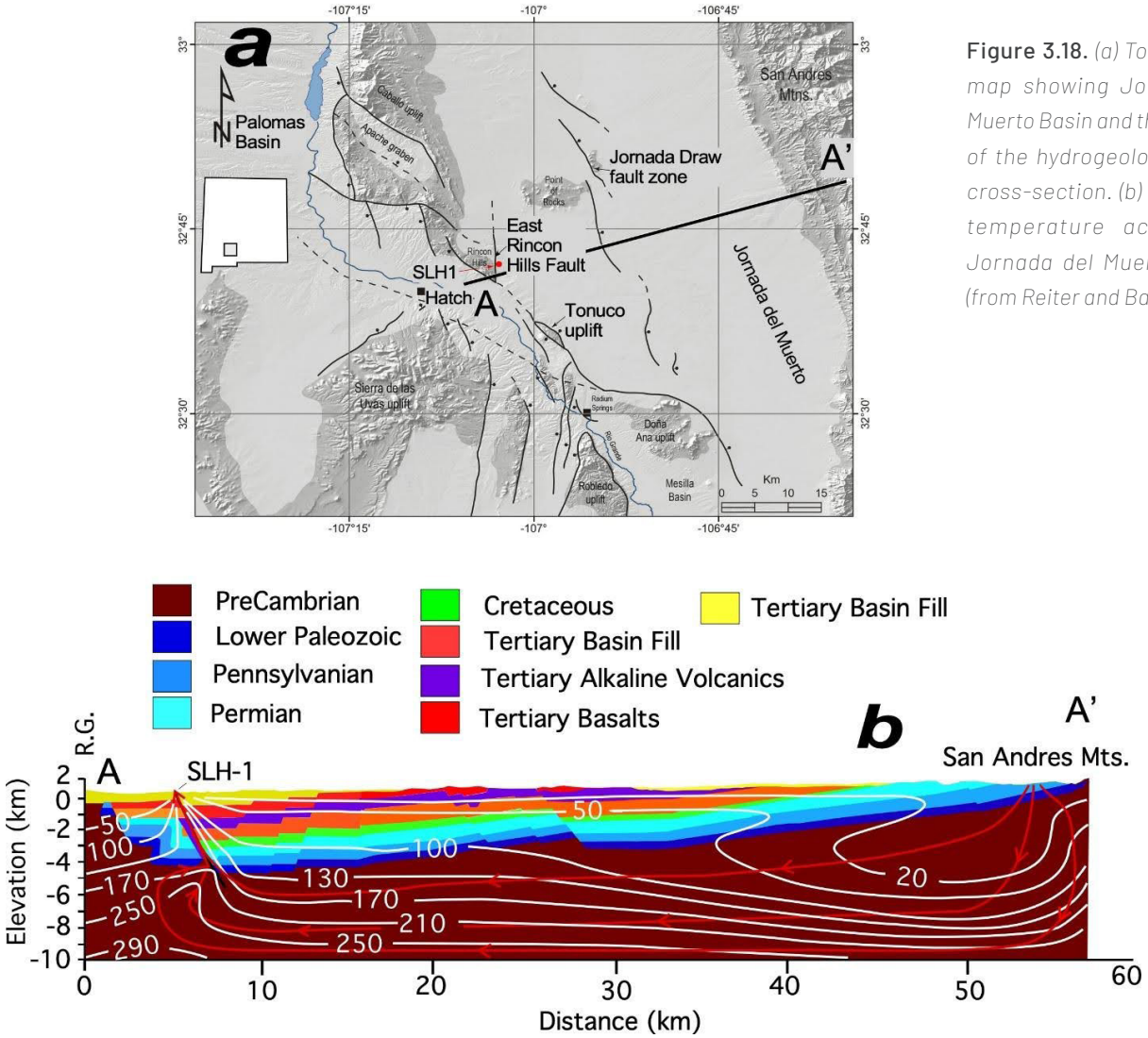

Figure 3.18. *(a) Topographic map showing Jornada del Muerto Basin and the location of the hydrogeologic model cross-section. (b) Simulated temperature across the Jornada del Muerto Basin. (from Reiter and Barroll, 1990)*

Jornada del Muerto and Hatch-Rincon Basins

The southern Jornada del Muerto and Hatch-Rincon Basins host the Rincon geothermal system, which is located at the intersection of the two basins (**Figure 3.18**). The geothermal system is located just to the northeast of the Rio Grande. The southern Jornada del Muerto is bounded to the east by the San Andres Mountains (maximum elevation 2,755 meters) and to the west by the Caballo Mountains (maximum elevation 3,194 meters).

Reiter and Barroll analyzed bottom-hole temperature data from oil wells in the northern and central Jornada del Muerto (not shown on **Figure 3.18a**).[93] The heat flow is high (95 milliwatts per square meter), which is unusual in this area that has few extensional features. These authors pose several ideas to explain the elevated heat flow in this little-deformed area. High crustal radioactivity in buried Proterozoic plutons and intrusions into the middle to lower crust were among the ideas proposed. Identifying the cause of the elevated heat flow in this area warrants additional research.

REGIONAL WATER TABLE CONTOUR MAP ACROSS THE JORNADA DEL MUERTO BASIN

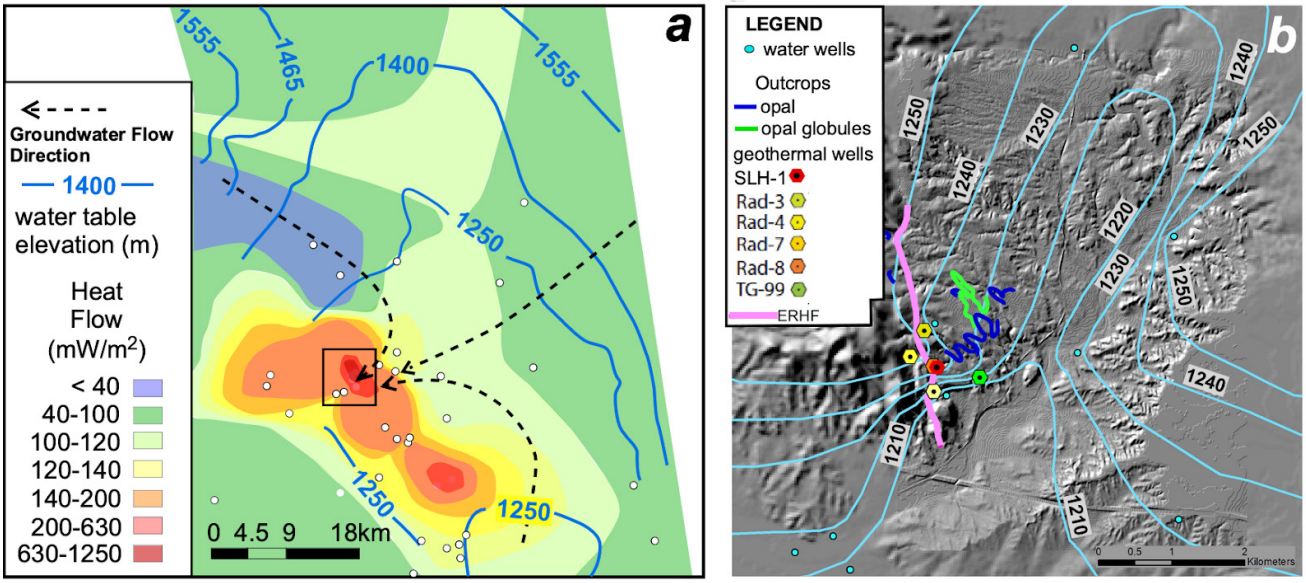

Figure 3.19. (*a) Regional water table contour map (blue lines) across the Jornada del Muerto Basin. Green to red shaded patterns denote temperature gradients contours (°C/km). White circles denote location of temperature gradient drill holes. (b) Expanded water table contours near the East Rincon Hills Fault (purple line) near the southwest edge of the basin. Temperature gradient drill holes and water wells are indicated by the blue dots (data source James Witcher, personal communication). Outcrops of opal deposits are also shown as a green line.* Source: Mack, G. H., Jones, M. C., Tabor, N. J., Ramos, F. C., Scott, S. R., & Witcher, J.C. (2012). Mixed geothermal and shallow meteoric origin of opal and calcite beds in Pliocene-Lower Pleistocene axial-fluvial strata, Southern Rio Grande Rift, Rincon Hills, New Mexico, USA. *Journal of Sedimentary Research, 82, 616-631.* https://doi.org/10.2110/jsr.2012.55

The Rincon geothermal prospect is a blind geothermal system (in other words, no geothermal features are present on the surface). The system was initially identified by the presence of opal deposits (**Figure 3.19b, green lines**).[94] Witcher found anomalous radon soil-gas levels (up to 322 picocuries per liter) in the Rincon Hills, and he mapped potential upflow zones in the vicinity of the East Rincon Hills fault using radon soil-gas surveys.[95] Subsequent drilling of thermal gradient boreholes in the Rincon area showed very high geothermal gradients within the vadose zone (> 400°C/km; 219°F/100 ft)(**Figure 3.20**). The gradients in RAD-8 and RAD-4 are conductive, whereas the thermal gradients in RAD-3 and RAD-7 (**Figures 3.19b and 3.20c**) decrease below the water table, indicative of an outflow plume. Self-potential surveying by Ross and Witcher further refined the shape and extent of the shallow upflow and outflow zones of the system.[96]

RAD-7, northeast of SHL-1 (**Figure 3.20**), was sampled for water chemistry via airlifting.[97] RAD-7 intersects the water table at around 90 meters deep and has a water table temperature of 60°C, or 140°F (**Figure 3.19.c**). The water is predominantly a sodium-chloride fluid with a total dissolved solids of 1924 milligrams per liter. A suite of geothermometry calculations yielded potential reservoir temperatures ranging from 94°C to 177°C (201°F–351°F). The 120°C (248°F) chalcedony geothermometer yields results similar to the sodium-lithium geothermometer (**Figure 3.21**). The sodium/potassium/calcium geothermometer may be unreliable because these waters have flowed through carbonate rocks.[98] Using this information, SLH-1 was drilled in 1992 (**Figure 3.20**).

A second temperature log was obtained in SHL-1 in 2018 (**Figure 3.20c**), and the results are presented in an article by Person and colleagues, who concluded that the temperature overturn observed in SLH-1 had to be due to a three-dimensional hydrologic flow system with components of flow of cold water from the northwest in addition to upflow along the East Rincon Hills fault.[99]

WELLS NEAR THE SAN ANDRES MOUNTAINS AND THE RIO GRANDE

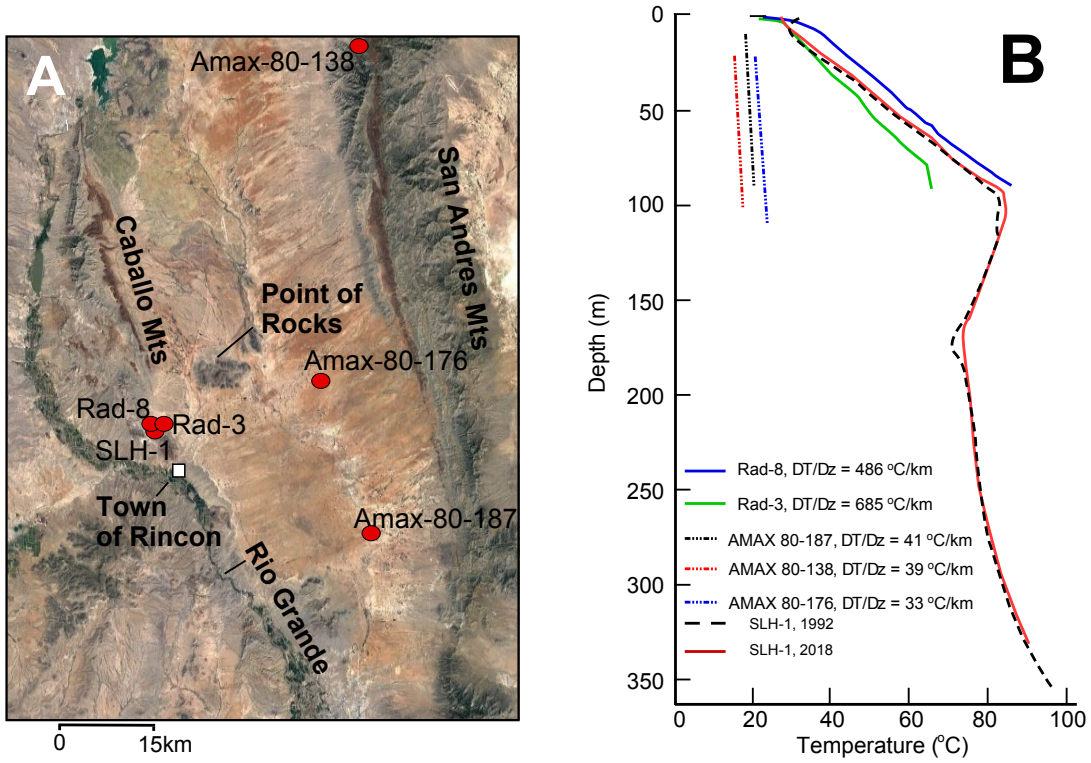

Figure 3.20. *(A) Map showing wells to the west of the recharge area in the San Andres Mountains and in the discharge area near the Rio Grande. (B) Upland temperature profiles on the east side of the Jornada del Muerto Basin to the west of the recharge area. Lowland wells RAD-8, RAD-3, and SLH-1 are located near a geothermal upflow zone east of the East Rincon Hills fault. Repeat temperature profiles were collected for SLH-1 in 1993 and 2018.* Sources: Witcher, J.C. (1998). The Rincon SLH1 geothermal well. *New Mexico Geological Society Guidebook,* (35–38). https://doi.org/10.56577/FFC-49; Person, M., Stone, W. D., Horne, M., Witcher, J., Kelley, S., Lucero, D., Gomez-Velez, J., & Gonzalez-Duque, D. (2023). Analysis of convective temperature overturns near the East Rincon Hills Fault Zone using semi-analytical models. *Geothermal Resources Council Transactions, 47,* 3093–3117.

RINCON GEOTHERMOMETER RESULTS

Na/K/Ca	Na/Li	Mg/Li	quartz	chalcedony	alpha-cristobalite
177°C	117°C	94°C	146°C	120°C	96°C

Figure 3.21 *Estimated reservoir temperatures (in oC) for fluids from well SLH-1 using chemical geothermometers. Source:* Horne, M. (2019). *Assessing the Rincon geothermal system using transient electromagnetic surveys and hydrothermal modeling* [Master's thesis]. New Mexico Institute of Mining and Technology.

MAP OF THE MESILLA BASIN

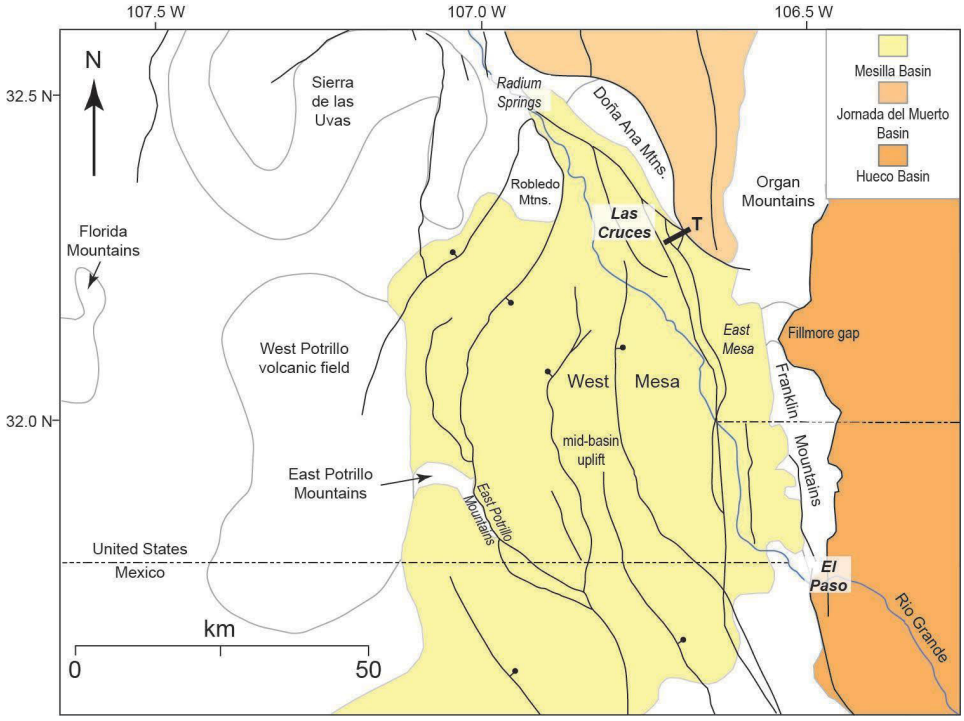

Figure 3.22. *Map of the Mesilla Basin showing the locations of geographic features, major faults (bar and ball on downthrown side), and known geothermal systems (names in italics). The cross-section shown in Figure 3.22 is the bold line labeled T (Tortugas Mountain) in this figure.*

They used semi-analytical mathematical models to evaluate flow rates up the fault and within the water table aquifer. The vertical and horizontal flow rates had to be of the same order of magnitude. Vertical flow up the East Rincon Hills fault was estimated to be about 22 meters per year. This rate is an order of magnitude higher than the estimated upflow based on measurements in the Truth or Consequences upflow zone.[100]

Mesilla Basin

The Mesilla Basin has been the target of extensive geothermal exploration since the early 1970s. Pepin and colleagues recently reported on the analysis of 397 temperature-depth profiles collected between 1972 and 2018 from the basin.[101,102] Known geothermal systems discovered in the basin during this time frame include the East Mesa, Radium Springs, and East Potrillo Mountains fields (**Figure 3.22**).[103,104]

The East Mesa geothermal system is associated with the Mesilla Valley fault zone and a horst located just east of the fault. The developed part of the system in the vicinity of Tortugas Mountain was originally found when the Clary and Ruther State 1 oil test produced steam[105] and hot water in 1949 and when warm salty water in shallow wells was noted during the construction of the Las Alturas neighborhood.[106] New Mexico State University decided to develop the geothermal system from the mid-1970s to early 1980s to save on heating costs. A direct-use heating system was built in 1981 and 1982 to heat athletic buildings and other facilities on the east side of campus. Greenhouse and aquaculture business incubators were added to the system in 1985. This was one of the first attempts to use a geothermal resource to directly heat large facilities on a university campus. Because this was a groundbreaking use of this resource, several mistakes in the initial design led to maintenance problems in later years,[107] and the system was taken offline in 2001. Numerous geophysical surveys, shallow thermal gradient holes, two deep test wells, and four deep production wells were used to define the resource.[108,109,110,111] The resource is associated with a structural bench that is cut by the 3- to 4-mile-wide Mesilla Valley fault zone that generally steps up and down across a series of faults (**Figure 3.23**). All of the wells, except PG-4, are completed in the middle to lower Santa Fe Group. The deepest 12 meters of PG-4 are in breccia in Permian limestone that may represent a fault zone or a karst feature (**Figure 3.23**).[112]

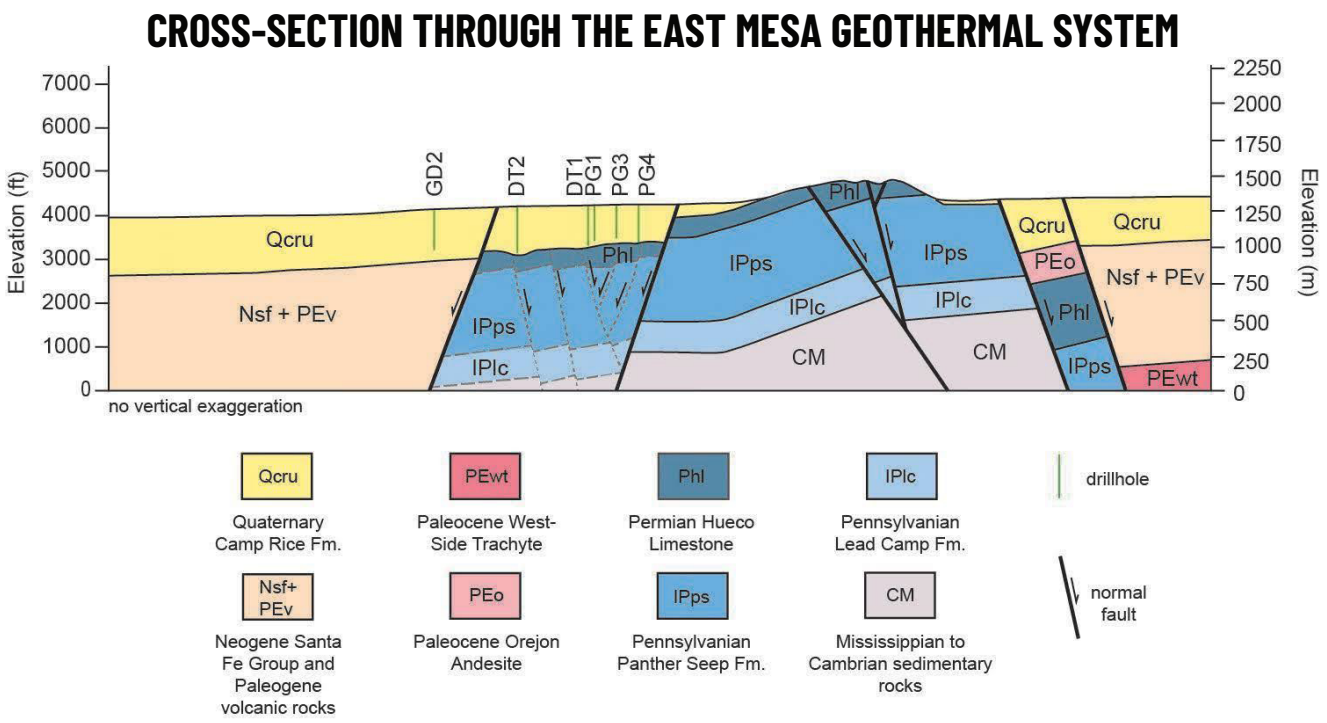

Figure 3.23. *Cross-section through the East Mesa geothermal system. The dashed gray lines show the geometry of faults and layering of rock units imaged by a seismic reflection line.* Sources: Witcher, J. C., Schoenmackers, R., Polka, R., & Cunniff, R. A. (2002). Geothermal energy at New Mexico State University in Las Cruces. *Geo-Heat Center Bulletin, 23,* 30–36; Jochems, A. P., Kelley, S. A., & Seager, W. R. (2020). *Geologic map of the Tortugas Mountain 7.5-minute quadrangle, Doña Ana County, New Mexico* (Open-file Geologic Map 282: scale 1:24,000). New Mexico Bureau of Geology and Mineral Resources.

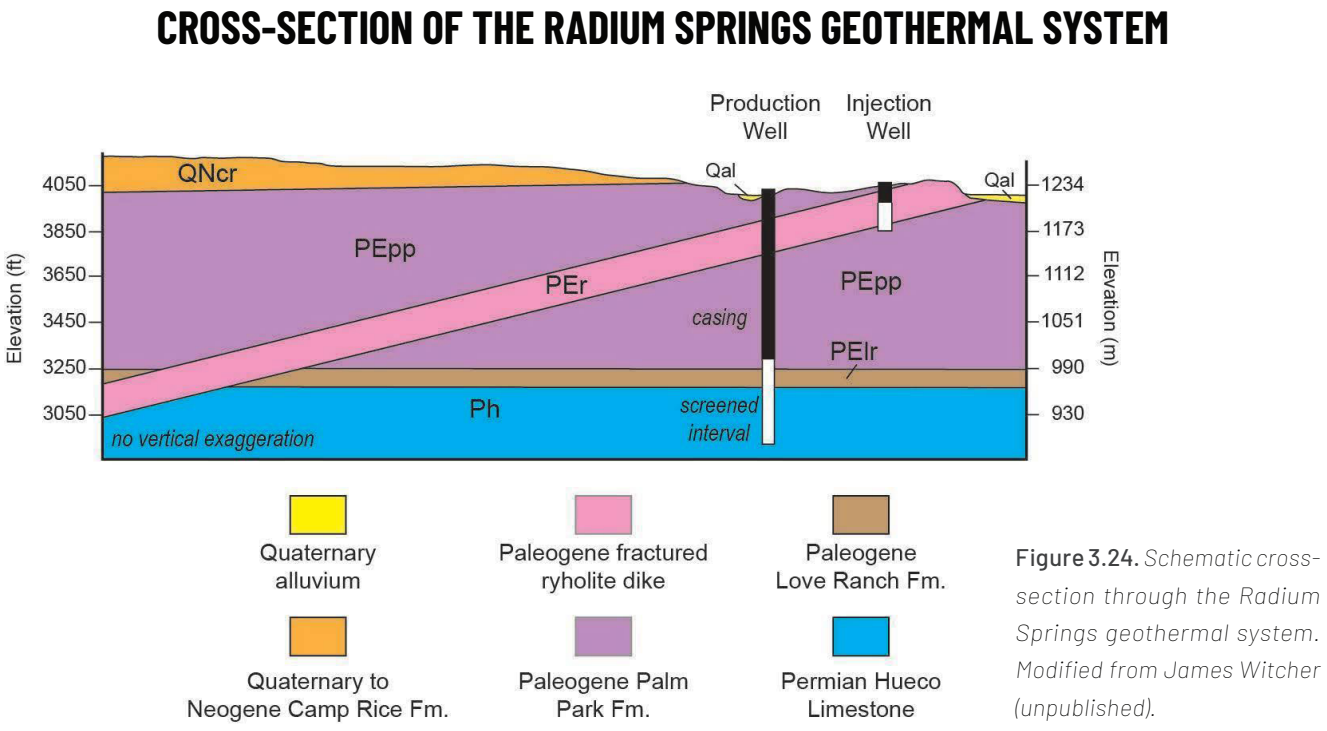

Figure 3.24. *Schematic cross-section through the Radium Springs geothermal system. Modified from James Witcher (unpublished).*

The Radium Springs system is at the very northern edge of the Mesilla Basin; this system is used to heat the greenhouse at the Masson Radium Springs Farm. The reservoir for this system is in fractured Permian limestone (**Figure 3.24**). The limestone is overlain by less than 30 meters of sand and gravel of the Paleocene to Eocene Love Ranch Formation and more than 216 meters of Eocene Palm Park Formation (**Figure 3.24**).[113] The Palm Park Formation in this area is a low-permeability andesitic lahar that acts as an aquitard. The aforementioned rock units at Radium Springs are cut by a rhyolite dike that is intensely fractured. Geothermal fluids in the limestone move to the surface through the fractured dike to form the natural springs in this area. The 30 meter to 46 meter dike is a hydrogeologic window through the Palm Park aquitard. The production well that heats the greenhouse is 244 meters deep and has a discharge temperature of 92.7°C (198.9°F).[114]

Geologic structures in the East Potrillo Mountains include Laramide thrust, low-angle normal and high-angle normal faults.[115] An oil well (Pure 1 Fed H) was drilled in 1962 about halfway along the eastern side of the range. The well was spudded in middle Permian limestone and penetrated a normal Permian, Mississippian, Devonian, and Silurian section to a depth of 1,343 meters. A repeat of the Permian and Mississippian section was then encountered, suggesting the presence of a fault at this depth. Marble and Cenozoic diorite were penetrated between 1902 and the total depth at 2,239 meters. The bottom-hole temperature for this well is 70°C (158°F). The undeveloped geothermal system along the east side of the southern East Potrillo Mountains is located in fractured carbonate rocks along the East Potrillo fault zone, a major basin boundary fault in the southwest part of the basin. Snyder used temperature-depth data from more than 140 geothermal industry shallow- and intermediate-depth wells to identify a heat flow anomaly within the carbonates that extends from the south end of the Eastern Potrillo Mountains southward toward the Mexican border.[116] Thermal logs from three wells that are close together at the south end of the East Potrillo uplift indicate strong upflow of fluids in the carbonates along the fault.[117,118] A possible reservoir in the form of thick eolian deposits may occur in the early Santa Fe Group deposits east of the East Potrillo fault zone.[119] Pepin and colleagues also note a single well to the north of the East Potrillo Mountains that indicates upflow along the projected trend of the East Potrillo fault zone;[120] elevated temperatures were noted to the northeast, suggesting the presence of an outflow plume.

Lightning Dock

The Lightning Dock known geothermal resource area was established in 1974. In 1995, Damon Seawright developed a geothermally heated aquaculture facility (AmeriCulture Inc., **Figure 3.4**). Americulture currently provides tilapia fry to aquaculture facilities across the USA. Since the initial discovery in 1948, a variety of greenhouses have utilized the resource, and a 15 MWe binary electrical plant was built by Cyrq Energy in 2013. Today, a step-out well drilled by Zanskar in late 2024 produces 163°C (325°F) water from more than 2,287 meters with a flow rate of roughly 19,000 liters per minute. Zanskar believes this new well can power the existing power plant without use of the earlier wells.[121]

The origin of the hot water is a matter of some discussion. Elston and colleagues proposed that the hot water was associated with upwelling along a Quaternary fault, which might coincide with a ring fracture of the Muir caldera preserved in the Pyramid Mountains to the east of Lightning Dock.[122] Geophysical data defined the extent of thermal anomaly, which overlies a buried horst.[123,124] In addition, the geophysical data shows that the mapped late Pleistocene fault has very little displacement and that larger faults delineate a graben between the thermal anomaly and the Pyramid Mountains to the east. Witcher used volcanic and sedimentary stratigraphic data from three wells in the Lightning Dock region to document Jurassic rift extension, Laramide compression, caldera collapse, and basin and range extension, which caused intense fracturing of rocks in this area, creating the wide fault zone discovered by Zanskar.[125]

Petroleum Basins

Bottom-hole temperatures and circulation information from geophysical well logs measured in the New Mexico portions of the Raton, San Juan, and Delaware Basins were compiled in the New Mexico Bureau of Geology and Mineral Resources Geothermal Database by Shari Kelley and her students starting in 2010. Colorado data for the San Juan Basin were sourced from Dixon.[126] Morgan compiled bottom-hole temperature data for the Colorado portion of the Raton Basin.[127] More than 800 bottom-hole temperature records were integrated

PETROLEUM WELLS WITH BOTTOM-HOLE TEMPERATURE DATA

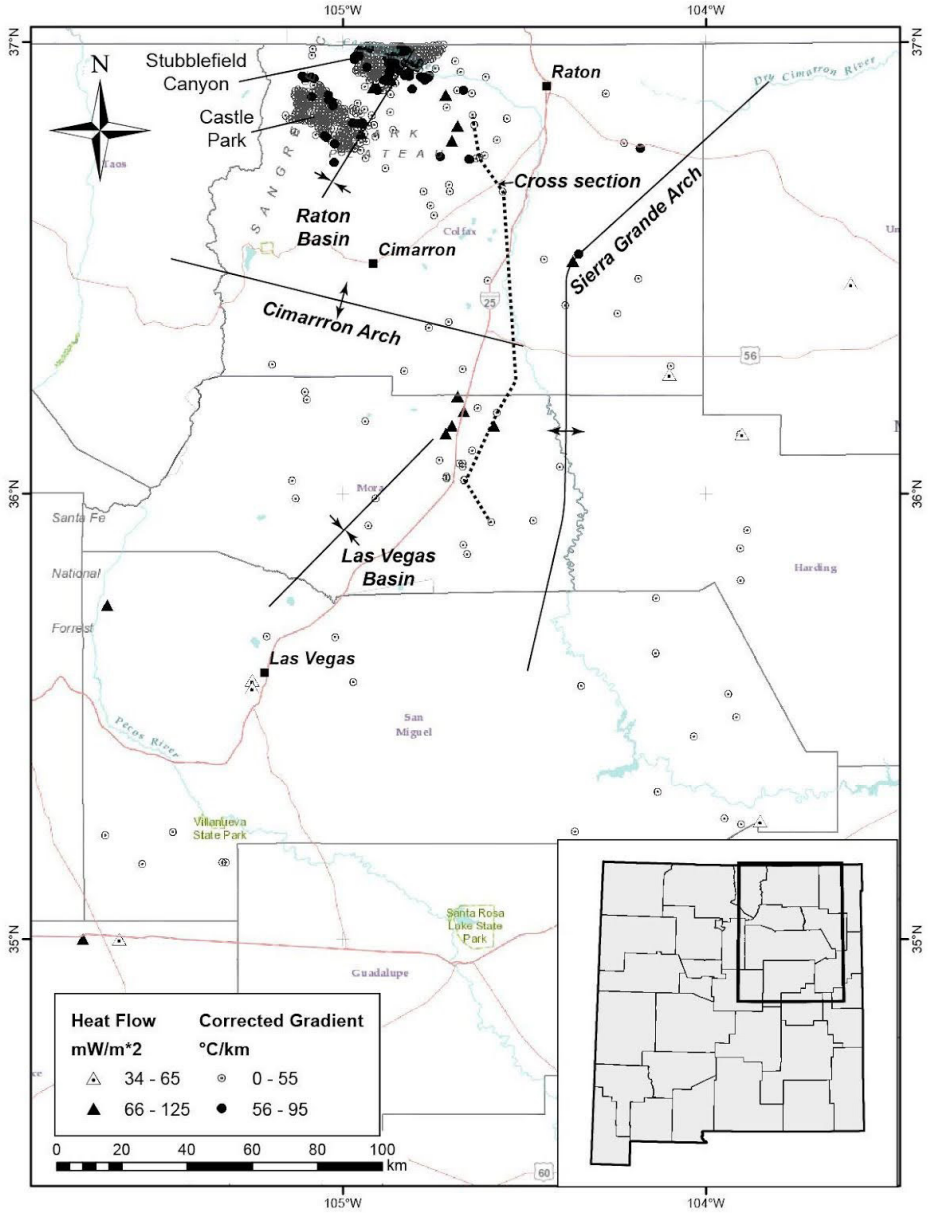

Figure 3.25. *Location of petroleum wells with bottom-hole temperature data (circles) and heat flow (triangle) data measured by Reiter and colleagues, and Edwards and colleagues in and near the Raton and Las Vegas Basins in northeastern New Mexico. The location of the cross-section in Figure 3.23 and Pennsylvanian and Laramide structural features are also shown.* Sources: Reiter, M., Edwards, C. L., Hartman, H., & Weidman, C. (1975). Terrestrial heat flow along the Rio Grande rift, New Mexico and southern Colorado. *GSA Bulletin, 86*(6), 811–818. https://doi.org/10.1130/0016-7606(1975)86<811:THFATR>2.0.CO;2; Edwards, C. L., Reiter, M., Shearer, C., & Young, W. (1978). Terrestrial heat flow and crustal radioactivity in northeastern New Mexico and southeastern Colorado. *GSA Bulletin, 89*(9), 1341–1350. https://doi.org/10.1130/0016-7606(1978)89%3C1341:THFACR%3E2.0.CO;2

in this analysis to assess geothermal potential within the Delaware Basin in New Mexico. Kelley described the challenges of determining an accurate correction for the bottom-hole temperature data in the Raton Basin in great detail.[128] Similar challenges were encountered when trying to correct bottom-hole temperature data for the San Juan and Delaware Basins. In the end, we decided to evaluate uncorrected bottom-hole temperature measurements for the San Juan and Delaware Basins and used corrected values in the Raton Basin. Once interesting anomalies are identified, we will refine our corrections for each anomalous area in these basins. The method for determining the geothermal gradient is outlined in Kelley.[129]

Raton Basin and Las Vegas Basin

The locations of the wells in the Raton and Las Vegas basins analyzed by Kelley are shown in **Figures 3.25** and **3.26.**[130] Kelley developed a bottom-hole temperature correction for the Raton Basin.[131] Both the map and the cross-section in the figures highlight the fact that

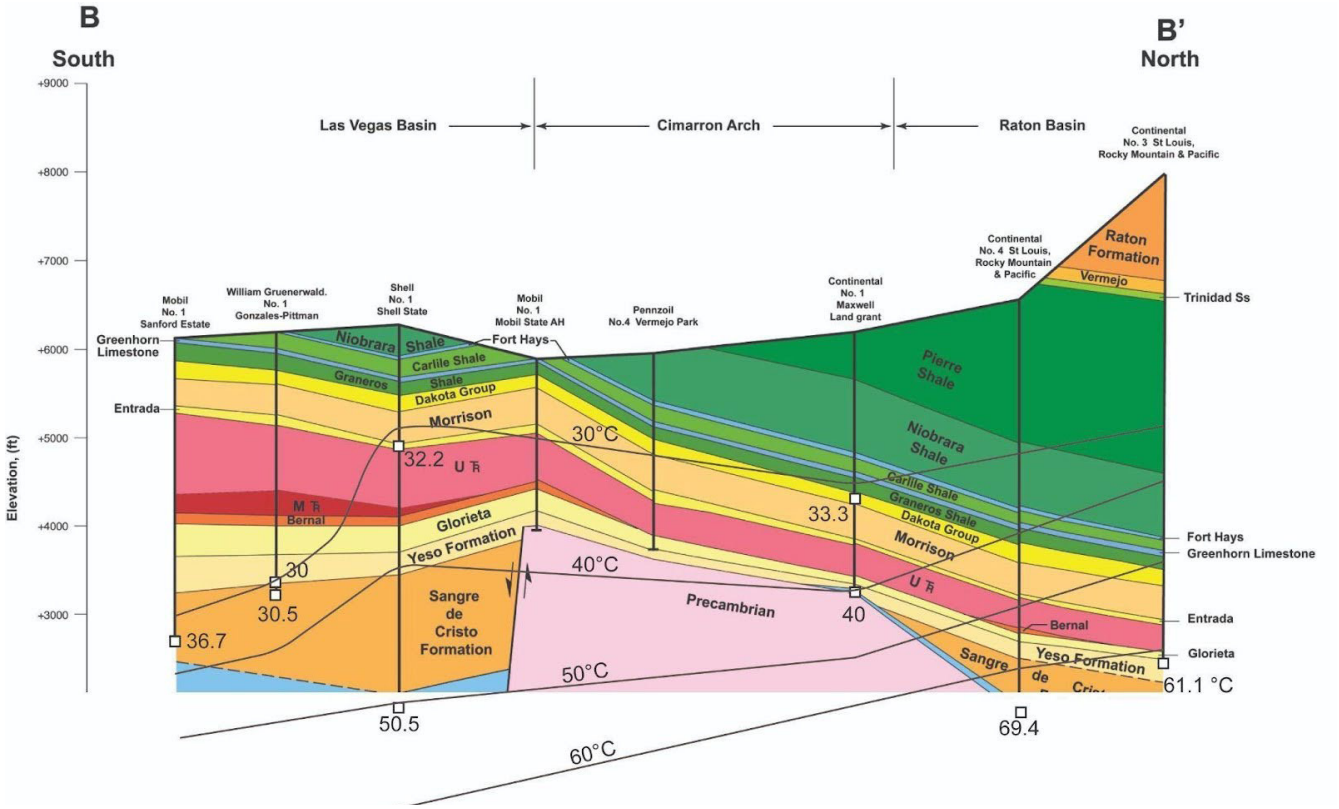

Figure 3.26. *South to north cross-section through northeastern New Mexico modified from Broadhead. Dashed lines are isotherms based on bottom-hole temperature data. Elevated geothermal gradients coincide with preserved Pierre Shale, which has a low thermal conductivity. UTr = upper Triassic strata. MTr = middle Triassic strata. Source:* Broadhead, R. F. (2008). *The natural gas potential of north-central New Mexico: Colfax, Mora, and Taos Counties* (Open-file Report 510). New Mexico Bureau of Geology and Mineral Resources. http://geoinfo.nmt.edu/publications/openfile/details.cfml?Volume=510

geothermal gradients and the subsurface temperatures are higher in the Raton Basin near the Colorado–New Mexico state line. Regional-scale gradients using corrected bottom-hole temperatures from drill holes deeper than 1 kilometer are 31.2°C ± 2.6°C/kilometer (88.2°F ± 36.7°F/kilometer) for the Las Vegas Basin and 46.1°C ±9.6°C/km (115.0°F ± 49.3°F/kilometer) for the Raton Basin with surface intercept values of 10.8°C (51.4°F) and 6.3°C (43.3°F), respectively. The highest measured bottom-hole temperature in northeastern New Mexico is 135°C (275°F), corrected to 150°C (302°F) at 2,156 meters.

Kelley concluded that the thermal structure of the Raton Basin is controlled in part by the thermal conductivity structure of the basin.[132] The presence of the thick low-thermal-conductivity Pierre Shale section in the northern part of the basin causes the subsurface temperatures to be higher compared with the southern part of the basin, where the Pierre Shale has been removed by erosion. Although the 150°C (302°F) isotherm is at a depth of between 2.6 and 2.7 kilometers below Stubblefield Canyon (**Figure 3.25**), low fluid-production rates in the underpressured Entrada and Glorieta Sandstones may preclude economic development of geothermal resources in the Raton Basin.

San Juan Basin

Both published heat flow data[133,134] and the industry temperature logs and bottom-hole temperature data analyzed by Kelley[135] record elevated modern subsurface temperatures in the northern part of the basin, consistent with the elevated observed heat flow and the high modern elevation of the San Juan Mountains to the north.[136] **Figure 3.27A** shows the distribution of data used in this analysis of the San Juan Basin. The San Juan Basin

BOTTOM-HOLE TEMPERATURES IN THE SAN JUAN BASIN

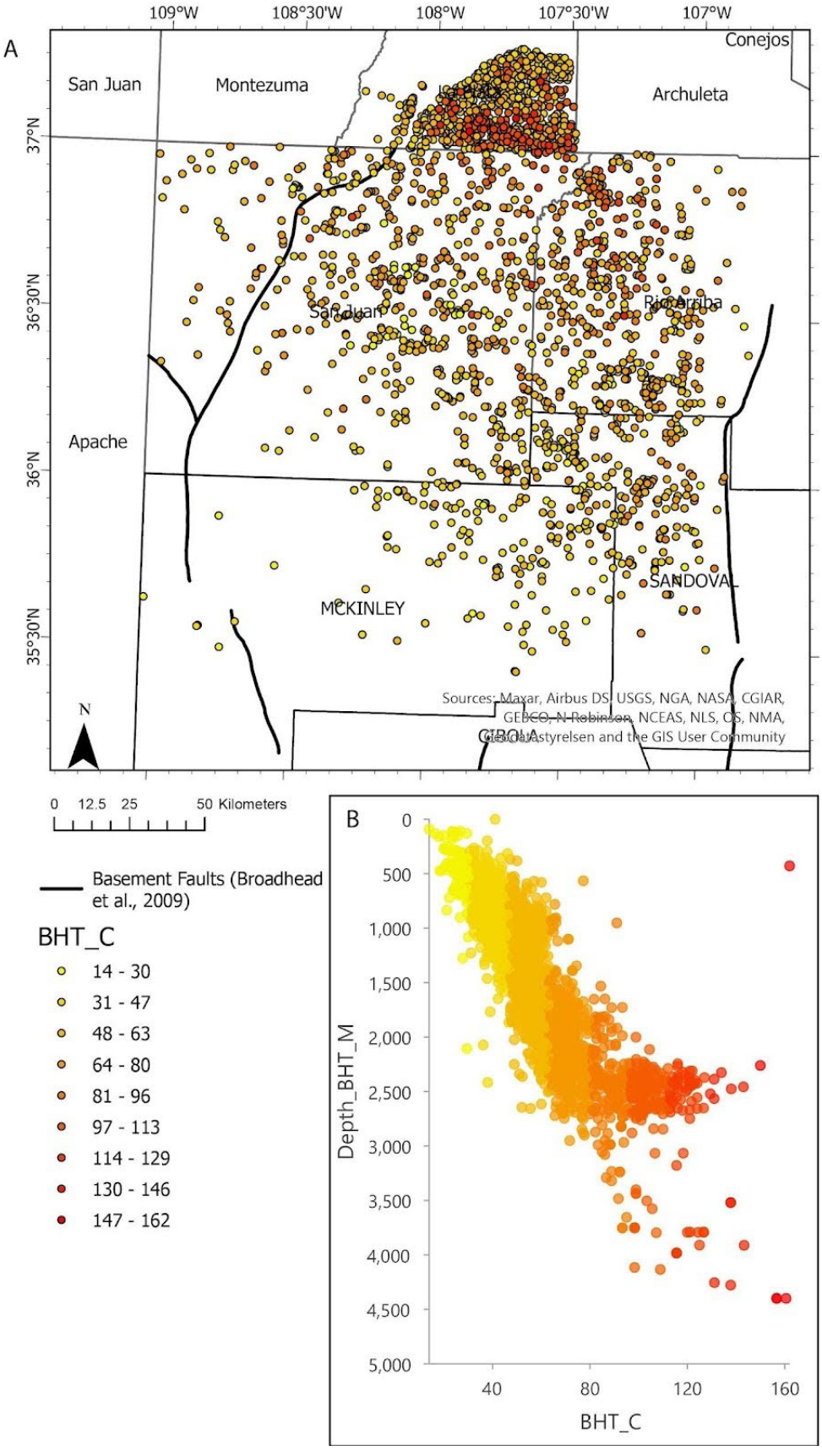

Figure 3.27. *(A) Bottom-hole temperature data locations in the San Juan Basin color scaled by temperature magnitude. Black lines are basement faults from Broadhead et al, (2009). (B) Plot of uncorrected BHT (°C) versus depth (meters), color scale same as A. Bottom-hole temperature data from New Mexico Bureau of Geology and Mineral Resources Subsurface Library and Dixon (2002).* Sources: Broadhead, R. F., Mansell, M., & Jones, G. (2009). *Carbon dioxide in New Mexico: Geologic distribution of natural occurrences* (Open-file Report 514). New Mexico Bureau of Geology and Mineral Resources. https://doi.org/10.58799/OFR-514; New Mexico Bureau of Geology and Mineral Resources. (n.d.). *New Mexico Subsurface Library*. https://geoinfo.nmt.edu/libraries/subsurface/search/; Dixon, J. (2002). *Evaluation of bottom-hole temperatures in the Denver and San Juan Basins of Colorado* (Open-file Report OF-02-15). Colorado Geological Survey, Division of Minerals and Geology, Department of Natural Resources. https://coloradogeologicalsurvey.org/publications/evaluation-bottom-hole-temperatures-denver-san-juan-basins-colorado

bottom-hole temperature data span a depth range of 90 meters to 4,400 meters, with uncorrected temperatures ranging from 14°C to 162°C (57°F–324°F; **Figure 3.27B**, compare with **Figure 3.10**). The mean geothermal gradient, calculated from uncorrected bottom-hole temperatures, for the entire San Juan Basin is 29°C/km (1.6°F/100 ft). Note the higher temperatures at depths of about 2,500 meters on the temperature-depth plot in **Figure 3.27B**; these points are from the warmer northern part of the basin (**Figure 3.28**). The cause of high geothermal gradients in north-central McKinley County (lower-left corner of the map; **Figure 3.28**) is uncertain.

Isotherm mapping was performed using uncorrected bottom-hole temperature data, extracting key temperatures for mapping subsurface grids. Data cleaning for mapping was accomplished by selecting one data point per well, and in the case of multiple bottom-hole temperature measurements per well, the deepest bottom-hole temperature data point was used. In the southwestern portion of the basin, an area with sparse drilling control, two equilibrium temperature logs from the New Mexico Bureau of Geology and Mineral Resources (2024) subsurface library were projected using their calculated gradient. The 90°C (194°F) isotherm was chosen

GEOTHERMAL GRADIENT IN THE SAN JUAN BASIN

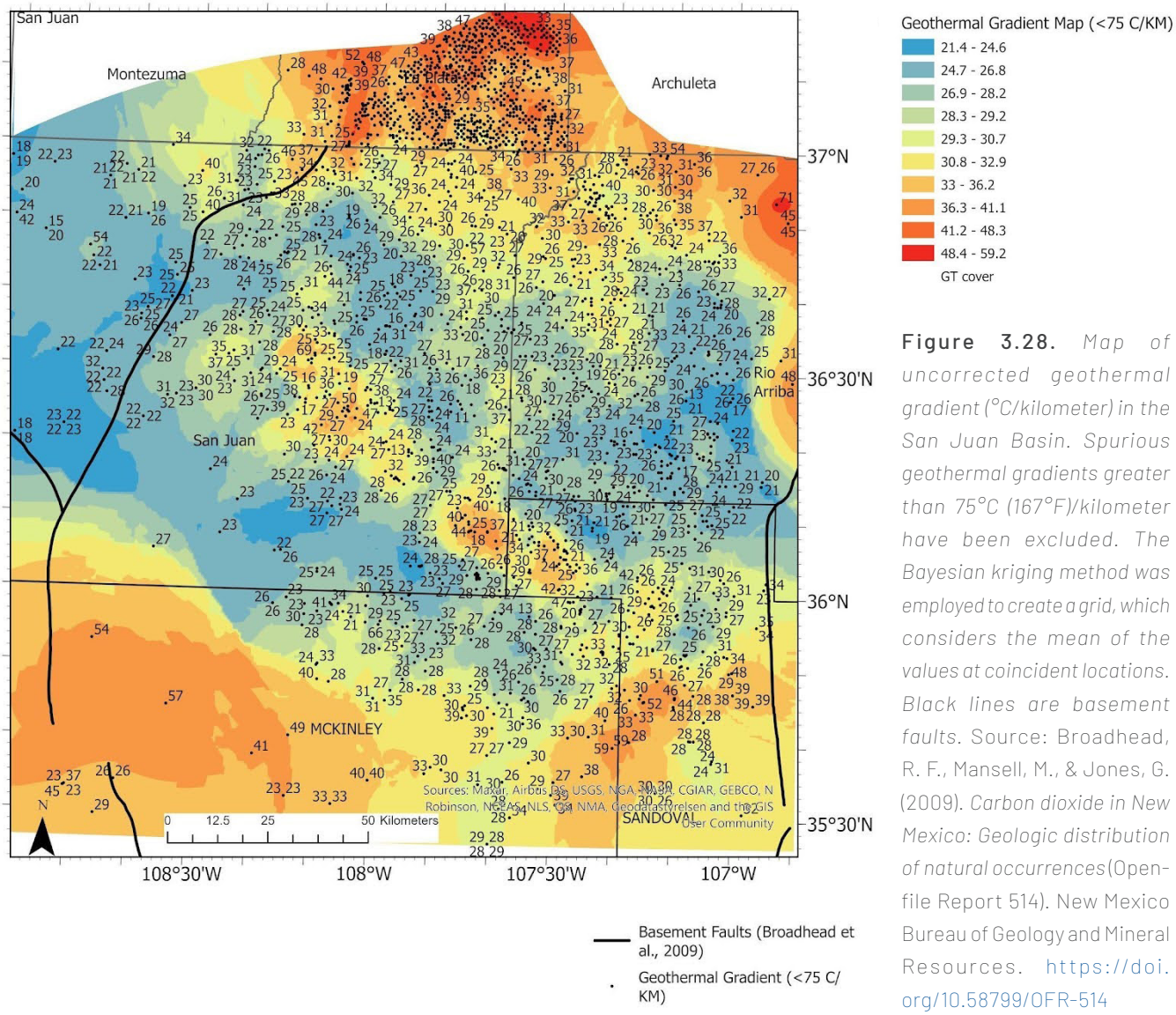

Figure 3.28. *Map of uncorrected geothermal gradient (°C/kilometer) in the San Juan Basin. Spurious geothermal gradients greater than 75°C (167°F)/kilometer have been excluded. The Bayesian kriging method was employed to create a grid, which considers the mean of the values at coincident locations. Black lines are basement faults.* Source: Broadhead, R. F., Mansell, M., & Jones, G. (2009). *Carbon dioxide in New Mexico: Geologic distribution of natural occurrences* (Open-file Report 514). New Mexico Bureau of Geology and Mineral Resources. https://doi.org/10.58799/OFR-514

ISOTHERM MAP FOR THE SAN JUAN BASIN

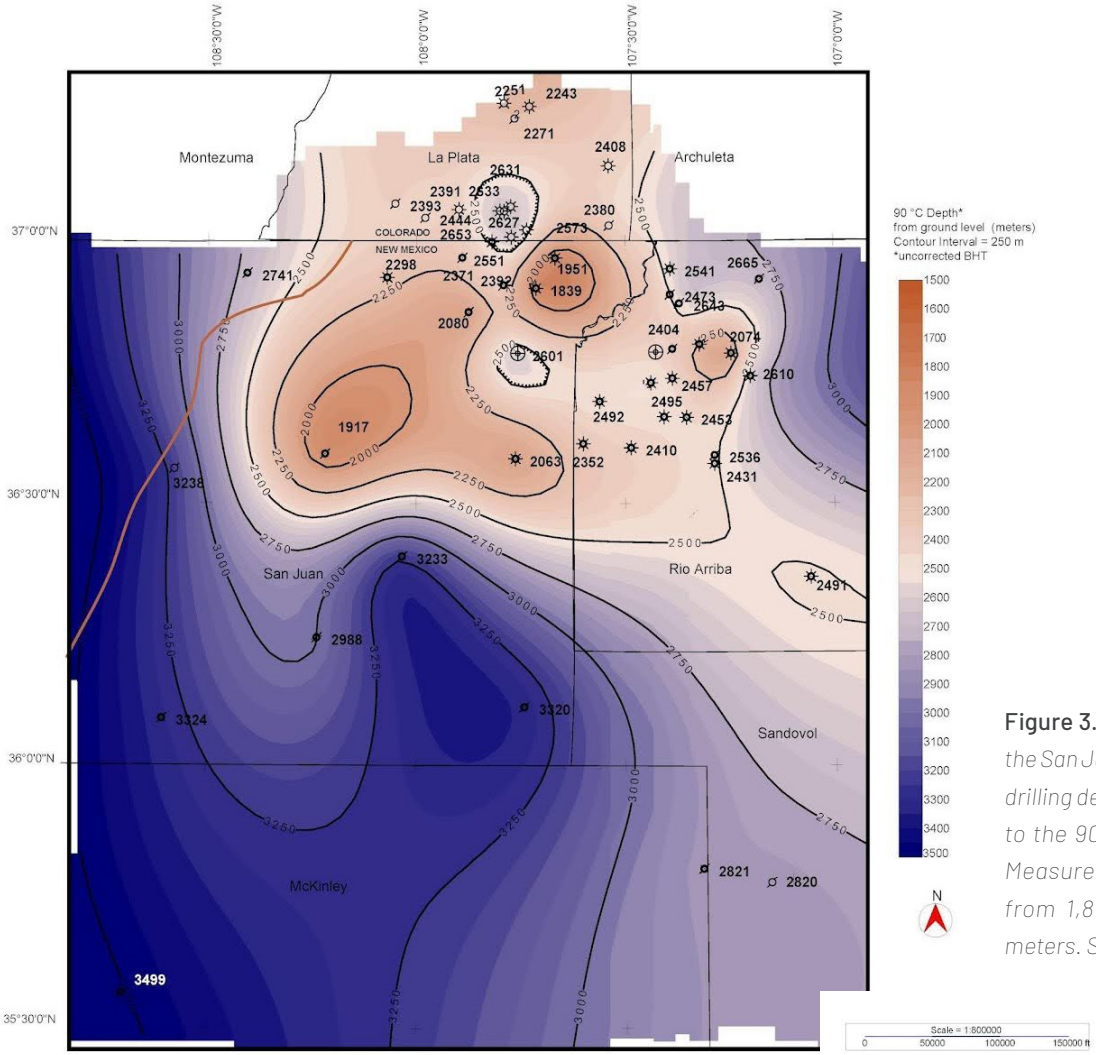

Figure 3.29. *Isotherm map for the San Juan Basin showing the drilling depth from ground level to the 90°C (194°F) isotherm. Measured drilling depths are from 1,890 meters to 3,500 meters. Source: Luke Martin.*

as a modeling decision point because a minimum of 90°C (194°F) is required for binary power plant production[137] where a working fluid with a boiling point lower than water is utilized. Many other cultural, environmental, reservoir, and economic parameters affect the viability of a geothermal project. Here, we present a depth-to-90°C (194°F) isotherm map, subtracting the ground level to 90°C (194°F) isotherm (**Figure 3.29**).

In summary, the San Juan Basin is a conductive basin with an approximately 29°C (84°F)/kilometer (1.6 °F/100 ft) average geothermal gradient. The basin has undergone tectonic influences that contribute to the fracture density of the basin. The northern portion of the basin contains the highest geothermal gradients and a greater density of higher bottom-hole temperatures, and it is the deepest portion structurally. Mapping of uncorrected bottom-hole temperature isotherms indicates that the lowest temperature threshold for binary geothermal power generation (90°C or 194°F) may be found at depths from 1,890 meters to 3,500 meters below ground level across the basin.

Delaware Basin

The Delaware Basin is the deep-water portion of the larger Permian Basin in southeastern New Mexico and west Texas (**Figure 3.30**). During the Late Cretaceous-Paleogene, the Permian Basin was affected by the Laramide orogeny. The few compressional and transpressional structures

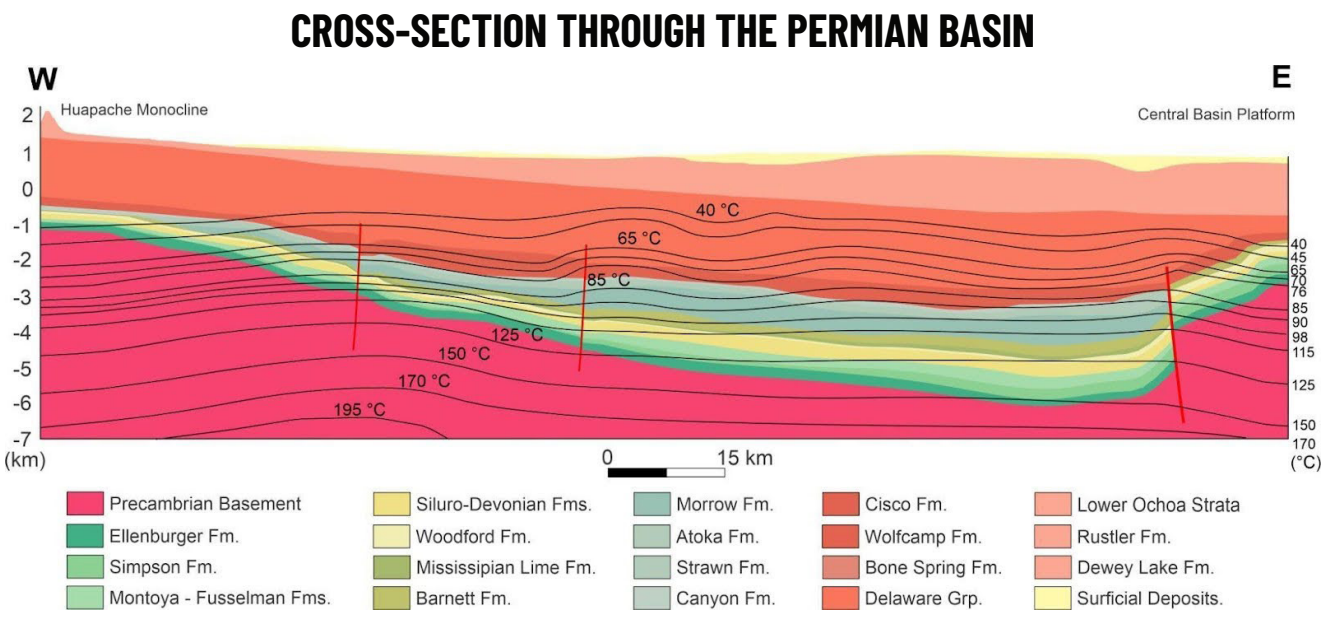

Figure 3.30. *Cross-section through the Permian Basin, New Mexico. The line of section is shown in Figure 3.31.* Sources: Lavery, D., Reyes Correa, M., Baca, A., Martin, L., & Attia, S. (2024). *3D geologic framework of the Delaware Basin, Eddy and Lea Counties, New Mexico* (Open-file Geologic Map 318). New Mexico Bureau of Geology and Mineral Resources. https://doi.org/10.58799/OF-GM-318; Aljubran, M. J., & Horne, R. N. (2024). Thermal Earth model for the conterminous United States using an interpolative physics-informed graph neural network. *Geothermal Energy, 12*(1), 25. https://doi.org/10.1186/s40517-024-00304-7

are located on the west side of the Permian Basin. The Huapache Monocline located to the west of the Delaware Basin in New Mexico is identified as a Laramide structure, and other structures on this side of the basin are the folds located at the north shelf and have been interpreted as inherited reactivated Precambrian-Paleozoic structures (see the present basin geometry in **Figure 3.30**)

More than 800 bottom-hole temperature records were integrated in this analysis to assess geothermal potential within the Delaware Basin in New Mexico (**Figures 3.10 and 3.31**). Bottom-hole temperatures in the Delaware Basin range from 23°C (73°F) to approximately 139°C, or 282°F (**Figure 3.10**), with data collected from depths between 116 meters and 6,984 meters. A total of 192 boreholes have bottom-hole temperatures values exceeding 100°C (212°F); the higher temperatures are located on the western side of the Delaware Basin near the border with the Guadalupe Mountains. The highest bottom-hole temperature recorded in the basin is 138.89°C (282.00°F), measured at 6,984 meters (22,913 feet). This value was obtained in the southern part of the Delaware Basin depocenter in New Mexico and is associated with the Precambrian basement.

The distribution of bottom-hole temperatures in the Delaware Basin is not uniform; it spans from the northwest to the southeast of the basin in New Mexico (**Figure 3.32a**). In terms of depth, temperature values exceeding 100°C (212°F) range from 8,000 feet to 22,000 feet, with the shallower values concentrated in the northwest side of the basin (**Figure 3.32b**).

In summary, **Figure 3.5A** in the introduction and **Figure 3.32b** both indicate that temperatures needed for power production lie at great depths (about 7 kilometers) in the Permian Basin.

CONCLUDING REMARKS

As noted in the introduction to this chapter, a tremendous amount of geothermal exploration and research was done in New Mexico during the 1970s and 1980s, with most exploration wells drilled to depths of less than 200 meters. Despite these efforts, very little is known about the deep thermal and geological structure of the rift basins, particularly south of the Albuquerque Basin, because few deep wells were drilled during the early exploration

TEMPERATURE PREDICTION IN THE DELAWARE BASIN

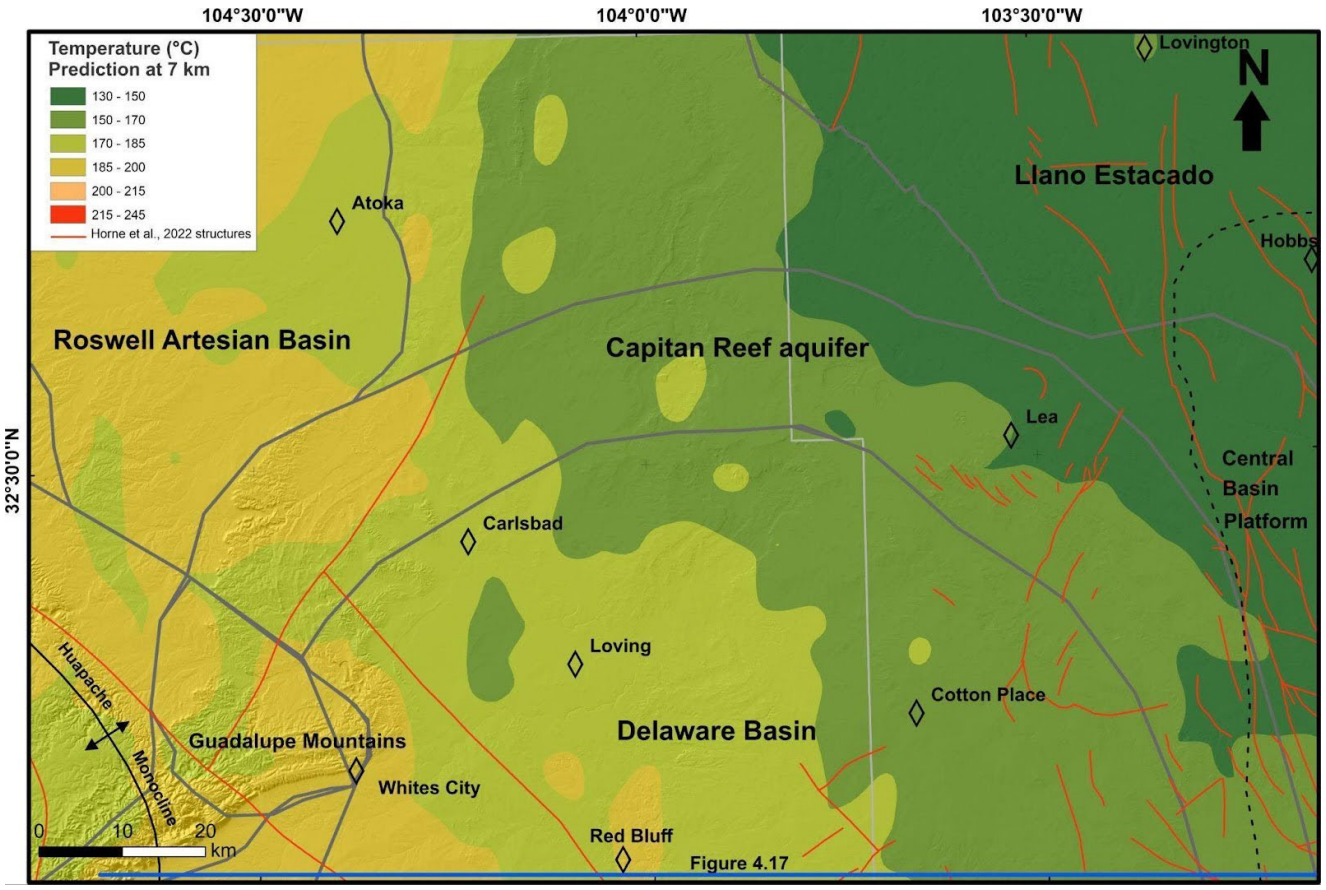

Figure 3.31. *Temperature prediction at 7 kilometers in the Delaware Basin. The blue line at the bottom of the map is the location of the cross section in Figure 4.16. White line is the boundary between Lea and Eddy counties in New Mexico. Sources:* Aljubran, M. J., & Horne, R. N. (2024). Thermal Earth model for the conterminous United States using an interpolative physics-informed graph neural network. *Geothermal Energy, 12*(1), 25. https://doi.org/10.1186/s40517-024-00304-7; Horne, E. A., Hennings, P. H., Smye, K. M., Staniewicz, S., Chen, J., & Savvaidis, A. (2022). Structural characteristics of shallow faults in the Delaware Basin. *Interpretation, 10*(4), T807–T835. https://doi.org/10.1190/INT-2022-0005.1

efforts. **Figure 3.33** shows that temperatures above 150°C (302°F) have been measured in a few wildcat oil wells in the southern part of the state and in oil wells drilled by Shell Oil Company during the 1970s in the Albuquerque Basin. Understanding the deep subsurface is key to successful siting of future next-generation projects. This gap in knowledge about the deep subsurface can be addressed by collecting new geophysical data (e.g., via SkyTEM, magnetotellurics, passive seismic), reprocessing old seismic lines, and ultimately drilling deep wells.

During earlier geothermal exploration efforts in New Mexico, an important observation was noted by Witcher and colleagues: Much of southwestern and west-central New Mexico was impacted by an episode of andesitic volcanism during the Eocene that deposited low-permeability debris flows that serve as aquitards within regional-scale hydrologic flow systems.[138] In places, highly fractured Proterozoic rocks that core Laramide highlands were buried beneath the debris flows, thus masking the presence of possible geothermal reservoirs in fractured basement rocks. Witcher and colleagues recognized that intrusions or faults that cut through the debris flows can act as conduits that bring hot water to the surface as hot springs (e.g., **Figures 3.12** and **3.24**).[139] These breaches through regional aquitards are called *hydrogeologic windows*. These authors created a subcrop map (**Figure 3.13**) that may serve as a useful tool for guiding future exploration efforts.

DISTRIBUTION OF BOTTOM-HOLE TEMPERATURE VALUES IN THE DELAWARE BASIN

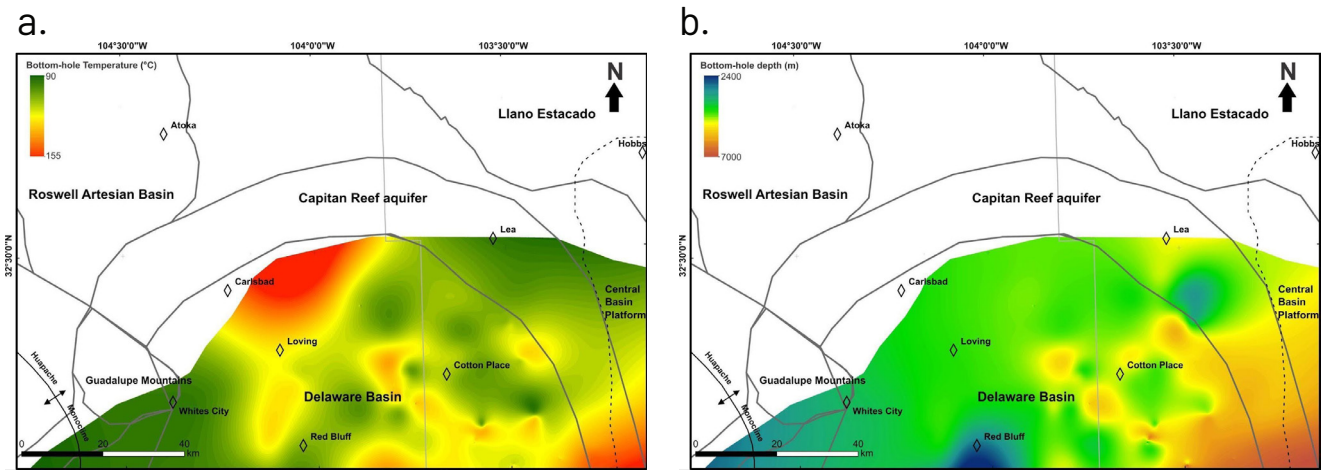

Figure 3.32. *(a) Map showing the distribution of bottom-hole temperature values greater than 91°C (196°F) in the New Mexico portion of the Delaware Basin. (b) Map depicting the depths at which bottom hole temperatures values exceed 100°C (212°F) within the Delaware Basin. Source: Martin Reyes.*

HOTTEST OIL WELLS IN NEW MEXICO

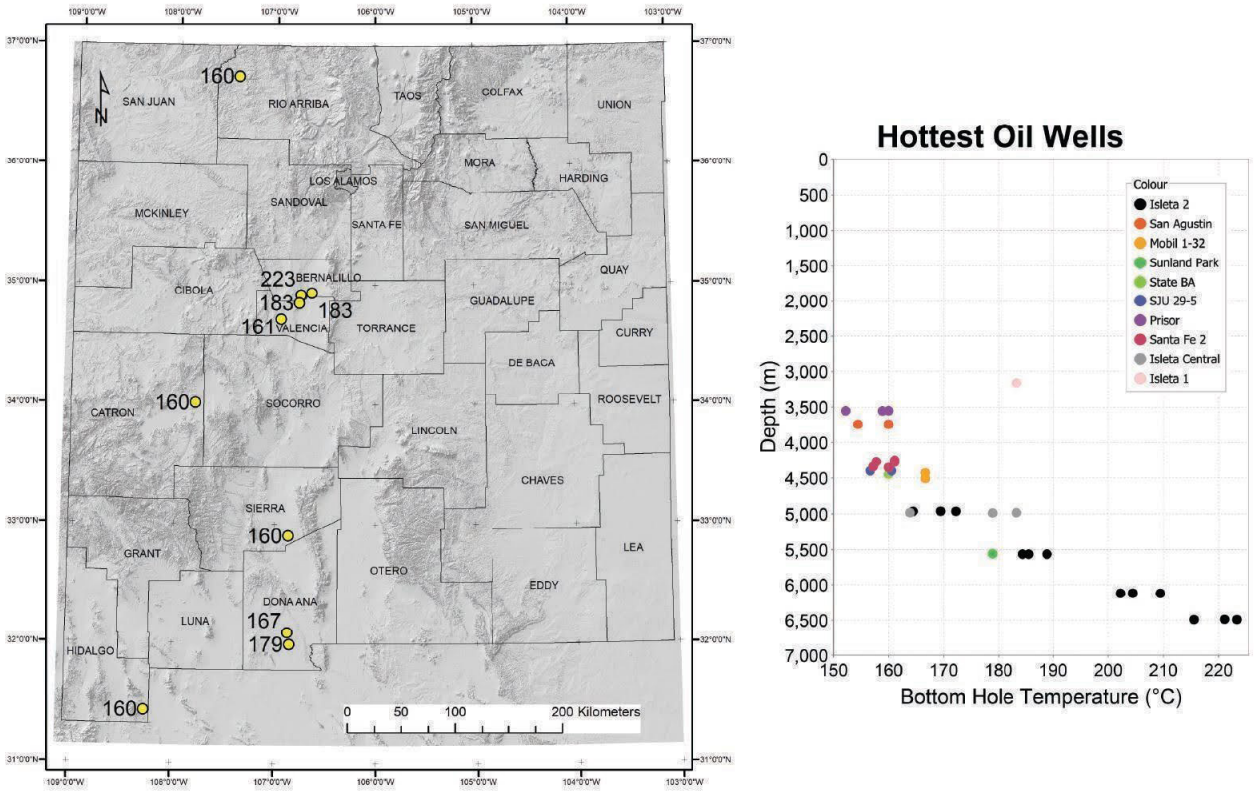

Figure 3.33. *Map and plot depicting examples of some of the hottest bottom-hole temperature data from deep oil wells across New Mexico. The bottom-hole temperature data points are uncorrected because there are few wells available in the vicinity of these sites to formulate a proper correction. Source: Shari Kelley.*

Expanding the Scope: Next-Generation Geothermal Opportunities

Veit Matt and Trent McFadyen, Project InnerSpace

New Mexico holds significant potential for the development of next-generation geothermal technologies in the state's sedimentary basins and deep subsurface for a variety of use cases, including heating and cooling for the built environment, industrial process heat, and the production of electricity.

New Mexico is one of only seven U.S. states that creates electricity from conventional hydrothermal systems—and as readers can see in the previous pages of this chapter, the state has plenty of subsurface resources it can use to develop much more conventional hydrothermal. Add to that: many portions of the state have substantial potential for conductive geothermal systems—also known as *next-generation geothermal*.

As explained in Chapter 1, "Geothermal 101," next-generation geothermal uses oil and gas technologies—horizontal drilling and/or hydraulic fracturing—to tap into subsurface heat even where there is no (or very slow) natural fluid flow as there is in hydrothermal geothermal and deep groundwater systems. By drilling into these hot dry rocks or hot (sedimentary or naturally fractured rock) aquifers, developers can enable the spread of a new era of geothermal projects across New Mexico.

The maps and text in this section complement the information in the previous pages, which is largely an examination of New Mexico's classic hydrothermal systems. By expanding the scope to look at heat extracted from all types of geothermal systems, we get a more comprehensive picture of New Mexico's geothermal potential. This section serves as a guide for readers without extensive geothermal

ESTIMATED SUBSURFACE TEMPERATURE AT 1 KM: 110°F (43°C) OR COLDER

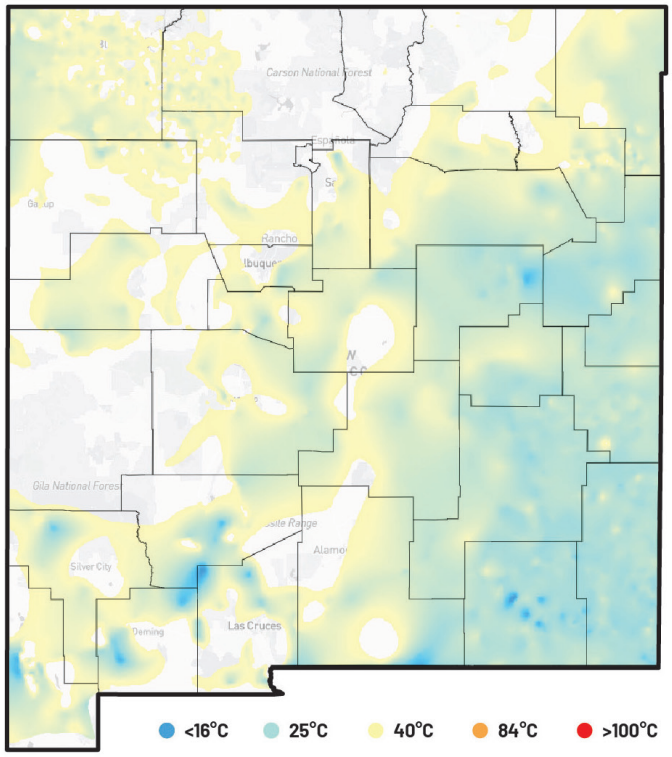

Figure 3.34. Based on available uncorrected well temperature data from both convective hydrothermal and conductive geothermal systems. The legend provides reference colors on a sliding scale of gradients. Source: Project InnerSpace (n.d.). GeoMap.

Disclaimer: Although the maps and analyses in this chapter highlight areas of geothermal potential, additional site-specific analyses—including economic and engineering and rock hydraulic property, fluid pressure, fluid composition, and fluid production rate analyses—are required to identify viable potential uses and drill-ready prospects.

ESTIMATED SUBSURFACE TEMPERATURE AT 1 KM: HOTTER THAN 110°F (43°C)

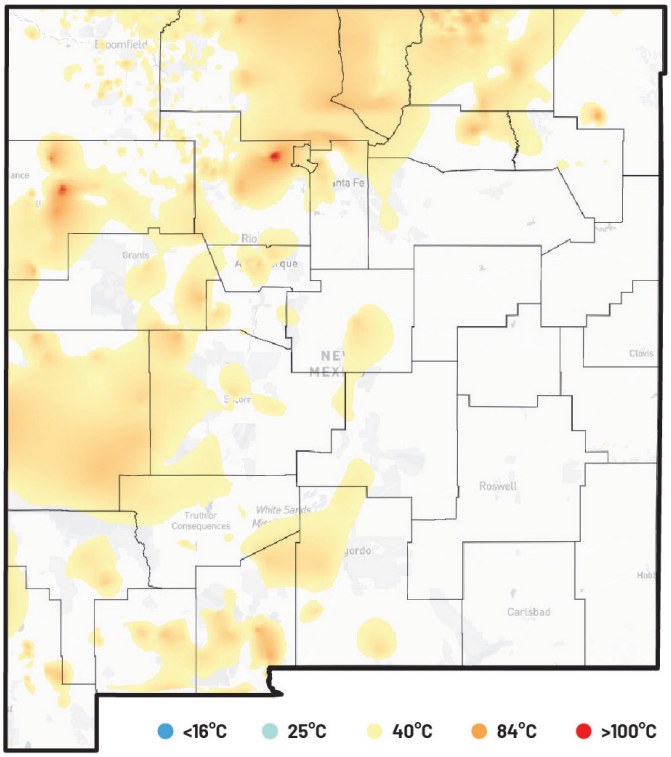

Figure 3.35. Based on available uncorrected well temperature data from both convective hydrothermal and conductive geothermal systems. The legend provides reference colors on a sliding scale of gradients. Source: Project InnerSpace, GeoMap

Note: While Figures 3.34 and 3.35 use red and blue shading, with red indicating hotter temperatures at 1 kilometer, red in Figures 3.36 and 3.37 represents areas requiring greater depth to reach the specified temperatures. Green shading shows shallower, more favorable geothermal locations (see legends for the figures).

expertise and provides additional analysis of New Mexico's subsurface. It also highlights the next-generation geothermal potential in the state's sedimentary basins and deep subsurface, with summary temperature-depth maps. Finally, it aims to help identify the lowest-hanging fruit: the geothermal applications that can most easily and most economically be developed.

The analysis uses data from Project InnerSpace's open-access GeoMap tool, which provides essential data and analytics for assessing the development potential of next-generation geothermal systems worldwide. Some of those data points and methods differ from the inputs used in the other part of this chapter. Although the maps in this chapter do not denote what kind of system should be developed where, the individual spatial analysis throughout the chapter guides towards potential "sweet spots", where additional investigation and exploration might be warranted.

In summary, New Mexico's observed and modeled subsurface temperatures show potential for geothermal to be used to (1) heat and cool buildings with both ground source heat pumps and thermal energy networks, (2) power industrial processes with direct-use geothermal, and (3) generate geothermal electricity in selected "hot spots." Regardless of what maps and methods are used, the findings remain clear: New Mexico has significant geothermal potential, as it is possible to develop one or another kind of geothermal energy solution in many locations across the entire state. (See **Figure 3.38** for a map of what geothermal applications are likely possible in which parts of the state.)

OVERVIEW OF NEW MEXICO'S SUBSURFACE

Subsurface Temperature

Whether based on directly measured or modeled data, determining the depths required to reach a given subsurface temperature is a fundamental aspect of assessing a location's potential for geothermal energy.

Temperature at 1 Kilometer

Figure 3.34 shows areas of New Mexico colder than about 110°F at a depth of 3,281 feet underground (≤43°C at 1 kilometer). Although deeper drilling can access hotter temperatures, geothermal energy at or below 110°F is limited to heating and cooling buildings and certain low-temperature industrial or agricultural processes.

As a complement to the previous map, **Figure 3.35** shows locations in New Mexico with subsurface temperatures hotter than 110°F at 3,281 feet deep (>43°C at 1 kilometer). These hotter locations, whether classic hydrothermal or next-generation conductive, lend themselves to increasingly high-energy applications, including possible electricity generation under the best circumstances. See Chapter 1, "Geothermal 101," for additional details about the temperatures of various geothermal applications.

Depth to a Given Temperature

While **Figures 3.34 and 3.35** show different temperatures at a constant depth of 1 kilometer, the following figures illustrate how different depths are required to reach a specific temperature. **Figure 3.36** shows the depths needed to reach 212°F (100°C) across New Mexico, a temperature that could power many industrial processes (see Chapter 4, "Geothermal Heating and Cooling," for more information).

Figure 3.37 shows the depths needed to reach 300°F (≈150°C), the general minimum temperature threshold for generating geothermal electricity.[1] Green, yellow, and light orange areas reach 300°F (≈150°C) at shallower than 15,000 feet (≈4,600 meter)—depths regularly reached by U.S. oil and gas drillers.

OVERVIEW OF GEOTHERMAL APPLICATIONS GIVEN AVAILABLE ESTIMATED SUBSURFACE TEMPERATURES

New Mexico can develop geothermal energy in some form across the entire state. As suggested in the previous maps, given the temperatures and depths shown in **Figures 3.34 through 3.37**, certain geothermal

1 Franzmann, D., Heinrichs, H., & Stolten, D. (2025). Global geothermal electricity potentials: A technical, economic, and thermal renewability assessment. Renewable Energy, 250, 123199. https://doi.org/10.1016/j.renene.2025.123199.

ESTIMATED MINIMUM DEPTH TO REACH TEMPERATURES OF 212°F (100°C)

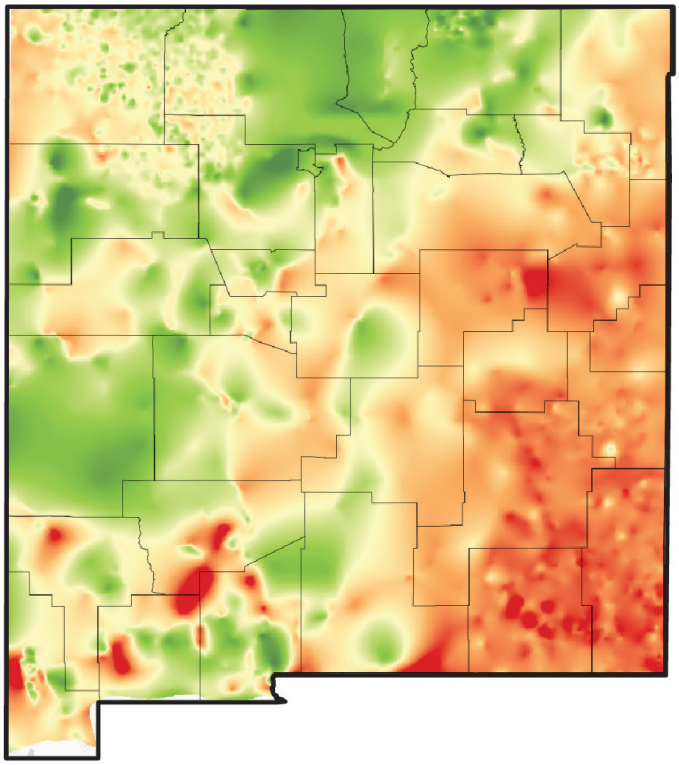

Figure 3.36. Based on available uncorrected well temperature data. The legend provides reference colors on a sliding scale of gradients. Source: Project InnerSpace, GeoMap.

- <1500m
- 1500-2500m
- 2500-3500m
- 3500-5000m
- >8000m

ESTIMATED MINIMUM DEPTH TO REACH TEMPERATURES OF 300°F (150°C)

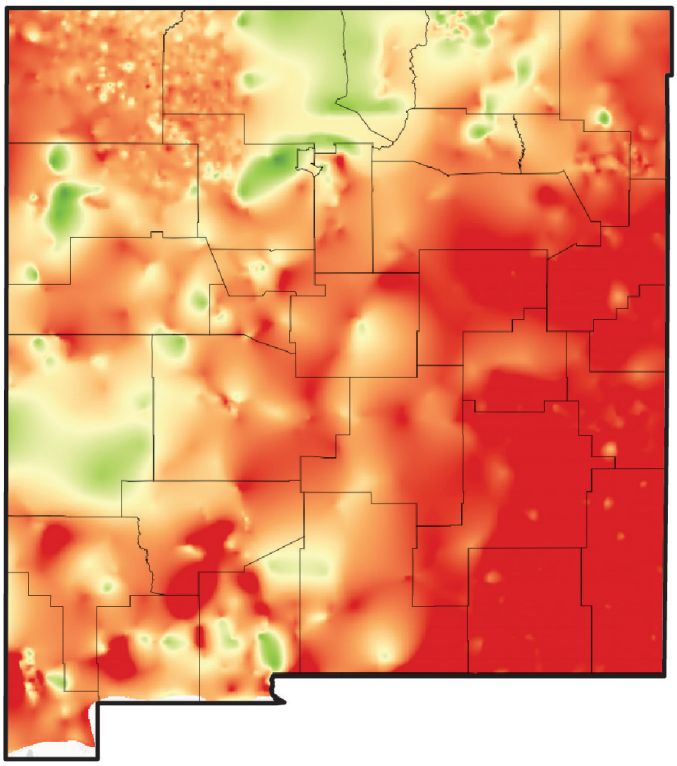

Figure 3.37. Based on available uncorrected well temperature data. The legend provides reference colors on a sliding scale of gradients. Two of the locations with the highest electricity potential—Gila Wilderness in the southwest and the Valles Caldera National Preserve in the north—currently have bans on development. Source: Project InnerSpace. GeoMap.

- <1500m
- 1500-2500m
- 2500-3500m
- 3500-5000m
- >8000m

GEOTHERMAL OPPORTUNITIES IN NEW MEXICO

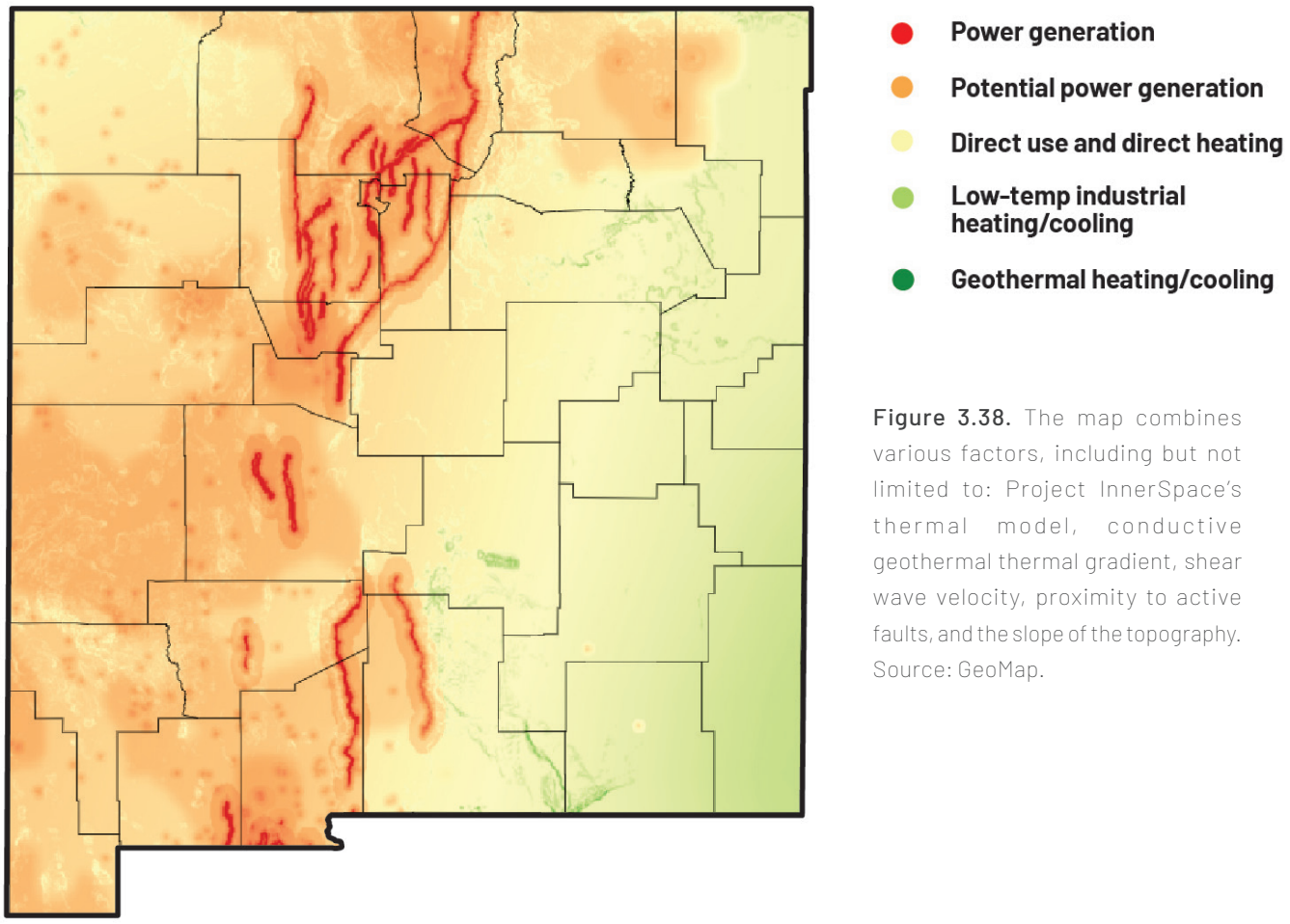

Figure 3.38. The map combines various factors, including but not limited to: Project InnerSpace's thermal model, conductive geothermal thermal gradient, shear wave velocity, proximity to active faults, and the slope of the topography. Source: GeoMap.

applications are more viable in some parts of New Mexico. **Figure 3.38** uses a weighted overlay analysis to map the favorability of developing different geothermal technologies across the state. Orange into red areas may be suitable for electricity generation. Lime green to yellow areas provide opportunities to use geothermal for low-temperature industrial and agricultural processes and for thermal energy networks. Dark green portions of the map are likely limited to using ground source heat pumps for heating and cooling buildings. Deeper drilling adds costs but might open up more opportunities.

Significant basin-by-basin analysis underlies the entirety of this analysis and can be viewed online in a draft report at https://storage.googleapis.com/project-innerspace-beta/pdf_resources/State-Geothermal-Evaluation-New-Mexico.pdf.

This full analysis reviews the methodologies used to develop the temperature maps in this section and introduces additional favorability-related analyses, such as conductive geothermal gradients, formation depth structures, and general rock-property information. The full scope of analysis is valuable for anyone attempting to further explore for specific geothermal development sites.

NEW MEXICO TEMPERATURE DATA AND CONDUCTIVE GEOTHERMAL GRADIENTS

The Project InnerSpace temperature data used to evaluate the deep next-generation geothermal potential of New Mexico is part of a U.S.-wide data set that has been compiled from numerous publicly available data sets.

INPUTS AND FACTOR CLASS

Inputs			Factor Class					
Used in Global Weighted Overlay Analysis (GeoMap)	**unit**	**weight% of total**	**0**	**1**	**2**	**3**	**4**	**5**
Proximity to Active/Recent Volcanoes	km	10	>10km	10km-5km	5km-3km	3km-2km	2km-1km	<1
Proximity to Thermal Springs	km	10	>5km	5km-3km	3km-2km	2km-1km	1km-0.5km	<0.5
Project InnerSpace Geothermal Gradiant Model	mW/m^2	30	<30	30-50	50-60	60-75	75-100	>100
Proximity to Active/Recent Faulting	km	30	>15km	5km-15km	5km-3km	3km-2km	2km-1km	<1
Average (Vs) in the Lithospheric Mantel Depth Range Between 110k m and 150 km	mW/m^2	20	>4.4189	4.3411-4.4189	4.2633-4.3411	4.1856-4.2633	4.1078-4.1856	<=4.1078

This analysis is based on the deep conductive geothermal gradient calculated based on temperature measurements taken at depths greater than 200 meters (≈650 ft) to minimize erroneous values related to "deep" circulating cold meteoric surface waters. To further improve the geothermal gradient map, erroneous negative values (<0.0°C/Km, <0.0°F/1,000ft) as well as excessively high thermal gradient values possibly associated with classic shallow hydrothermal systems (>100°C/Km, >55°F/1,000ft) have been removed (see **Equation 1**, **Figure 3.39, Figure 3.40**).

Well temperature data is concentrated in areas with current and historic oil and gas exploration and production (for example, the Permian, San Juan, and Raton basins). Data suitable for analyzing next-generation geothermal potential is less reliable outside these areas because most of the publicly available temperature measurements come from water wells. These wells are usually drilled to shallower depths to produce fresh or low-salinity water suitable for consumption and agricultural use (such as irrigation, livestock). In these low-density or no-data areas, detailed geophysical inversion modeling could improve estimated geothermal gradients.

The temperature-depth plot (**Figure 3.39**) shows the difference between the raw measured well temperature data and the provided corrected well temperature data. The difference in average regional thermal gradient between raw and corrected temperature values is highlighted by the "best-fit" linear trend lines. The average geothermal gradient based on the corrected temperatures is about 12% higher than the gradient based on the raw temperature data. Locally, the difference in geothermal gradient estimates can be significantly higher or lower.

To evaluate the geothermal potential of an area, one of the basic parameters to be calculated and mapped is the geothermal gradient, representing the increase of the rock temperature with depth:

Equation 1:

$$\textit{Geothermal Gradient} = \frac{\textit{Subsurface Temperature} - \textit{Surface Temperature}}{\textit{Measurement Depth}}$$

The calculation of the regional geothermal gradient maps for New Mexico is based on a smoothed average surface temperature National Oceanic and Atmospheric Administration (NOAA) map and the depth-temperature data collected by Project InnerSpace (**Figure 3.39**).

LOCATION AND DISTRIBUTION OF TEMPERATURE DATA IN NEW MEXICO

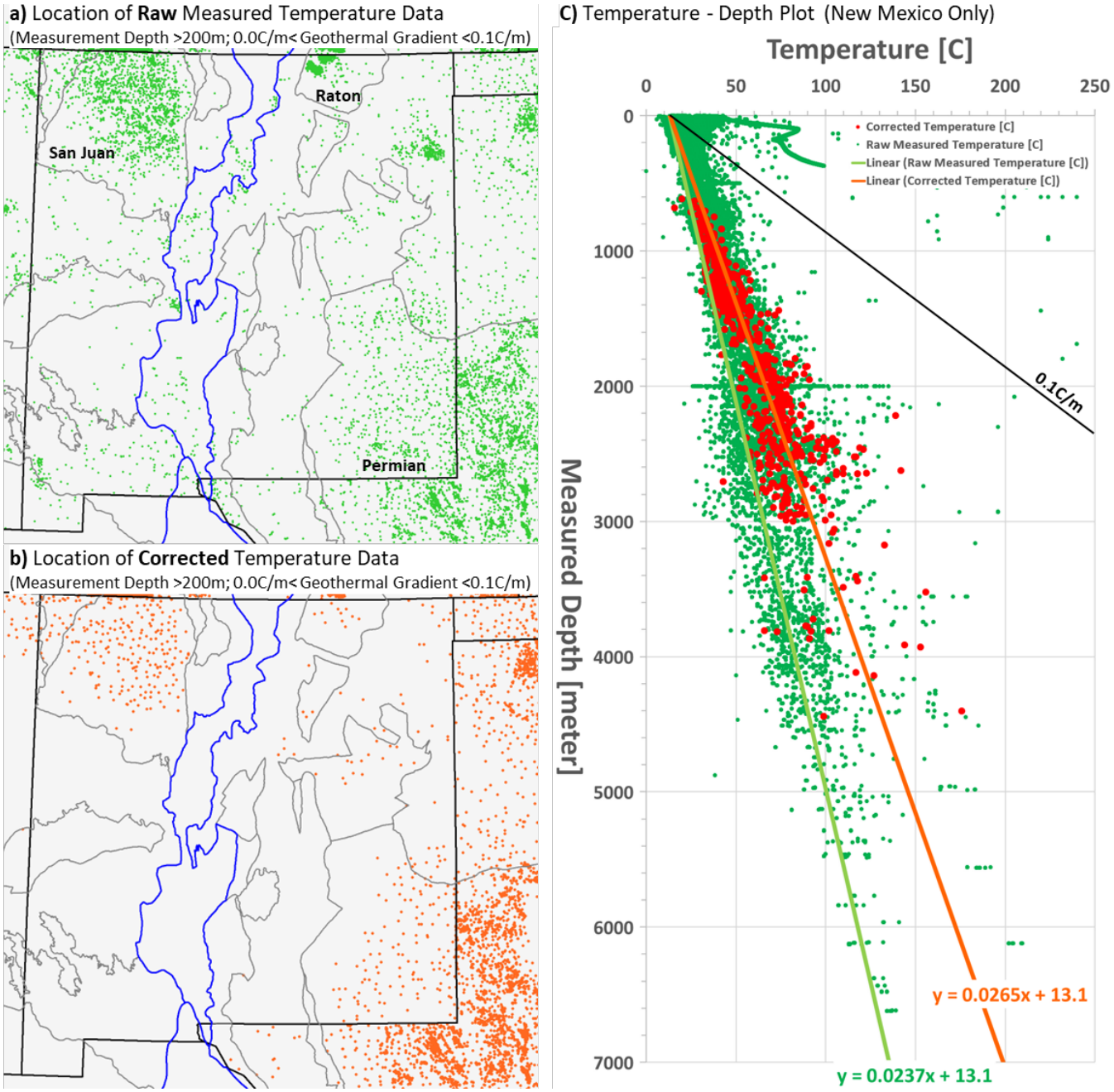

Figure 3.39. Location and distribution of (a) the raw measured temperature-depth and (b) the provided corrected temperature-depth data used. (c) Temperature-depth plot showing the difference between the used raw measured temperature data and the provided corrected temperature data. The equations for the linear best-fit lines are shown at the bottom of the plot area. The blue polygons show key basins along the central Rio Grande rift system. The gray polygons represent the outline of other prominent Paleozoic, Laramide, and Tertiary basins. Source: Project InnerSpace

UNCORRECTED AND CORRECTED DEEP CONDUCTIVE GEOTHERMAL GRADIENT MAPS FOR NEW MEXICO

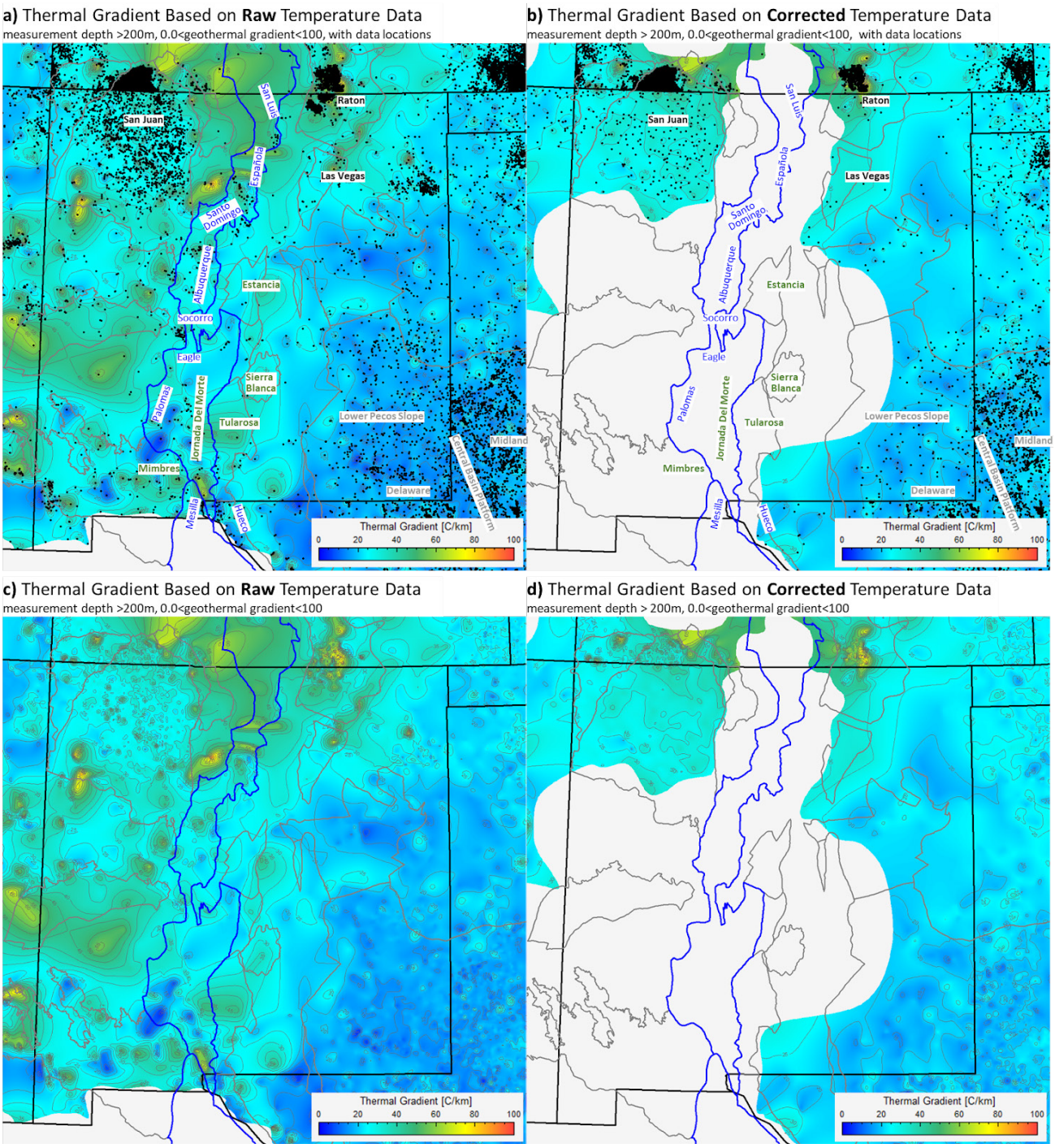

Figure 3.40. (a) and (b) include data control point locations, and (c) and (d) do not include data control point locations. The blue polygons show key basins along the central Rio Grande rift system. The gray polygons represent the outline of other prominent Paleozoic, Laramide, and Tertiary basins. Source: Project InnerSpace

UNCORRECTED AND CORRECTED DEEP CONDUCTIVE GEOTHERMAL GRADIENT MAPS FOR NEW MEXICO

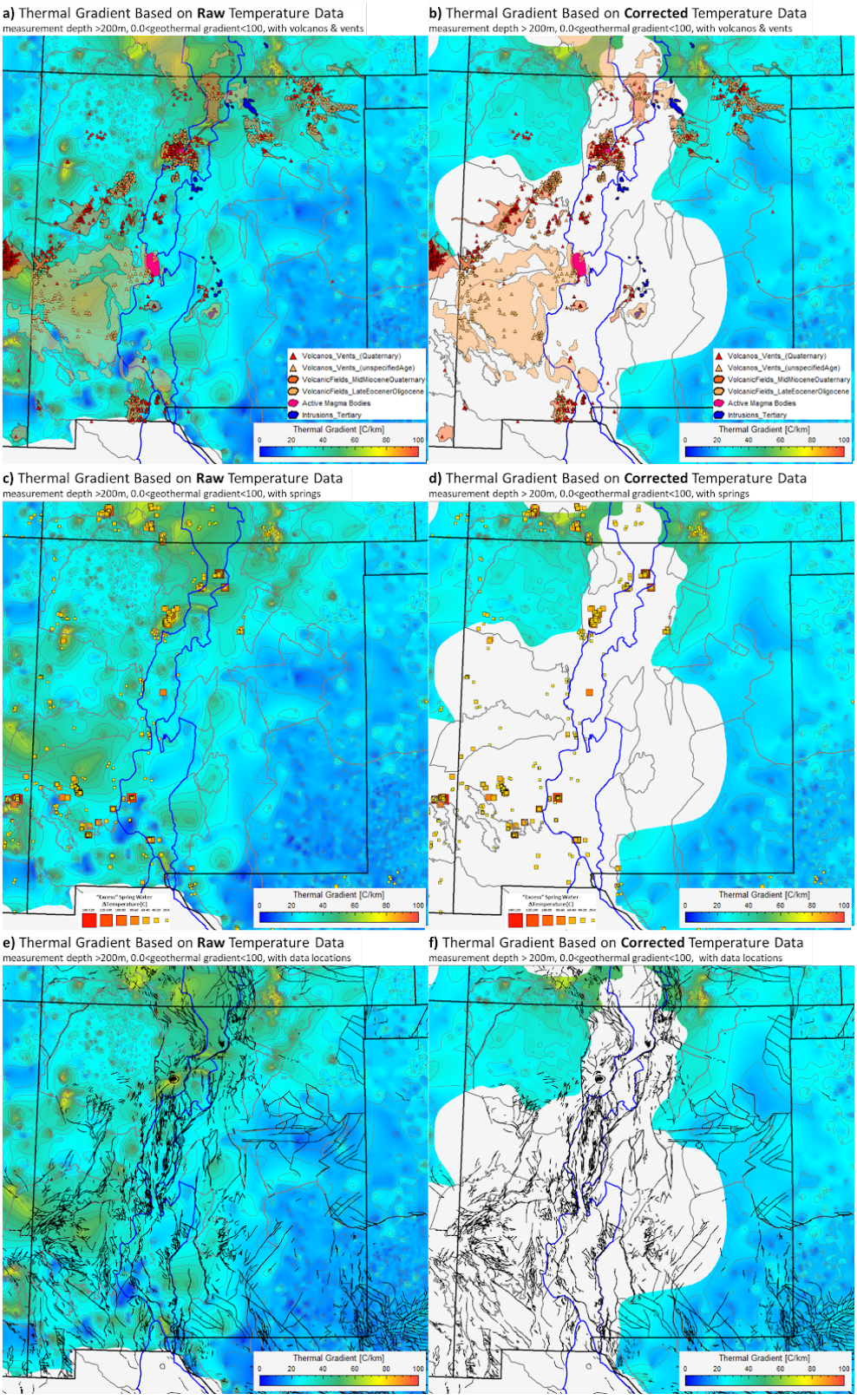

Figure 3.41: (a) and (b) with identified volcanoes and volcanic vents Tertiary and Quaternary in age; (c) and (d) with mapped "hot" springs (the provided Δ temperature represents the spring water temperature in excess of the average surface temperature); (e)and(f)with mapped faults. The blue polygons show key basins along the central Rio Grande rift system. The gray polygons represent the outline of other prominent Paleozoic, Laramide, and Tertiary basins. Sources: Repasch, M., Karlstrom, K., Heizler, M., & Pecha, M. (2017). Birth and evolution of the Rio Grande fluvial system in the past 8 Ma: Progressive downward integration and the influence of tectonics, volcanism, and climate. Earth-Science Reviews, 168, 113–164. https://doi.org/10.1016/j.earscirev.2017.03.003; Sussman, A. J., Lewis, C. J., Mason, S. N., Geissman, J. W., Schultz-Fellenz, E., Oliva-Urcia, B., & Gardner, J. (2011). Paleomagnetism of the Quaternary Bandelier Tuff: Implications for the tectonic evolution of the Española Basin, Rio Grande rift. Lithosphere, 3(5), 328–345. https://doi.org/10.1130/L128.1; Zimmerer, M. J. (2024) A temporal dissection of the late Quaternary volcanism and related hazards with the Rio Grande rift and along the Jemez Lineament of New Mexico, USA. Geosphere, 20(2), 505–546. https://doi.org/10.1130/GES02576.1

ISOTHERMAL DEPTH MAPS

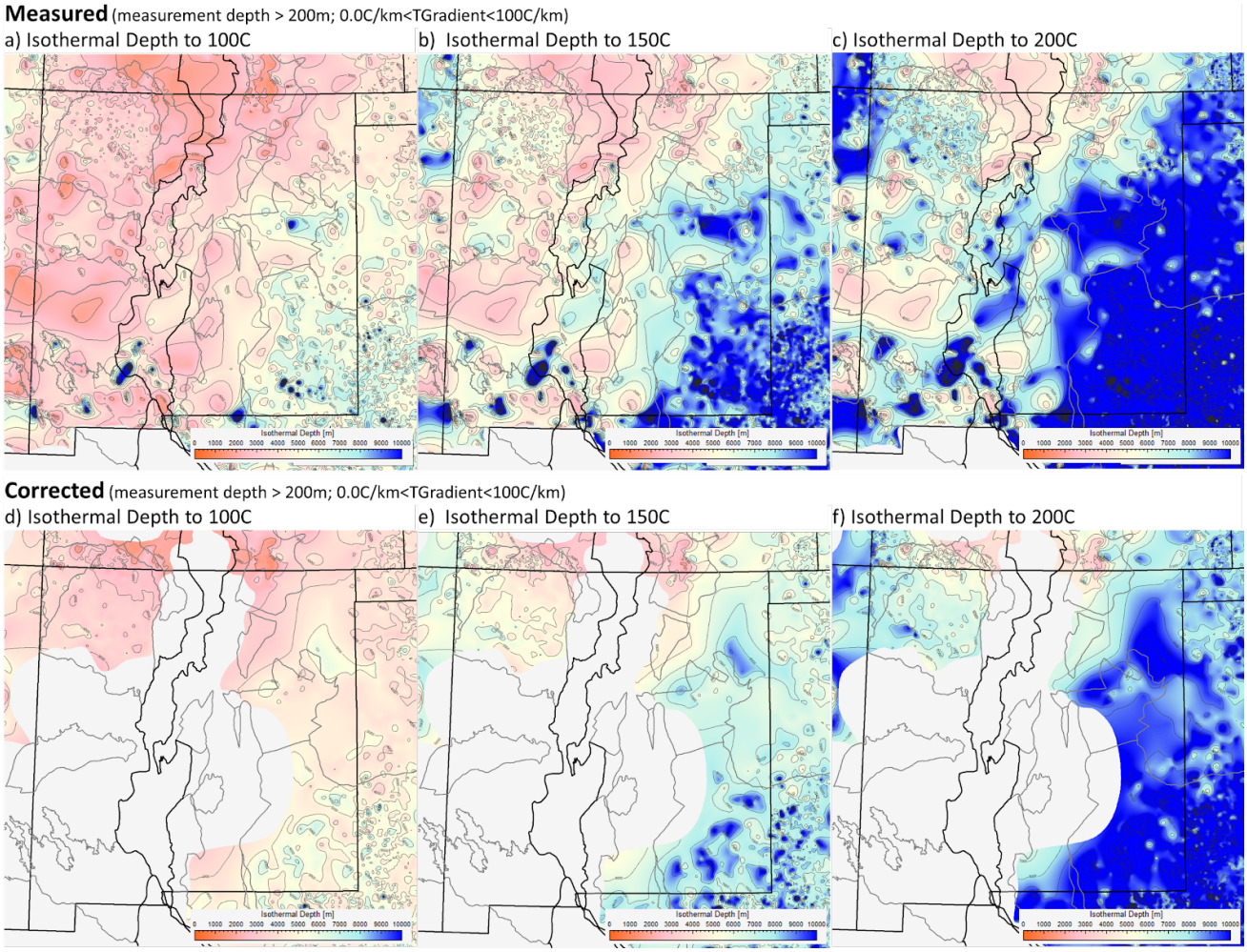

Figure 3.42: Isothermal depth maps based on uncorrected thermal gradients: (a) 100°C; (b) 150°C; and (c) 200°C. Isothermal depth maps based on corrected thermal gradients: (d) 100°C; (e) 150°C; and (f) 200°C. The black polygons show key basins along the central Rio Grande rift system. The gray polygons represent the outline of other prominent Paleozoic, Laramide, and Tertiary basins. Source: Project InnerSpace

ISOPACH AND TEMPERATURE MAPS

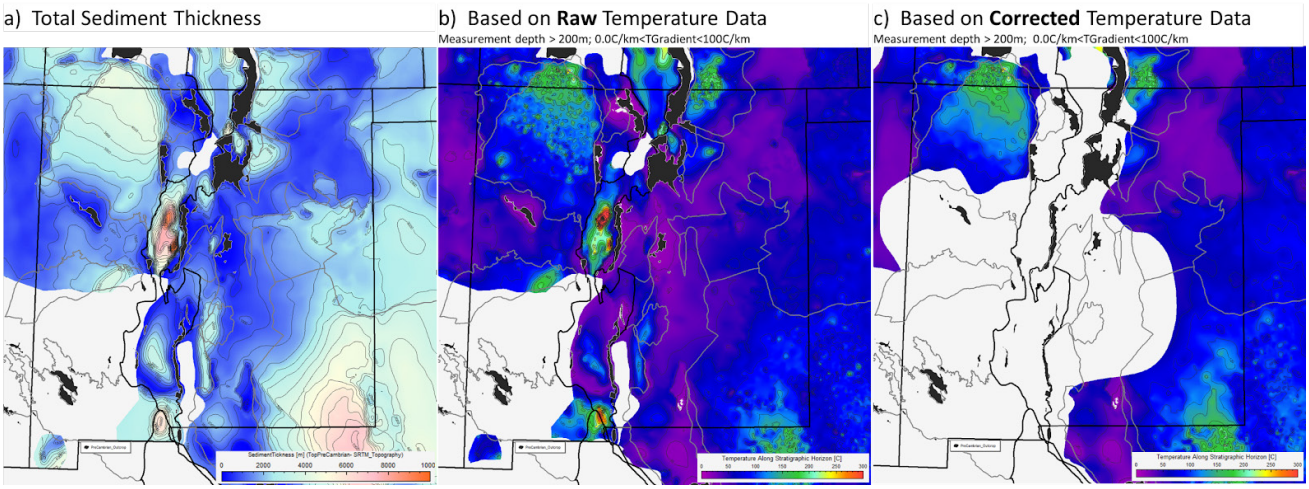

Figure 3.43. (a) Estimated total thickness of sediments (= depth to Precambrian basement); (b) Temperature along the top Precambrian basement based on the uncorrected thermal gradient map; (c) Temperature along the top Precambrian basement based on the corrected thermal gradient map. The black polygons show key basins along the central Rio Grande rift system. The gray polygons represent the outline of other prominent Paleozoic, Laramide, and Tertiary basins. Project InnerSpace..

New Mexico can be subdivided into two main sectors: the "cold" southeast corner of the state vs. the "hot" rest of the state. The "cold" sector is dominated by "old" Paleozoic tectonics and structures and related stratigraphic intervals and sediments, while the "hot" sector has been very active in the Cenozoic, as shown by the extensional tectonics and related Tertiary and Quaternary igneous and volcanic activity (**Figure 3.41a and b**). The high thermal gradient areas align well with the identified volcanoes and volcanic vents, as well as with the identified hot springs (**Figure 3.41c and d**). A mismatch between the igneous, volcanic, and hydrothermal features and the shown geothermal map is most likely related to the lack of available depth-temperature data. These possibly low thermal gradient areas represent areas for future studies and could benefit from additional new deep geothermal test wells.

While a slight correlation between the presence of hot springs and available faults can be seen, correlation between the available mapped faults (**Figures 3.41e** and **f**) and the presented geothermal gradient map is difficult to evaluate; not every existing fault at every scale has been, or can be mapped.

As shown in **Figures 3.36** and **3.37** and again in **Figure 3.42**, in New Mexico's "hot" sector, 100°C can be reached at between 2 kilometers and 3 kilometers, 150°C is reached at between 4 kilometers and 5 kilometers depth, and 200°C requires drilling to between 6 kilometers and 7 kilometers.

Figure 3.43 shows the temperature along the top of the Precambrian basement. By definition, the deeper the basement, the hotter the temperature (i.e., the deepest parts of the various basins). As expected, zones of decreased or increased rock temperature also coincide with the areas of decreased or increased geothermal gradient (**Figure 3.40**). This is most prominent in the deeper parts of the Delaware Basin, which shows relatively low temperatures due to the low local geothermal gradients *and* the higher temperatures in the San Juan and Raton Basins at moderate depths. The large amount of "white space" is due to the lack of temperature data as well as missing top Precambrian basement depth information. We encourage other researchers to gather additional top basement depth data to update, correct, and extend the existing map data set.

CHAPTER REFERENCES

1 Roberts, B. J. (2018). *Geothermal resources of the United States: Identified hydrothermal sites and favorability of deep enhanced geothermal systems (EGS)*. National Renewable Energy Laboratory. https://www.nrel.gov/docs/libraries/gis/high-res-images/geothermal-identified-hydrothermal-and-egs.jpg?sfvrsn=94d5211_1

2 Aljubran, M. J., & Horne, R. N. (2024). Thermal Earth model for the conterminous United States using an interpolative physics-informed graph neural network. *Geothermal Energy*, *12*(1), 25. https://doi.org/10.1186/s40517-024-00304-7

3 Gao, W., Grand, S. P., Baldridge, W. S., Wilson, D., West, M., Ni, J. F., & Aster, R. (2004). Upper mantle convection beneath the central Rio Grande Rift imaged by P- and S-wave tomography. *Journal of Geophysical Research*, *109*(B3). https://doi.org/10.1029/2003JB002743

4 Wilson, D., Aster, R., Ni, J., Grand, S., West, M., Gao, W., Baldridge, W. S., & Semken, S. (2005). Imaging the seismic structure of the crust and upper mantle beneath the Great Plains, Rio Grande Rift, and Colorado Plateau using receiver functions. *Journal of Geophysical Research*, *110*(B5), B05306. https://doi.org/10.1029/2004JB003492

5 Schmandt, B., & Humphreys, E. (2010). Complex subduction and small-scale convection revealed by body-wave tomography of the western United States upper mantle. *Earth and Planetary Science Letters*, *297*, 435–445. https://doi.org/10.1016/j.epsl.2010.06.047

6 MacCarthy, J. K., Aster, R. C., Dueker, K., Hansen, S., Schmandt, B., & Karlstrom, K. (2014). Seismic tomography of the Colorado Rocky Mountains upper mantle from CREST: Lithosphere–asthenosphere interactions and mantle support of topography. *Earth and Planetary Science Letters*, *402*, 107–119. https://doi.org/10.1016/j.epsl.2014.03.063

7 Wilgus, J., Schmandt, B., Maguire, R., Jiang, C., & Chaput, J. (2023). Shear velocity evidence of upper crustal magma storage beneath Valles Caldera. *Geophysical Research Letters*, *50*(5), e2022GL101520. https://doi.org/10.1029/2022GL101520

8 Anderson, J., Wills, O., James, N., Broadhurst, T., Lenci, T., Brambila, I., Laferriere, L., Bedrosian, P., Peacock, J., Kelley, S., Ferguson, J. F., Anderson, M. L., Azevedo, O., & Smith, E. (2024). *Investigating the Valles and Toledo Calderas, New Mexico, using gravity and magnetotelluric methods* [Abstract GP11A-3563]. American Geophysical Union.

9 Goff, F., & Kelley, S. A. (2021). Facts and hypotheses regarding the Miocene–Holocene Jemez Lineament, New Mexico, Arizona and Colorado. *New Mexico Geological Society Guidebook*, *71*, 101–116. https://doi.org/10.56577/FFC-71.101

10 Zimmerer, M. J. (2024). A temporal dissection of late Quaternary volcanism and related hazards within the Rio Grande rift and along the Jemez lineament of New Mexico, USA. *Geosphere*, *20*(2), 505–546. https://doi.org/10.1130/GES02576.1

11 Burnham, J. B., & Stewart, D. H. (1970). Economics of plowshare geothermal power. In *Proceedings of the Symposium on Engineering with Nuclear Explosives* (pp. 1376–1383). International Atomic Energy Agency.

12 Smith, M. C. (1983). A history of hot dry rock geothermal energy systems. *Journal of Volcanology and Geothermal Research*, *15*, 1–20. https://doi.org/10.1016/0377-0273(83)90093-8

13 Swanberg, C. A. (1980). *Chemistry, origin, and geothermal potential of thermal and non-thermal waters in New Mexico* [Unpublished report submitted under U.S. Geological Survey Grant 14-08-0001-6-255]

14 Swanberg, C. A. (1984). *Geothermal resources of the Rio Grande rift* (Report NMERDI 2-69-2208). New Mexico Energy Research and Development Institute.

15 Icerman, L., & Lohse, R. L. (1983). *Geothermal low-temperature reservoir assessment in Doña Ana County, New Mexico* (Report NMERDI 2-69-2202). New Mexico Energy Research and Development Institute. https://doi.org/10.2172/6801873

16 Witcher, J. C. (1988). Geothermal resources of southwestern New Mexico and southeastern Arizona. *New Mexico Geological Society Guidebook*, *49*, 191–197. https://doi.org/10.56577/FFC-39.191

17 Jiracek, G. R., Gustafson, E. P., & Parker, M. D. (1982). Geophysical exploration for geothermal prospects west of Albuquerque, New Mexico. *New Mexico Geological Society Guidebook*, *33*, 333–342. https://doi.org/10.56577/FFC-33.333

18 Reiter, M., Edwards, C. L., Hartman, H., & Weidman, C. (1975). Terrestrial heat flow along the Rio Grande rift, New Mexico and southern Colorado. *GSA Bulletin*, *86*(6), 811–818. https://doi.org/10.1130/0016-7606(1975)86<811:TFATR>2.0.CO;2

19 Summers, W. K. (1976). *Catalog of thermal waters in New Mexico* (Hydrologic Report 4). New Mexico Bureau of Mines and Mineral Resources.

20 Norman, D. E., & Bernhardt, C. A. (1982). *Assessment of geothermal reservoirs by analysis of gases in thermal waters* (Report EMD 2-68r2305). New Mexico Research and Development Institute.

21 Barroll, M. W., & Reiter, M. (1990). Analysis of the Socorro hydrogeothermal system: Central New Mexico. *Journal of Geophysical Research*, *95*, 21949–21964. https://doi.org/10.1029/JB095iB13p21949

22 Dadi, S., Norbeck, J., Tiov, A., Dyer, B., Mohammadi, A., Geng, Y., Obinna, K., Nakata, N., & Matson, G. (2024). Microseismic monitoring during a next generation Enhanced Geothermal System at Cape Modern, Utah. *GRC Transactions*, 48, 1673–1698.

23 Fercho, S., Matson, G., McConville, E., Rhodes, G., Jordan, R., & Norbeck, J. (2024, February 12–14). *Geology, temperature, geophysics, stress orientations, and natural fracturing in the Milford Valley, UT, informed by the drilling results of the first horizontal wells at the Cape Modern Geothermal Project*. 49th Workshop on Geothermal Reservoir Engineering, Stanford University, Stanford, CA, United States.

24 Kelley, S. A., & Price, L. J. (2020). A brief introduction to the geology of southern New Mexico. In P. A. Scholle, D. S. Ullmer-Scholle, S. M. Cather, & S. A. Kelley (Eds.), *The geology of southern New Mexico's parks, monuments, and public lands* (pp. 7–15). New Mexico Bureau of Geology and Mineral Resources.

25 Kelley, S. A., & Price, L. J. (2020). A brief introduction to the geology of southern New Mexico. In P. A. Scholle, D. S. Ullmer-Scholle, S. M. Cather, & S. A. Kelley (Eds.), *The geology of southern New Mexico's parks, monuments, and public lands* (pp. 7–15). New Mexico Bureau of Geology and Mineral Resources.

26 Berglund, H. T., Sheehan, A. F., Murray, M. H., Roy, M., Lowry, A. R., Nerem, R. S., & Blume, F. (2012). Distributed deformation across the Rio Grande Rift, Great Plains, and Colorado Plateau. *Geology*, *40*(1), 23–26. https://doi.org/10.1130/G32418.1

27 Zimmerer, M. J., Lafferty, J., & Coble, M. A. (2016). The eruptive and magmatic history of the youngest pulse of volcanism at the Valles Caldera: Implications for successfully dating late Quaternary eruptions. *Journal of Volcanology and Geothermal Research*, *310*, 50–57. https://doi.org/10.1016/j.jvolgeores.2015.11.021

28 Nielson, D. L., & Hulen, J. B. (1984). Internal geology and evolution of the Redondo Dome, Valles Caldera, New Mexico. *Journal of Geophysical Research*, *89*(B10), 8695–8711. https://doi.org/10.1029/JB089iB10p08695

29 Hulen, J. B., Nielson, D. L., & Little, T. M. (1991). Evolution of the Western Valles Caldera Complex, New Mexico: Evidence from intracaldera sandstones, breccias, and surge deposits. *Journal of Geophysical Research*, *96*(B5), 8127–8142. https://doi.org/10.1029/91JB00374

30 Goff, F., Gardner, J., Baldridge, W., Hulen, J., Nielson, D., Vaniman, D., Heiken, G., Dungan, M., & Broxton, D. (1989). *Excursion 17B: Volcanic and hydrothermal evolution of the Valles Caldera and Jemez volcanic field.* New Mexico Bureau of Mines and Mineral Resources.

31 Goff, F., & Gardner, J. N. (1994). Evolution of a mineralized geothermal system, Valles Caldera, New Mexico. *Economic Geology*, *89*(8), 1803–1832. https://doi.org/10.2113/gsecongeo.89.8.1803

32 Goff, F., & Goff, C.J. (2017). *Energy and mineral resources of New Mexico: Overview of the Valles caldera (Baca) geothermal system.* New Mexico Bureau of Geology and Mineral Resources. https://doi.org/10.58799/M-50F

33 Goff, F., & Goff, C.J. (2017). *Energy and mineral resources of New Mexico: Overview of the Valles caldera (Baca) geothermal system.* New Mexico Bureau of Geology and Mineral Resources. https://doi.org/10.58799/M-50F

34 Laughlin, A. W. Eddy, A. C., Laney, R., & Aldrich, M. J., Jr. (1983). Geology of the Fenton Hill, New Mexico, hot dry rock site. *Journal of Volcanology and Geothermal Research*, *15*, 21–41. https://doi.org/10.1016/0377-0273(83)90094-X

35 Kelkar, S. M., WoldeGabriel, G., & Rehfeldt, K. (2016). Lessons learned from the pioneering hot dry rock project at Fenton Hill, USA. *Geothermics*, *63*, 5–14. https://doi.org/10.1016/j.geothermics.2015.08.008

36 Goff, F., Shevenell, L., Gardner, J. N., Vuataz, F.-D., & Grigsby, C. O. (1988). The hydrothermal outflow plume of Valles Caldera, New Mexico, and a comparison with other outflow plumes. *Journal of Geophysical Research*, *93*(B6), 6041–6058. https://doi.org/10.1029/JB093iB06p06041

37 Goff, F., & Gardner, J. N. (1994). Evolution of a mineralized geothermal system, Valles Caldera, New Mexico. *Economic Geology*, *89*(8), 1803–1832. https://doi.org/10.2113/gsecongeo.89.8.1803

38 Goff, F., & Goff, C.J. (2017). *Energy and mineral resources of New Mexico: Overview of the Valles caldera (Baca) geothermal system.* New Mexico Bureau of Geology and Mineral Resources. https://doi.org/10.58799/M-50F

39 Kutscher, C. (2001). *Small-scale geothermal power plant field verification projects* (No. NREL/CP-550-30275). National Renewable Energy Lab.

40 Mailloux, B. J., Person, M., Kelley, S., Dunbar, N., Cather, S., Strayer, L., & Hudleston, P. (1999). Tectonic controls on the hydrogeology of the Rio Grande Rift, New Mexico. *Water Resources Research*, *35*(9), 2641–2659. https://doi.org/10.1029/1999WR900110

41 Pepin, J., Person, M., Phillips, F., Kelley, S., Timmons S., Owens, L., Witcher, J., & Gable, C. (2015). Deep fluid circulation within crystalline basement rocks and the role of hydrologic windows in the formation of the Truth or Consequences, New Mexico low-temperature geothermal system. *Geofluids*, *15*, 139–160. https://doi.org/10.1111/gfl.12111

42 Pepin, J., Person, M., Phillips, F., Kelley, S., Timmons S., Owens, L., Witcher, J., & Gable, C. (2015). Deep fluid circulation within crystalline basement rocks and the role of hydrologic windows in the formation of the Truth or Consequences, New Mexico low-temperature geothermal system. *Geofluids*, *15*, 139–160. https://doi.org/10.1111/gfl.12111

43 Jolie, E., Scott, S., Faulds, J., Chambefort, I., Axelsson, G., Gutiérrez-Negrín, L. C., Regenspurg, S., Ziegler, M., Ayling, B., Richter, A., & Zemedkun, M. T. (2021). Geological controls on geothermal resources for power generation. *Nature Reviews Earth & Environment*, *2*(5), 324–339. https://doi.org/10.1038/s43017-021-00154-y

44 Snow, D. T. (1965). *A parallel plate model of fractured permeable media* [Doctoral dissertation]. University of California, Berkeley.

45 Mailloux, B. J., Person, M., Kelley, S., Dunbar, N., Cather, S., Strayer, L., & Hudleston, P. (1999). Tectonic controls on the hydrogeology of the Rio Grande Rift, New Mexico. *Water Resources Research*, *35*(9), 2641–2659. https://doi.org/10.1029/1999WR900110

46 Pepin, J., Person, M., Phillips, F., Kelley, S., Timmons S., Owens, L., Witcher, J., & Gable, C. (2015). Deep fluid circulation within crystalline basement rocks and the role of hydrologic windows in the formation of the Truth or Consequences, New Mexico low-temperature geothermal system. *Geofluids*, *15*, 139–160. https://doi.org/10.1111/gfl.12111

47 Barroll, M. W., & Reiter, M. (1990). Analysis of the Socorro hydrogeothermal system: Central New Mexico. *Journal of Geophysical Research*, *95*, 21949–21964. https://doi.org/10.1029/JB095iB13p21949

48 Mailloux, B. J., Person, M., Kelley, S., Dunbar, N., Cather, S., Strayer, L., & Hudleston, P. (1999). Tectonic controls on the hydrogeology of the Rio Grande Rift, New Mexico. *Water Resources Research*, *35*(9), 2641–2659. https://doi.org/10.1029/1999WR900110

49 Witcher, J. C., Schoenmackers, R., & Whittier, J. (1988). *Geologic, geohydrologic, and thermal settings of southern New Mexico geothermal resources* (Technical Report DE-FG07-84ID12546). New Mexico Statewide Geothermal Energy Program.

50 Mailloux, B. J., Person, M., Kelley, S., Dunbar, N., Cather, S., Strayer, L., & Hudleston, P. (1999). Tectonic controls on the hydrogeology of the Rio Grande Rift, New Mexico. *Water Resources Research*, *35*(9), 2641–2659. https://doi.org/10.1029/1999WR900110

51 Morgan, P., & Witcher, J. C. (2011). Geothermal resources along the southern Rocky Mountains and the Rio Grande rift. *The Mountain Geologist*, *48*(4), 81–93.

52 Witcher, J. C. (1991). Radon soil-gas surveys with diffusion-model corrections in geothermal exploration. *Geothermal Resources Council Transactions*, *15*, 301–308.

53 Witcher, J. C. (1991). The Rincon geothermal system, southern Rio Grande Rift, New Mexico: A preliminary report on a recent discovery. *Geothermal Resources Council Transactions*, *15*, 202–212.

54 Bielicki, J., Blackwell, D., Harp, D., Karra, S., Kelley, R., Kelley, S., Middleton, R., Pepin, J., Person, M., Sutula, G., & Witcher, J. (2015). *Hydrogeologic windows: Regional signature detection for blind and traditional geothermal Play Fairways applied to Southwestern New Mexico*. [Data set]. Geothermal Data Repository. Los Alamos National Laboratory. https://gdr.openei.org/submissions/611

55 Witcher, J. C., Schoenmackers, R., & Whittier, J. (1988). *Geologic, geohydrologic, and thermal settings of southern New Mexico geothermal resources* (Technical Report DE-FG07-84ID12546). New Mexico Statewide Geothermal Energy Program.

56 Vesselinov, V. V., Ahmmed, B., Mudunuru, M. K., Pepin, J. D., Burns, E. R., Siler, D. L., Karra, S., & Middleton, R. S. (2022). Discovering hidden geothermal signatures using non-negative matrix factorization with customized k-means clustering. *Geothermics*, *106*, 102576. https://doi.org/10.1016/j.geothermics.2022.102576

57 Holmes, R. C., & Fournier, A. (2022). Machine learning-enhanced Play Fairway Analysis for uncertainty characterization and decision support in geothermal exploration. *Energies*, *15*(5), 1929. https://doi.org/10.3390/en15051929

58 See Table 3 in Vesselinov, V. V., Ahmmed, B., Mudunuru, M. K., Pepin, J. D., Burns, E. R., Siler, D. L., Karra, S., & Middleton, R. S. (2022). Discovering hidden geothermal signatures using non-negative matrix factorization with customized *k*-means clustering. *Geothermics*, *106*, 102576. https://doi.org/10.1016/j.geothermics.2022.102576

59 Swanberg, C. (1979). Chemistry of thermal and non-thermal groundwaters in the Rio Grande Rift and adjacent tectonic provinces. In R. R. Riecker (Ed.), *Rio Grande rift: Tectonics and magmatism* (pp. 279–288). American Geophysical Union.

60 Holmes, R. C., & Fournier, A. (2022). Machine learning-enhanced Play Fairway Analysis for uncertainty characterization and decision support in geothermal exploration. *Energies*, *15*(5), 1929. https://doi.org/10.3390/en15051929

61 Holmes, R. C., & Fournier, A. (2022). Machine learning-enhanced Play Fairway Analysis for uncertainty characterization and decision support in geothermal exploration. *Energies*, *15*(5), 1929. https://doi.org/10.3390/en15051929

62 Sanford, A. R., Alptekin, Ö., & Topozada, T. R. (1973). Use of reflection phases on microearthquake seismograms to map an unusual discontinuity beneath the Rio Grande rift. *Bulletin of the Seismology Society of America*, *63*(6-1), 2021–2034. https://doi.org/10.1785/BSSA0636-12021

63 Axen, G., van Wijk, J., Phillips, F., Harrison, B., Sion, B., Yao, S., & Love, D. (2019). The Socorro Magma Body. *New Mexico Earth Matters*, *19*(1), 1–6.

64 Brown, L. D., Krumhans, P. A., Chapin, C. E., Sanford, A. R., Cook, F. A., Kaufman, S., Oliver, J. E., & Schlit, F. S. (1979). COCORP reflection studies of the Rio Grande rift. In R. E. Reicker (Ed.), *Rio Grande Rift: Tectonics and magmatism* (pp. 127–145). American Geophysical Union.

65 Rinehart, E. J., Sanford, A. R., & Ward, R. M. (1979). Geographic extent and shape of an extensive magma body at mid-crustal depths in the Rio Grande rift near Socorro, New Mexico. In R. E. Reiker (Ed.), *Rio Grande rift: Tectonics and magmatism* (pp. 237–251). American Geophysical Union. https://doi.org/10.1029/SP014p0237

66 Rinehart, E. J., Sanford, A. R., & Ward, R. M. (1979). Geographic extent and shape of an extensive magma body at mid-crustal depths in the Rio Grande rift near Socorro, New Mexico. In R. E. Reiker (Ed.), *Rio Grande rift: Tectonics and magmatism* (pp. 237–251). American Geophysical Union. https://doi.org/10.1029/SP014p0237

67 Balch, R. S., Hartse, H. E., Sanford, A. R., & Lin, K.-w. (1997). A new map of the geographic extent of the Socorro mid-crustal magma body. *Bulletin of the Seismological Society of America*, *87*(1), 174–182. https://doi.org/10.1785/BSSA0870010174

68 Williams, A. J., Crossey, L. J., Karlstrom, K. E., Newell, D., Person, M., & Woolsey, E. (2013). Hydrogeochemistry of the Middle Rio Grande aquifer system—Fluid mixing and salinization of the Rio Grande due to fault inputs. *Chemical Geology*, *351*, 281–298. https://doi.org/10.1016/j.chemgeo.2013.05.029

69 Fialko, Y., & Simons, M. (2001). Evidence for on-going inflation of the Socorro Magma Body, New Mexico, from interferometric aperture radar imaging. *Geophysical Research Letters*, *28*(18), 3549–3552. https://doi.org/10.1029/2001GL013318

70 Fialko, Y., & Simons, M. (2001). Evidence for on-going inflation of the Socorro Magma Body, New Mexico, from interferometric aperture radar imaging. *Geophysical Research Letters*, *28*(18), 3549–3552. https://doi.org/10.1029/2001GL013318

71 Axen, G., van Wijk, J., Phillips, F., Harrison, B., Sion, B., Yao, S., & Love, D. (2019). The Socorro Magma Body. *New Mexico Earth Matters*, *19*(1), 1–6.

72 Stankova, J., Bilek, S. L., Rowe, C. A., & Aster, R. C. (2008). Characteristics of the October 2005 microearthquake swarm and reactivation of similar event seismic swarms over decadal time periods near Socorro, New Mexico. *Bulletin of the Seismological Society of America*, *98*, 93–105. https://doi.org/10.1785/0120070108

73 Ruhl C., Bilek S. L., & Stankova-Pursley, J. (2010). Relocation and characterization of the August 2009 microearthquake swarm above the Socorro magma body in the central Rio Grande Rift. *Geophysical Research Letters*, *37*(23), L23304. https://doi.org/10.1029/2010GL045162

74 Stankova, J., Bilek, S. L., Rowe, C. A., & Aster, R. C. (2008). Characteristics of the October 2005 microearthquake swarm and reactivation of similar event seismic swarms over decadal time periods near Socorro, New Mexico. *Bulletin of the Seismological Society of America*, *98*, 93–105. https://doi.org/10.1785/0120070108

75 Ruhl C., Bilek S. L., & Stankova-Pursley, J. (2010). Relocation and characterization of the August 2009 microearthquake swarm above the Socorro magma body in the central Rio Grande Rift. *Geophysical Research Letters*, *37*(23), L23304. https://doi.org/10.1029/2010GL045162

76 Reiter, M., Chamberlin, R. M., & Love, D.W. (2010). New data reflect on the thermal antiquity of the Socorro magma body locale, Rio Grande Rift, New Mexico. *Lithosphere, 2*(6), 447–453. https://doi.org/10.1130/L115.1

77 Reiter, M., Chamberlin, R. M., & Love, D.W. (2010). New data reflect on the thermal antiquity of the Socorro magma body locale, Rio Grande Rift, New Mexico. *Lithosphere, 2*(6), 447–453. https://doi.org/10.1130/L115.1

78 Woolsey, E. E. (2017). *Hydrologic modeling assessment of deep regional flow systems within the Albuquerque Basin using thermal, geochemical, and geomechanical tracers* [Master's thesis]. New Mexico Institute of Mining and Technology.

79 Woolsey, E. E. (2017). *Hydrologic modeling assessment of deep regional flow systems within the Albuquerque Basin using thermal, geochemical, and geomechanical tracers* [Master's thesis]. New Mexico Institute of Mining and Technology.

80 Reiter, M., Simmons, G., Chessman, M., England, T., Hartman, H., & Weidman, C. (1976). Terrestrial heat flow near Datil, New Mexico. In F. E. Kottlowski and staff (Eds.), *New Mexico Bureau of Mines and Mineral Resources annual report July 1, 1975 to June 30, 1976* (pp. 33–37). New Mexico Bureau of Mines and Mineral Resources.

81 Reiter, M., Simmons, G., Chessman, M., England, T., Hartman, H., & Weidman, C. (1976). Terrestrial heat flow near Datil, New Mexico. In F. E. Kottlowski and staff (Eds.), *New Mexico Bureau of Mines and Mineral Resources annual report July 1, 1975 to June 30, 1976* (pp. 33–37). New Mexico Bureau of Mines and Mineral Resources.

82 Theis, C. V., Taylor, G. C., & Murray, C. R. (1941). *Thermal waters of the Hot Springs Artesian Basin, Sierra County, NM: Fourteenth and fifteenth biennial reports of the State Engineer of New Mexico.* State Engineer of New Mexico.

83 Pepin, J. (2018). *New approaches to geothermal resource exploration and characterization* [Doctoral dissertation]. New Mexico Institute of Mining and Technology.

84 Person, M., Phillips, F., Kelley, S., Timmons, S., Pepin, J., Blom, L., Haar, K., & Murphy, M. (2013). *Assessment of the sustainability of geothermal development within the Truth or Consequences Hot-Springs District, New Mexico* (Open-file Report 551). New Mexico Bureau of Geology and Mineral Resources. https://doi.org/10.58799/OFR-551

85 Person, M., Phillips, F., Kelley, S., Timmons, S., Pepin, J., Blom, L., Haar, K., & Murphy, M. (2013). *Assessment of the sustainability of geothermal development within the Truth or Consequences Hot-Springs District, New Mexico* (Open-file Report 551). New Mexico Bureau of Geology and Mineral Resources. https://doi.org/10.58799/OFR-551

86 Pepin, J., Person, M., Phillips, F., Kelley, S., Timmons S., Owens, L., Witcher, J., & Gable, C. (2015). Deep fluid circulation within crystalline basement rocks and the role of hydrologic windows in the formation of the Truth or Consequences, New Mexico low-temperature geothermal system. *Geofluids*, *15*, p. 139–160. https://doi.org/10.1111/gfl.12111

87 Pepin, J. (2018). *New approaches to geothermal resource exploration and characterization* [Doctoral dissertation]. New Mexico Institute of Mining and Technology.

88 Pepin, J. (2018). *New approaches to geothermal resource exploration and characterization* [Doctoral dissertation]. New Mexico Institute of Mining and Technology.

89 Pepin, J. (2018). *New approaches to geothermal resource exploration and characterization* [Doctoral dissertation]. New Mexico Institute of Mining and Technology.

90 Person, M., Phillips, F., Kelley, S., Timmons, S., Pepin, J., Blom, L., Haar, K., & Murphy, M. (2013). *Assessment of the sustainability of geothermal development within the Truth or Consequences Hot-Springs District, New Mexico* (Open-file Report 551). New Mexico Bureau of Geology and Mineral Resources. https://doi.org/10.58799/OFR-551

91 Pepin, J. (2018). *New approaches to geothermal resource exploration and characterization* [Doctoral dissertation]. New Mexico Institute of Mining and Technology.

92 Theis, C. V., Taylor, G. C., & Murray, C. R. (1941). *Thermal waters of the Hot Springs Artesian Basin, Sierra County, NM: Fourteenth and fifteenth biennial reports of the State Engineer of New Mexico.* State Engineer of New Mexico.

93 Reiter, M., & Barroll, M. W. (1990). High heat flow in the Jornada del Muerto: A region of crustal thinning in the Rio Grande rift without upper crustal extension. *Tectonophysics*, *174*, 183–195. https://doi.org/10.1016/0040-1951(90)90391-K

94 Mack, G. H., Jones, M. C., Tabor, N. J., Ramos, F. C., Scott, S. R., & Witcher, J.C. (2012). Mixed geothermal and shallow meteoric origin of opal and calcite beds in Pliocene-Lower Pleistocene axial-fluvial strata, Southern Río Grande Rift, Rincon Hills, New Mexico, USA. *Journal of Sedimentary Research*, *82*, 616–631. https://doi.org/10.2110/jsr.2012.5

95 Witcher, J. C. (1991). Radon soil-gas surveys with diffusion-model corrections in geothermal exploration. *Geothermal Resources Council Transactions*, *15*, 301–308.

96 Ross, H. P., & Witcher, J. C. (1998). Self-potential surveys of three geothermal areas in the southern Rio Grande rift, New Mexico. *New Mexico Geological Society Guidebook*, *49*, 93–100. https://doi.org/10.56577/FFC-49

97 Witcher, J. C. (1991). The Rincon geothermal system, southern Rio Grande Rift, New Mexico: A preliminary report on a recent discovery. *Geothermal Resources Council Transactions*, *15*, 202–212.

98 Witcher, J. C. (1991). The Rincon geothermal system, southern Rio Grande Rift, New Mexico: A preliminary report on a recent discovery. *Geothermal Resources Council Transactions*, *15*, 202–212.

99 Person, M., Stone, W. D., Horne, M., Witcher, J., Kelley, S., Lucero, D., Gomez-Velez, J., & Gonzalez-Duque, D. (2023). Analysis of convective temperature overturns near the East Rincon Hills Fault Zone using semi-analytical models. *Geothermal Resources Council Transactions*, *47*, 3093–3117.

100 Person, M., Phillips, F., Kelley, S., Timmons, S., Pepin, J., Blom, L., Haar, K., & Murphy, M. (2013). *Assessment of the sustainability of geothermal development within the Truth or Consequences Hot-Springs District, New Mexico* (Open-file Report 551). New Mexico Bureau of Geology and Mineral Resources. https://doi.org/10.58799/OFR-551

101 Pepin, J. D., Robertson, A. J., & Kelley, S. A. (2019). *Borehole temperature profiles measured in the Mesilla Basin, New Mexico during the period 1972 through 2018* [Data set]. U.S. Geological Survey. https://doi.org/10.5066/P9FQ9BEN.

102 Pepin, J. D., Robertson, A. J., & Kelley, S. A. (2021). Salinity contributions from geothermal waters to the Rio Grande and shallow aquifer system in the transboundary Mesilla (United States)/Conejos-Médanos (Mexico) Basin. *Water*, *14*(1), 33. https://doi.org/10.3390/w14010033

103 Witcher, J. C. (1995). *New Mexico Geothermal Resource Database: New Mexico State University, Southwest Technology Development Institute report*. Geo-Heat Center, Oregon Institute of Technology.

104 Pepin, J. D., Robertson, A. J., & Kelley, S. A. (2021). Salinity contributions from geothermal waters to the Rio Grande and shallow aquifer system in the transboundary Mesilla (United States)/Conejos-Médanos (Mexico) Basin. *Water*, *14*(1), 33. https://doi.org/10.3390/w14010033

105 Gunaji, N. N., Thode, E. F., Chaturvedi, L., Walvekar, A., LaFrance, L., Swanberg, C. A., Jiracek, & G. R. (1978). *Geothermal application feasibility study for the New Mexico State University campus* (Technical Report NMEI13). Department of Energy.

106 Witcher, J. C., Schoenmackers, R., Polka, R., & Cunniff, R. A. (2002). Geothermal energy at New Mexico State University in Las Cruces. *Geo-Heat Center Bulletin*, *23*, 30–36.

107 Millennium Energy. (2006). *New Mexico State University geothermal system feasibility study*. National Renewable Energy Laboratory.

108 Chaturvedi, L. (1979). *Analysis of geological and geophysical logs of two geothermal exploration wells drilled on NMSU land, Las Cruces, NM* (NMSU Engineering Experiment Station Report prepared for the U.S. Department of Energy under contract EW-78-0500701717). U.S. Department of Energy.

109 Chaturvedi, L. (1981). *New Mexico State University Geothermal Production Well* (New Mexico Energy Research and Development Institute Report EMD 77-2218). New Mexico Energy Research and Development Institute.

110 Gross, J., & Icerman, L. (1983). *Subsurface investigations for the area surrounding Tortugas Mountain, Doña Ana County, New Mexico* (Report NMERDI 2-67-2238). New Mexico Research and Development Institute.

111 Icerman, L., & Lohse, R. L. (1983). *Geothermal low-temperature reservoir assessment in Doña Ana County, New Mexico* (Report NMERDI 2-69-2202). New Mexico Energy Research and Development Institute. https://doi.org/10.2172/6801873

112 Witcher, J. C., Schoenmackers, R., Polka, R., & Cunniff, R. A. (2002). Geothermal energy at New Mexico State University in Las Cruces. *Geo-Heat Center Bulletin*, *23*, 30–36.

113 Witcher, J. C., & Mack, G. H. (2018). Masson Farm Geothermal Greenhouses at Radium Springs: Third-day (C) Road Log from Las Cruces to Geothermal Greenhouses of the Masson Farm at Radium Springs. *New Mexico Geological Society Guidebook*, *69*, 47–51. https://doi.org/10.56577/FFC-69.47

114 Witcher, J. C., & Mack, G. H. (2018). Masson Farm Geothermal Greenhouses at Radium Springs: Third-day (C) Road Log from Las Cruces to Geothermal Greenhouses of the Masson Farm at Radium Springs. *New Mexico Geological Society Guidebook*, *69*, 47–51. https://doi.org/10.56577/FFC-69.47

115 Seager, W. R., & Mack, G. H. (1994). *Geology of East Potrillo Mountains and vicinity, Doña Ana County, New Mexico*. Bulletin 113. New Mexico Bureau of Mines and Mineral Resources. https://doi.org/10.58799/B-113

116 Snyder, J. T. (1986). *Heat flow in the southern Mesilla Basin, with an analysis of East Potrillo geothermal system, Doña Ana County, New Mexico* [Master's thesis]. New Mexico State University.

117 Pepin, J. D., Robertson, A. J., & Kelley, S. A. (2021). Salinity contributions from geothermal waters to the Rio Grande and shallow aquifer system in the transboundary Mesilla (United States)/Conejos-Médanos (Mexico) Basin. *Water*, *14*(1), 33. https://doi.org/10.3390/w14010033

118 Snyder, J. T. (1986). *Heat flow in the southern Mesilla Basin, with an analysis of East Potrillo geothermal system, Doña Ana County, New Mexico* [Master's thesis]. New Mexico State University.

119 Witcher, J. C., King, J. P., Hawley, J. W., Kennedy, J. F., Williams, J., Cleary, M., & Bothern, L. R. (2004). *Sources of salinity in the Rio Grande and Mesilla Basin groundwater* (Technical Completion Report no. 330). New Mexico Water Resources Research Institute.

120 Pepin, J. D., Robertson, A. J., & Kelley, S. A. (2021). Salinity contributions from geothermal waters to the Rio Grande and shallow aquifer system in the transboundary Mesilla (United States)/Conejos-Médanos (Mexico) Basin. *Water*, *14*(1), 33. https://doi.org/10.3390/w14010033

121 Zanskar. (2025, February 3). *Lightning Dock update.* Zanskar (Blog). https://www.zanskar.com/blog/betting-on-an-underperforming-geothermal-resource-zanskars-new-step-out-production-well-at-lightning-dock-is-a-world-beating-gusher

122 Elston, W. E., Deal, E. G., & Logsdon, M. J. (1983). *Geology and geothermal waters of Lightning Dock region, Animas Valley and Pyramid Mountains, Hidalgo County, New Mexico*. New Mexico Bureau of Mines and Mineral Resources. https://doi.org/10.2172/5228760

123 Jiracek, G. R., Smith, C., Ander, M. E., Holcombe, H. T., Gerety, M. T., & Swanberg, C. A. (1977). Geophysical studies at the Lightning Dock KGRA, Hidalgo County, New Mexico. *Geothermal Resources Council Transactions*, *1*, 157–158.

124 Smith, C. S. (1978). Geophysics, geology, and geothermal leasing status of the Lightning Dock KGRA, Animas Valley, New Mexico. *New Mexico Geological Society Guidebook*, *29*, 343–348. https://doi.org/10.56577/FFC-29.343

125 Witcher, J. C. (2008). Evidence for large-scale Laramide tectonic inversion and a mid-Tertiary caldera ring fracture zone at the Lightning Dock geothermal system, New Mexico. *New Mexico Geological Society Guidebook*, *59*, 177–187. https://doi.org/10.56577/FFC-59.177

126 Dixon, J. (2002). *Evaluation of bottom-hole temperatures in the Denver and San Juan Basins of Colorado* (Open-file Report OF-02-15). Colorado Geological Survey, Division of Minerals and Geology, Department of Natural Resources. https://coloradogeologicalsurvey.org/publications/evaluation-bottom-hole-temperatures-denver-san-juan-basins-colorado.

127 Morgan, P. (2009). A preliminary analysis of geothermal resources in the central Raton Basin, Colorado, from bottom-hole temperature data. *Geothermal Resources Council Transactions*, *33*, 509–513.

128 Kelley, S. A. (2015). Geothermal potential of the Raton Basin, New Mexico. *New Mexico Geological Society Guidebook*, *66*, 261–275. https://doi.org/10.56577/FFC-66.261

129 Kelley, S. A. (2015). Geothermal potential of the Raton Basin, New Mexico. *New Mexico Geological Society Guidebook*, *66*, 261–275. https://doi.org/10.56577/FFC-66.261

130 Kelley, S. A. (2015). Geothermal potential of the Raton Basin, New Mexico. *New Mexico Geological Society Guidebook*, *66*, 261–275. https://doi.org/10.56577/FFC-66.261

131 Kelley, S. A. (2015). Geothermal potential of the Raton Basin, New Mexico. *New Mexico Geological Society Guidebook*, *66*, 261–275. https://doi.org/10.56577/FFC-66.261

132 Kelley, S. A. (2015). Geothermal potential of the Raton Basin, New Mexico. *New Mexico Geological Society Guidebook*, *66*, 261–275. https://doi.org/10.56577/FFC-66.261

133 Reiter, M., & Clarkson, G. (1983). A note on terrestrial heat flow in the Colorado Plateau. *Geophysical Research Letters*, *10*, 929–932.

134 Reiter, M., & Mansure, A. J. (1983). Geothermal studies in the San Juan Basin and the Four Corners area of the Colorado Plateau, I: Terrestrial heat flow measurements. *Tectonophysics*, *91*, 233–251.

135 Kelley, S. (2019). Thermal structure and exhumation history of the San Juan Basin, New Mexico. *Geological Society of America Abstracts with Programs*, *51*(2).

136 Reiter, M. (2014). Heat flow data in the Four Corners area suggest Neogene crustal warming resulting from partial lithosphere replacement in the Colorado Plateau interior, southwest USA. *GSA Bulletin*, *126*(7/8), 1084–1092. https://doi.org/10.1130/B30951.1

137 Blankenship, D., Gertler, C., Kamaludeen, M., O'Connor, M., & Porse, S. (2024). *Pathways to commercial liftoff: Next-generation geothermal power.* U.S. Department of Energy.

138 Witcher, J. C., Schoenmackers, R., & Whittier, J. (1988). *Geologic, geohydrologic, and thermal settings of southern New Mexico geothermal resources* (Technical Report DE-FG07-84ID12546). New Mexico Statewide Geothermal Energy Program.

139 Witcher, J. C., Schoenmackers, R., & Whittier, J. (1988). *Geologic, geohydrologic, and thermal settings of southern New Mexico geothermal resources* (Technical Report DE-FG07-84ID12546). New Mexico Statewide Geothermal Energy Program.